EKSU
JOURNAL OF SCIENCE AND TECHNOLOGY (EJST)

Vol.9 Issue 2
2024

AGRICULTURE, ENGINEERING, MEDICINE AND SCIENCE

ISSN: 2489-0456

EKITI STATE UNIVERSITY
ADO-EKITI, EKITI STATE NIGERIA
OFFICE OF RESEARCH, DEVELOPMENT AND INNOVATION

tetfund
TERTIARY EDUCATION TRUST FUND
TETFund/DR&D/CE/UNI/ADO-EKITI/ARJ/1&2

EKSU JOURNAL OF SCIENCE AND TECHNOLOGY (EJST)

ISSN: 2489-0456

Published by:
OFFICE OF RESEARCH, DEVELOPMENT AND INNOVATION
EKITI STATE UNIVERSITY,
ADO-EKITI, EKITI STATE UNIVERSITY, NIGERIA

E-mail: ejst@eksu.edu.ng
website: https:/ejst.eksu.edu.ng

EKSU JOURNAL OF SCIENCE AND TECHNOLOGY (EJST)

EDITORIAL POLICY

EKSU Journal of Science and Technology (EJST) is a biannual Journal published by Ekiti State University, Office of Research, Development and Innovation. The Journal aims at periodically exhibiting and advertising the potential of research results within and outside the university as well as promoting dissemination of intellectual publications generally. The Journal, which is multidisciplinary and multicultural in nature covers the publication of original findings in Science and Engineering. It serves as a platform for academics, researchers, professionals, practitioners and students in the Science and Technology field to impart and share knowledge in the form of high quality practical, empirical and theoretical research papers, case studies, literature review and book reviews etc. from all over the world.

CALL FOR PAPERS

ABOUT EJST

Ekiti State University has been publishing journals at the Faculty and Departmental levels, But there is no university based journal. As part of the mandate of Ekiti State University, Office of Research, Development and Innovation (EKSUORD) to periodically exhibit and advertise the potentials of research results within the University as well as promoting the dissemination of intellectual publications generally, EKSUORDI announces the publication of a Science and Engineering based University journal EKSU Journal of Science and Technology (EJST). The Journal which is an international academic journal provides a platform natural, agricultural, environmental, medical scientists and engineers as well as technologists to share and expand the knowledge of scientific advancements in the myriad disciplines of science and engineering and applied aspects.

2. AIMS AND FOCUS

EKSU Journal of Science and Technology aims to publish and disseminate original papers that:

a. address ethical or socioeconomic issues relating to modern agricultural and environmental science as applicable to developing countries;
b. contribute to the development of science and technology for economic advancement;
c. innovate near market or market ready technologies and processes
d. publish research findings on current topical issues in science and engineering of interest to both public and private sectors.

3. SCOPE

EJST will publish peer reviewed original research and critical reviews on agriculture, human nutrition or human health, scientific or technological information, with particular emphasis on interdisciplinary studies that explore the intersection of agriculture, science, engineering and environment.

4. DOMICILIATION

The Journal is domiciled in the Office of Research, Development and Innovation, Ekiti State University, Ado-Ekiti.

5. SECTION

In order to encourage researchers to publish their research articles in the field of Science and Technology, the following sections are introduced:

Section A- (Agricultural Science)
Section B - (Natural Sciences)
Section C - (Engineering and Technology)
Section D - (Medical Sciences)
Section E-(Environmental Sciences)

6. FREQUENCY

The frequency of the journal is bienial.

7. REVIEW PROCESS

There shall be a review process of manuscripts by independent referees who are conversant and versatile in the pertinent subject area.
Authors should strive for maximum clarity of expression. Material which is not essential to the continuity of the text (e.g., proofs, derivations, or calculations) should be placed in Appendices Materials which have been previously copyrighted, published, or accepted for publication will not be considered for publication in the journal.
The editorial board is highly committed to the quick review process of the paper, but not with the sacrifice of the right judgment of a paper. The review process takes maximum of six weeks.

8. PROCEDURE FOR MANUSCRIPTACCEPTANCE FOR PUBLICATION

The manuscript would be sent to three (3) reviewers, of which two (2) of the reviewers' comment must be positive before acceptance, and the authors would have to effect all the corrections pointed out by the reviewers in the reviewers form.

9. PAGE CHARGE PROOFAND REPRINTS

Manuscript should be submitted as e-mail attachment to the corresponding author who will be contacted via e-mail on the corrections of the manuscript. This volume of EJST is sponsored by Tertiary Education Trust Fund (TETFund). With the exception of minor typographical errors, no changes will be made on the manuscript at the proof stage. A hard copy of the appropriate section and five (5) off prints would be provided for the corresponding author of each paper.

10. ACCESSIBILITYAND SUBSCRIPTION

EJST will be available both in print (hardcopy) and online (softcopy) format at www.academix.ng Online accessibility is by subscription. Information on purchase of any section, biennial, quarterly or annual subscription can be obtained by contacting EKSUORD.

11. ARTICLE TYPES

Regular Articles, short communication, and review will be acceptable for publication in thejournal.

12. INFORMATION /GUIDES FOR AUTHOR

a. The title page should bear the author's full names and affiliation of the names of corresponding author along with phone. fax and e-mail information. Present addresses of authors should appear as a footnote.
b. Abstract should be informative and self-explanatory. Should be 100-200 words in length Abstract should be written in past tense-standard nomenclature should be used.

Abbreviation should be avoided and no literature should be cited. List of nonstandard abbreviation should be added.

c. Manuscript should not exceed 15-20 pages.

d. Introduction should provide a clear statement of the problem, the relevant literature on the subject, and the proposed approach or solution.

e. Materials and methods should be complete enough to allow experiments to bereproduced and results written in past tense should be presented with clarity and precision.

f. Results should be explained, but largely without referring to the literature.

g. Discussion should interprete findings in view of results obtained in present and past studies on the topic.

h. Conclusion should be stated in few sentences at the end of the paper.

i. Acknowledgment of people, grant, funds should be brief.

j. Manuscript should be typed in double-line spacing with microsoft word on A4 size paper using 12 font size (Time New Roman)

k. Table should be kept to a minimum, and are to be typed double line-spaced through outincluding headings and footnotes. The same data should not be presented in both table andgraph form or repeated in the text.

l Figure legend should be typed in numerical order on a separate sheet.

m. Graphics should be prepared using applications capable of generating high resolution Gif., TIFF, JPEG or Microsoft PowerPoint before pasting in Microsoft world manuscript file.

n. References. In the text, a reference identified by means of an author's name should be followed by the date of the reference in parentheses. When there are more than two authors' names mentioned, it should be the first author followed by et al. In the event that an author cited has two or more works published during the same year, the reference, both in text and in the reference list, should be identified by a lower case letter like, a' and, b'after the date to distinguish the works. Example: Abayomi (2000), Agindotan et al. (2003), (Kelebeni, 1983), (Usman and Smith, 1992), (Chege, 1998; Chukwura, 1987 a, b; Tijani 1993, 1995), (Kumasi et al., 2001).

References should be listed at the end of the paper in alphabetical order. Articles In preparation or articles submitted for publication, unpublished observations, Personal communications date, etc, should not be included in the reference but should only be mentioned in the article text (eg. A. Kingory, University of Nairobi, Kenya, personal communication, date) Journal names are abbreviated according to chemical abstracts.

Authors are fully responsible for the accuracy of references. Example: Chikere C. B, Omoni V.T, and Chikere B. 0. (2008). Distribution of potential nosocomial pathogens ina hospital environmental. Afr. J. Biotechnol. 7:3535-3539.

Moran G. J, Amii R. N, Abrahamian F. M, Talan D. A. (2005), Methicilin resistantstaphylococcus aureus in community- acquired skin infections. Emeg. Infect. Dis. 11: 928-930.

Pelczar J. R. Harley J. P, Klein D. A. (1993) Microbiology: Concept and applications, McGraw-Hill Inc., New York, pp 591-603.

13. Short Communication: Short communication are limited to a maximum of two figures and one table. They should present a complete study that is more limited in scope than is found

in fullength papers. The items of manuscript preparation listed above apply to short communications with the following differences:

i. Abstracts are limited to 100 words:
i. Instead of a separate materials and methods section, experimental procedures may be incorporated into fiqure legends and table footnotes;
ii. Results and discussion should be combined into one section.

Copyrights

Submission of manuscript implies that the work described has not been published before, and that it is not under consideration for publication elsewhere. If and when the manuscript is accepted for publication, the authors will agree to automatically transfer the copyrights to the publisher.

CORRESPONDENCE

Please direct all correspondence(s) to:

The Managing Editor
Office of Research, Development and Innovation
Ekiti State University
P M B 5363, Ado Ekiti
E-mail: ejst@eksu.edu.ng

Editorial Board of Eksu Journal of Science and Technology (EJST)

Chairman:

Prof. Taiwo Owoeye
Director,
Office of Research, Development and Innovation (ORDI)
Ekiti State University, Ado-Ekiti
Phone +2348033518845

Editor-in-Chief

Prof. Richard Odunayo Akinyeye
Department of Industrial Chemistry
Faculty of Science
Ekiti State University, Ado-Ekiti
richard.akinyeye@eksu.ed@eksu.edu.ng

Managing Editor

Dr.(Mrs) Adenike O. Olubiyi
Department of Statistics
Faculty of Science
Ekiti State University, Ado-Ekiti
adenike.olubiyi@eksu.edu.ng

Administrative Officer

Dr.(Mrs) F. F. Daodu
Office of Research, Development and Innovation
Ekiti State University
P.M.B. 5363
florence.daodu2@gmail.com

Prof. Olusola O. Agbede
College of Agricultural Sciences,
Department of Crop and Soil Sciences,
Landmark University,
PMB 1001, Omu Aran,
Kwara State, Nigeria.
+2348037337617
Agbede,olusola@lmu.edu.ng

Mohibullah Mohibullah
Department of Geology,
University of Balochistan,
Quetta, Pakistan.
+92(0)3339323099
Mohibgeo1@yahoo.com

Dr. Fadiya Suyi Lawrence
Department of Geology,
Obafemi Awolowo University,
Ile-Ife, Osun State, Nigeria.
+2348033320230
slfadiya@oauife.edu.ng

Prof. J.F.Olorunfemi
Department of Geography and Environmental Management,
Faculty of Social Sciences,
University of Ilorin,
PMB 1515, Ilorin,
Kwara State, Nigeria.
+2348037208875
funshofem@unilorin.edu.ng

Table of Contents

EFFECTS OF SOME PLANT GROWTH REGULATORS ON THE GROWTH, NUTRITIONAL AND MEDICINAL ATTRIBUTES OF AFRICAN GARDEN EGG (*Solanum macrocarpon* L.)

[1,3]**Abdullahi Adeyemi ADEGOKE*;**
[2]**Anthony Wale OJEWUMI;**
[3]**Queeneth Abiola OGUNNIYI;**
[4]**Maryam Titilope AGBAJE;**
[1]**Mary Ololade AKINLADE;**
[5]**Olusegun Micheal AKANMU.**

*Corresponding Author: (adegokeabdullahi24@gmail.com; +2348068056396)
Authors' details

1. Department of Biological Sciences, Federal University of Agriculture, Abeokuta, Ogun state, Nigeria. **adegokeabdullahi24@gmail.com**; https://orcid.org/0000-0001-7208-9620; +2348068056396.
2. Department of Botany, Lagos State University, Lagos Nigeria. **anthony.ojewumi@lasu.edu.ng**; +2348121176267
3. Department of Pharmacognosy, University of Ibadan, Ibadan Nigeria. **queenethabiola@gmail.com**; +2348052272965
4. Department of Food Science and Technology, University of Ibadan, Ibadan Nigeria. **mtagbaje@gmail.com**; +2348039717815
5. Department of Environmental Biology, Ladoke Akintola University, Ogbomoso Oyo state, Nigeria. **olusegunmichealakanmu@gmail.com**; +2348060151983

ABSTRACT

The use of growth regulatory substances has been reported to have modulatory effects on growth and production efficiency of crops including African Garden egg (Solanum macrocarpon). Hence, this study was carried out to evaluate effects of different growth promoters; Naphthalene Acetic Acid, Coconut water and Bryophyllum pinnatum leaf extract on growth, nutritional and medicinal attributes of S. macrocarpon in a completely randomize design. Distilled water served as control. Proximate, mineral, vitamin and phytochemical contents of leaves of the vegetable were evaluated. Highest stem height (9.43 cm), number of leaf (6.25) and root length (11.15cm) were recorded in S. macrocarpon treated with 10% CW while highest leaf area (12.21cm^2) was observed in control. Highest moisture (8.84%), ash (0.22%) and crude protein (4.77%), were recorded in plant treated with Coconut Water, crude fibre (1.26%) and fat (0.71 %) were recorded in control while highest carbohydrate (86.44%) was determined the vegetable treated Naphthalene Acetic Acetic. Sodium (21.45mg/100g) and Potassium (620.52mg/100g) were higher in plant treated with Bryophyllum

pinnatum leaf extract, while highest phosphorus (59.88mg/100g) was recorded in treatment with Naphthalene Acetic Acid. In conclusion, Coconut Water promoted the growth and improved the nutritional parameters of the vegetable; therefore, the treatments can be used to enhance production of the vegetable.

Keywords: *Naphthalene Acetic Acid; Solanum macrocarpon; Bryophyllum extracts; Growth regulator, proximate contents*

INTRODUCTION

Plant hormones (phytohormones) are signal molecules produced by plants in small quantities to modulate changes in growth of plants (Méndez-Hernández *et al*., 2019), protect plants against pathogens (Bürger and Chory, 2019) and stress tolerance (Ullah *et al*., 2018) and control their reproductive systems.

Several hormones such as auxins, indole acetic acid, indole butyric acid, naphthalene acetic acid, and 2,4-Dichloropheoxyacetic acid among others have been shown to encourage root and leaf formation in plants (Sourati *et al.*, 2022). When applied to cuttings and placed in an appropriate propagation media, napthelene acetic acid has been shown to induce root formation (Quainoo *et al.*, 2014). In contrast to Naphthalene Acetic Acid is involved in elongation of stems and roots of plants (Chen *et al.*, 2022). The creation of adventitious roots is often induced by low concentrations of auxins. Aside synthetic hormones, extracts of some plants have been reported to boost production of crops (Ojo *et al*., 2022). Typical example of such plants is *Bryophyllum pinnatum* L, a perennial herb in Crassulaceae family and *Cocus nucifera*, a perennial plant in Aracaceae (Palm family). Extracts or coconut water from these plants contains a variety of chemicals such as sugars, vitamins, minerals, electrolytes, enzymes, amino acids, cytokines, phytohormones suitable to promote growth of vegetables (Molnár *et al*., 2011) such as tomato, pepper and *S. macrocarpon*. These vegetables most especially *S. macrocarpon* is also known for its important nutritional and medicinal values.

It is a significant fruit and leafy vegetable grown both for the market and domestic consumption (Komlaga *et al.*, 2014; Tropical Plants Data Base, 2020). Also, various researchers have reported *S. macrocarpon* as analgesic, anti-inflammatory and anti-asthmatic (Odetola *et al.*, 2014), antioxidants, anti-glaucoma, anti-cancer, and anti-viral agent (Chinedu *et al.*, 2011).

Despite the enormous relevance of the vegetable the rate of their production is low due to poor viability of their seeds and the low rate of germination as affected by erratic change in meteorological conditions (Ojo *et al*., 2022). This often results in reduction in

mass production of the plants for both domestic and commercial values.

In an order to improve the production and nutritional values of the vegetable, several concerted efforts such as good farming practices, appropriate use of fertilizers and the use of growth promoters have been adopted by farmers or horticulturists, yet these efforts have yielded little or no desired results. On the other hand, most of the growth promoters used cannot be afforded by the farmers. Hence, there is need for cheap plant-based growth promoters as alternatives to synthetic growth promoters in order to enhance production of the vegetable. Hence, this study was carried out to evaluate effects of different growth promoters; Naphthalene Acetic Acid (NAA), Coconut water (CW) and *Bryophyllum pinnatum* leaf extract (BPLE) on growth, nutritional and medicinal attributes of *S. macrocarpon*.

Materials and Methods

Seed collection: African egg plant seeds (*Solanum macrocarpum*) and Coconut (*Cocos nucifera*) fruits were obtained from Osiele market, Abeokuta, Ogun State. *Bryophyllum pinnatum* leaves were obtained from Botanical Garden, Federal University of Agriculture, Abeokuta (FUNAAB).

Collection of soil sample: The top soil utilized was collated at 0-6cm depth from different locations of the study site using soil probe as describe in Ojewumi *et al*. (2022).

Experimental location and Seedling preparation: The experiment was carried out at the Forest Nursery, FUNAAB, Ogun State, Nigeria. Seedlings of *S. macrocarpon* were raised in the study area for 21 days, transplanted into 20 planting buckets and watered for another 7 days to ensure hardening.

Experiment Design and Preparation of treatments

The planting buckets with one seedling per bucket were arranged in a complete randomize design with four replicates.

Preparation of experimental treatments

The coconut water (CW) was obtained by inserting a needle into the soft region of the fruit eye, the water content of the fruits was produced. *Bryophyllum pinnatum* Leaf Extract (BPLE) was prepared according to the method of Ojo *et al.*, (2022) cited in Agboola and Adedire (1998) with little modifications**.** Leaves of the plants were thoroughly washed and grounded using mortar and pestle. Juicy contents of the grounded leaves were filtered using Whatman Paper, thereafter, 10% of the filtrate (extract) obtained was determined by diluting 100ml of the extract in 900ml distilled water (Ojewumi et al., 2022). Similar procedure was adopted for preparation of 10% CW used. Also, 0.1mg/L was prepared by dissolving weighed 0.1mg of Naphthalene acetic acid in a litre of water. Distilled water served as control.

Hundred (100 mL) of each treatment was applied using folia application at three days intervals.

Data collection

Parameters such as stem height and root length were determined using meter rule calibrated in cm while number of leaf was determined using counting methods according to (Kadiri 1999). The total leaf area was determined using LI-3000 C Portable Leaf Area Meter by DMP Ltd.

Determination of nutritional content of *S. macrocarpon*

Proximate, vitamins and **q**uantitative phytochemicalanalysiswere determined on *S. macrocarpon* according to Harborne (1973) cited in Chigozie *et al*., (2014) with little modification. Minerals elements were assayed using Atomic Absorption Spectrophotometer (Perkin-Elmer Model 2280)

Statistical analysis

Data collected were analyzed using statistical analysis system. Means were calculated using one-way analysis of variance and separated by Duncan's Multiple Range Test (DMRT) at $P<0.05$.

RESULTS

Parameters such as stem height, number of leaves, root length and leaf area investigated in this study increased ($p<0.05$) as affected by the different growth promoters over a period of 6 weeks. *S. macrocarpon* treated with 10% CW produced highest stem height (9.43 cm) followed by control (7.90 cm) while least of the parameter (4.50 cm) was recorded in the vegetable sprayed with 10% NAA (Table 1). Highest number of leaf (6.25) was also recorded in plants treated with 10% CW, followed by Control (6.25) while least number of leaf (4.50) was recorded in vegetable treated with 10% NAA (Table 2. Similarly, Table 3 showed responses of root length to the treatments. Results revealed that 10% Coconut water produced longest root length (11.15 cm), followed by 10% BPLE (8.92 cm). Highest leaf area were recorded in vegetable treatment with water control (12.21 m^2kg^{-1}) while least (2.12 m^2kg^{-1}) of the parameters was recorded in 10% NAA (Table 4).

In addition, highest crude fibre (1.26%) and fat (0.71%) were recorded in leaf of *S. macrocarpon* treated with distilled water, Crude Protein (4.77%) and ash (0.22%) were observed in 10% CW while highest carbohydrate (86.44%) was observed in vegetable treated with 10% NAA (Table 4).

Furthermore, potassium (620.52 mg/ 100g) and sodium (620. 52 mg/100g) were significantly higher in the vegetable sprayed with 10% BPLE, calcium (250.79 mg/100g) and Zinc (250.79 mg/100g) in 10% CW magnesium (50.94 mg/100g) control while highest Phosphorus (59.88) was observed in the vegetable treated with 10% NAA (Table 6)

Table 7 showed that Vitamin A (0.03), Vitamin B (0.23) and Vitamin C (43.08) were significantly higher in *S. macrocarpon* sprayed with 10% WC compared with other treatments while higher Vitamin E(0.7%) was observed in the vegetable sprayed with 10% NAA. It was observed that alkaloids (2.46%) Saponin (0.28 %) and anthocyanin (0.5%) were significantly higher in the vegetable treated with 10% Coconut water while higher flavonoid (0.52%) was observed in control (Table 8).

Table 1: Effect of different concentrations of growth promoters on stem height of *S. macrocarpon at* various weeks after treatment

Treatments	Weeks after treatment			
	3WAT	4WAT	5WAT	6WAT
10% NAA	3.72±0.24^{a}	4.18±0.35^{b}	4.62±0.43^{b}	4.50±0.55^{c}
10% BPLE	3.74±0.24^{a}	5.20±0.35^{ab}	5.86±0.43^{b}	6.33±0.49^{b}
10% Coconut water	3.76±0.24^{a}	5.60±0.35^{a}	8.50±0.43^{a}	9.43±0.55^{a}
Control (Water)	2.96±0.24^{b}	4.80±0.35^{b}	7.38±0.43^{a}	7.90±0.49^{ab}

Means followed by different superscripts are significantly different at P< 0.05 using Duncan multiple range test (DMRT). *Bryophyllum pinnatum* leaf extract = BPLE WAT= Weeks after treatment

Table 2: Effect of different concentrations of growth promoters on number of leaf of *S. macrocarpon* at various weeks after treatment

Treatments	Weeks after treatment			
	3WAT	4WAT	5WAT	6WAT
10% NAA	3.00±0.12^{b}	4.00±0.19^{c}	4.20±0.24^{c}	4.50±0.21^{b}
10% BPLE	3.00±0.12^{b}	4.20±0.19^{bc}	5.00±0.24^{b}	6.00±019^{a}
10% Coconut water	3.40±0.12^{a}	4.80±0.19^{a}	5.80±0.24^{a}	6.25±0.21^{a}
Control (Water)	3.00±0.12^{b}	4.60±0.19^{ab}	5.80±0.24^{a}	6.20±0.19^{ab}

Means followed by different superscripts are significantly different at P< 0.05 using Duncan multiple range test (DMRT).*Bryophyllum pinnatum* leaf extract = BPLE WAT= Weeks after treatment

Table 3: Effect of different concentrations of growth promoters on root length of *S. macrocarpon* at variousweeks after treatment

Treatments	Weeks after treatments			
	3WAT	4WAT	5WAT	6WAT
10% NAA	2.38±0.56^{b}	5.06±0.31^{b}	5.86±0.32^{b}	6.69±0.54^{c}
10% BPLE	4.58±0.56^{a}	5.76±0.31^{ab}	7.64±0.32^{a}	8.92±0.48^{b}
10% Coconut water	4.58±0.56^{a}	6.54±0.31^{a}	7.98±0.32^{a}	11.15±0.54^{a}
Control (Water)	4.64±0.56^{a}	5.78±0.31^{ab}	7.68±0.32^{b}	8.58±0.48^{b}

Means followed by different superscripts are significantly different at P< 0.05 using Duncan multiple range test (DMRT).*Bryophyllum pinnatum* leaf extract = BPLE WAT= Weeks after treatment

Table 4: Effect of different concentrations of growth promoters on leaf area of *S. macrocarpon* at various weeks after treatment

Treatments	Weeks after treatment			
	3WAT	4WAT	5WAT	6WAT
10% NAA	1.38±0.20^{b}	1.89±0.42^{b}	2.02±1.14^{c}	2.12±1.28^{c}
10% BPLE	1.74±0.20^{ab}	2.54±0.42^{ab}	5.56±1.14^{b}	5.62±1.14^{bc}
10% Coconut water	2.29±0.20^{a}	3.70±0.42^{a}	9.28±1.14^{a}	8.76±1.28^{ab}
Control (Water)	2.10±0.20^{a}	3.70±0.42^{a}	9.99±1.14^{a}	12.21±1.14^{a}

Means followed by different superscripts are significantly different at P< 0.05 using Duncan multiple range test (DMRT).*Bryophyllum pinnatum* leaf extract = BPLE WAT= Weeks after treatment

Table 5: The effect of growth substances on proximate composition of *S. macrocarpon*

Treatments	Proximate contents (%)					
	Crude Fibre	Crude Protein	Fat	Ash	Moisture c	Carbohydrate
10% NAA	1.12±0.00^{a}	4.40±0.08^{b}	0.22±0.01^{c}	0.14±0.00^{b}	8.79±0.16^{a}	86.44±0.19^{a}
10% BPLE	1.19±0.04^{a}	4.68±0.01^{a}	0.27±0.01^{bc}	0.15±0.00^{b}	8.84±0.02^{b}	86.01±0.01^{a}
10% Coconut water	1.24±0.01^{a}	4.77±0.05^{a}	0.40±0.08^{b}	0.22±0.11^{a}	8.84±0.07^{a}	85.77±0.30^{b}
Control (Water)	1.26±0.09^{a}	4.65±0.02^{a}	0.71±0.05^{a}	0.11±0.01^{c}	8.75±0.03^{a}	85.78±0.03^{b}

Means followed by different superscripts are significantly different at P< 0.05 using Duncan multiple range test (DMRT).*Bryophyllum pinnatum* leaf extract = BPLE

Table 6: Mineral composition of *Solanum macrocarpon* with different growth substance

Treatments	Mineral elements (mg.100g)					
	Magnesium	**Potassium**	**Calcium**	**Phosphorus**	**Sodium**	**Zinc**
10% NAA	50.90±0.05^{a}	604.87±2.22^{c}	246.72±0.99^{b}	59.88±0.06^{a}	604.87±2.22^{c}	246.72±0.99^{b}
10% BPLE	48.72±0.04^{b}	620.52±0.02^{a}	246.25±0.21^{b}	57.88±0.02^{b}	620.52±0.02^{a}	246.25±0.21^{b}
10% Coconut water	51.05±0.31^{a}	610.50±0.25^{c}	250.79±0.31^{a}	55.75±0.02^{c}	610.50±0.25^{c}	250.79±0.31^{a}
Control (Water)	50.94±0.33^{a}	615.48±0.28^{b}	245.79±1.00^{b}	50.56±0.15^{d}	615.48±0.28^{b}	245.79±1.00^{b}

Means followed by different superscripts are significantly different at P< 0.05 using Duncan multiple range test (DMRT).*Bryophyllum pinnatum* leaf extract = BPLE

Table 7: Vitamin composition of *Solanum macrocarpon* treated with different growth parameters.

Treatments	Vitamin (insert unit here)			
	Vitamin A	**Vitamin B**	**Vitamin C**	**Vitamin E**
10% NAA	0.02±0.00^{b}	0.02±0.00^{b}	42.23±0.37^{b}	0.7±0.06^{a}
10% BPLE	0.02±0.00^{b}	0.02±0.00^{b}	42.85±0.03^{ab}	0.12±0.01^{b}
10% Coconut water	0.03±0.01^{a}	0.23±0.00^{a}	43.08±0.22^{a}	0.11±0.01^{b}
Control (Water)	0.02±0.00^{b}	0.10±0.08^{b}	40.77±0.12^{c}	0.130±0.01^{b}

Means followed by different superscripts are significantly different at P< 0.05 using Duncan multiple range test (DMRT).*Bryophyllum pinnatum* leaf extract = BPLE

Table 8: Phytochemical composition of *S. macrocarpon* treated with different growth substances.

Treatments	Phytochemicals (%)				
	Alkaloids	**Flavonoids**	**Saponin**	**Steroids**	**Anthocyanin**
10% NAA	2.25±0.01^{c}	0.43±0.21^{ab}	0.13±0.01^{b}	0.08±0.01^{a}	0.12±0.01^{b}
10% BPLE	2.42±0.02^{b}	0.11±0.00^{b}	0.13±0.01^{b}	0.07±0.01^{ab}	0.2±0.01^{b}
10% Coconut water	2.46±0.01^{a}	0.12±0.00^{b}	0.28±0.02^{a}	0.06±0.01^{ab}	0.5±1.02^{a}
Control (Water)	2.41±0.01^{b}	0.52±0.00^{a}	0.12±0.01^{b}	0.03±0.02^{b}	0.02±0.00^{b}

Means followed by different superscripts are significantly different at P< 0.05 using Duncan multiple range test (DMRT).*Bryophyllum pinnatum* leaf extract = BPLE

DISCUSSION

The use of growth promoters or their substitutes is a promising approach in crop production. This is due to précised actions of the substances on targeted plants or plant organs (Rafeekher *et al*., 2002; Naeem *et al*., 2004). Results of the present findings demonstrated that growth promoters manipulated and modulated differential changes in morphological characters of *S. macrocarpon* studied. Variations observed in the characters may indicate that application of the treatments produced modulatory influence on elongation of stem (height) and root of the vegetable and enhance the formation of auxiliary bud which is often resulted into leaf development and general proliferation leaf number and leaf area as observed in *S. macrocarpon*. The observation is in agreement with submission of Mukhtar (2008) who opined that the application of growth substances such as coconut water induced increase in height and other morphological indices of *Hibiscus sabdariffa* (Gnasekaran *et al*., 2012) and Oyeyemi *et al., (*2015) who reported that inclusion of coconut water into culture medium promoted proliferation in Vanda Kasem's Delight orchid.

Effects of the growth promoters on nutritional indices of the vegetable revealed that the substances most especially coconut water contains bunch of nutrition contents such as vitamins, minerals, amino acids, and phyto- hormones necessary for enlargement of morphological parameters (Shamal *et al*., 2021) and improvement of the dietary importance of the vegetable.

Appreciable amount of crude protein and ash obtained in the vegetable sprayed with CW indicated although other t reatments investigated nutritionally relevance to the cultivation of the vegetable but coconut water contained required nutritional indices needed for the synthesis/repair vascular tissue and enzymatic actions in the vegetable (Achikanu *et al*., 2022).

Based on results of this study, leaves of *S. macrocarpon* treated with or WC contain a moderate quantity of ash, making it a suitable source of plant minerals required by man for regular metabolic activity of bodily tissues as well as proper assimilation (Umoh *et al*., 2013). The high moisture contents observed suggests that the vegetable cannot be stored for a long without deterioration and spoilage as moisture enhance microbial action (Eshun *et al*., 2013). Also, relatively high carbohydrate level noticed in the vegetable sprayed with 10% NAA and 10% BPLE may inform that the treatments induced higher amount of energy inform of adenosine triphosphate needed by the plants to power metabolic process of the parts. The energy may also be potential source of nutrient for plumule and radicle before the emergence of mature leaves

during germination process (Ashraf and Foolad 2005).

Higher mineral contents recorded in the leaves of *S. macrocarpon* as influenced by or WC infers that the treatment is a good source of a host of mineral elements such calcium, magnesium, potassium, sodium, phosphorus, iron, and zinc needed for skeletal integrity and gastrointestinal uptake of mineral elements (Adefisan *et al*., 2020).

In addition, presence of appreciable quantities of minerals in adequate amount in the vegetable treated with or WC may indicate ability of the treatment in enhancing normal physiological functions such as nutrient utilization and mineralization in the plants (Adeyeye, 2000) as well as prevention and control of ailments, Hence, the observation may denote contributions of WC to therapeutic potential of vegetable (Shamal *et al.*, 2021). Although, the nutritional responses of the vegetable showed variations across the treatments yet nutritional compassions of WC increased both primary and secondary metabolites the vegetable investigated. Therefore, WC may be considered the best treatment for cultivation of *S. macrocarpon* to ensure better morphological characters and high nutritional contents of the vegetable.

The quantitative phytochemical analysis of *S. macrocarpon* revealed appreciable amount of alkaloid, saponins, tannins, phenol, flavonoids, anthocyanin and steroids. These phytochemicals may signify substantial benefit of the vegetable to consumers an excellent source of therapeutic values (Aletan and Kwazo, 2019).

CONCLUSION

This study revealed that although differentgrowth treatments investigated influenced the vegetative growth and nutritional contents of *S. macrocarpon,* however Coconut water emerged as the most effective growth and nutritional enhancer in the vegetable, therefore the treatment is recommended for massive production of the vegetable

REFERENCES

Achikanu, CE; Ujah II and Ezenwali, MO (2022). Proximate and phytochemical composition of *Phyllantusamarus* . *World Journal of Advanced Research and Reviews*, 15(01), 041–047

Adefisan I. O., Ebuehi O. A. T. and Odesanmi O. S. (2020). Proximate, Mineral Composition and Phytochemical Screening of Aqueous Leaf Extract of Alafia barteri Oliv. (Apocynaceae). International Journal of Biochemistry Research & Review. 29(9): 2020: 108-112.

Adeyeye, E. I. (2000) Bio-Concentration of Macro and Trace Minerals in Four Prawns Living in Lagos Lagoons. Pakistan Journal of Scientific and Industrial Research, 43, 367-373.

Agboola, D. A. and Adedire, M. O. (1998). Responses of treated dormant seeds of three tropical tree species to germination promoters. *Nigerian Journal of Botany*, 11: 103 – 110.

Aletan U.I. and Kwazo H.A. (2019). Analysis of the Proximate Composition, Anti-Nutrients and Mineral Content of *Maerua Crassifolia* Leaves. Nigerian Journal of Basic and Applied Science 27(1): 89-96

Ashraf, M., & Foolad, M. R. (2005). Pre‐sowing seed treatment—A shotgun approach to improve germination, plant growth, and crop yield under saline and non‐saline conditions. *Advances in agronomy*, *88*, 223-271

Bürger M, Chory J (August 2019). "Stressed Out About Hormones: How Plants Orchestrate Immunity". *Cell Host & Microbe*. **26** (2): 163-172. doi:10.1016/j.chom.2019.07.006. PMC 7228804. PMID 31415749

Chen C., Wu, X., Pan L., Yang Y., Dai H., Hua B., Miao M., Zhang Z. (2022) Effects of Exogenous alpha- Naphthalene acetic acid and 24-Epibrassinolide on fruit size and assimilate Metabolism-related Sugars and enzyme Activities in giant Pumpkin. *International Journal of Molecular Sciences*; 23(21);13157

Chigozie, M. E., Chukwuma, S. E., Augustine, N. E. (2014) . Determination of physical and phytochemical constituent of some tropical timbers Indigenous to Niger delta area of Nigeria. *European scientific journal*. Vol.10:18

Chinedu, S. N., Olasumbo, A. C., Eboji, O. K., Emiloju, Arinola, O. K., and Dania, D. I (2011). Proximate and phytochemical analyses of Solanum athiopicum L. and Solanum macrocarpon L. fruits. Res. J. Chem. Sci., 1(3): 63-72

Eshun G, Amankwah EA and Barimah J. (2013) Nutrient's content and lipid characterization of seed pastes of four selected peanut (Arachis hypogaea) varieties from Ghana. *African Journal of Food Science*, 7(10): 375-381.

Gnasekaran, P., Poobathy, R., Mahmood, M., Samian, M. R., Subramaniam, S. (2012). Effects of complex organic additives on improving the growth of PLBs of Vanda Kasem's Delight. AJCS 6(8):1245-1248.

Harborne, J. B. (1973). Phytochemical methods; a guide to modern techniques of plant analysis. Chapman & Hall Ltd., London; 49-188

Kadiri, M. (1999). Effect of coconut milk and GA3 on the vegetative growth and transpiration rate of *Abelmoschum esculentus* and *Lycopersicum esculentus* . Personal communication.

Komlaga, G., Sam, G. H., Dickson, R. A., Mensah, M. L. K., Fleischer, T. C., (2014). Pharmacognostic

studiesand Antioxidant properties of the leaves of *Solanummacrocarpon*. Journal of Pharm. Sci. & Resources Vol. 6(1):1-4.

Méndez-Hernández H. A., Ledezma-Rodríguez M., Avilez-Montalvo R. N., Juárez-Gómez Y. L., Skeete A., Avilez-Montalvo J., (2019). "Signaling Overview of Plant Somatic Embryogenesis". *Frontiers in Plant Science*. **10**: 77. doi:10.3389/fpls.2019.00077. PMC 6375091. PMID 30792725

Molnár, Z., Virág, E., and Ördög, V. (2011). Natural substances in tissue culture media of higher plants. Acta BiologicaSzegediensis, 55 (1): 123-127.

Mukhtar, F. B. (2008). Effect of some plant regulators on the growth and nutritional value of *Hibiscus sabdariffa L.* (Red sorrel). *International Journal of Pure and AppliedSciences* Vol. 2(3):70-75.

Naeem, M., Iram, B., Raza, H. A. and Yasin, M. A. (2004). Effects of some growth hormones (GA_3, IAA and Kinetin) on the morphology and early or delayed initiation of bud of Lentil (LENS CULINARISMEDIK). *Pakistan Journal of Botany*, 36(4): 801 – 809.

Odetola A.A., Iranloye Y.O. and Akinloye O., (2014) Hypolipidaemic Potentials of Solanummelongena and Solanum gilo on Hypercholesterolemic Rabbits, Pak *J. Nutri.*, 3 (3), 180-187

Ojewumi, A. W.; Junaid, O. E. and Feyibunmi, G. O. (2022). Morpho-Physiological Assessment of Water Stress Ameliorative Potential of Some Osmoprotectants on Growth Performance and Chlorophyll Contents of Cayenne Pepper (Capsicum annum). FUOYE Journal of Pure and Applied Sciences, Vol. 7 (3) ISSN:2616-1419

Ojo, E. S., **Ojewumi, A. W.,** Fawibe, O.O. and Agboola, D.A. 2022**.** Seed Emergence And Seedling Growth Of Two Varieties Of Cucurbits As Affected By Varying Concentrations Of Hormones Nigerian Journal of Botany , 35 (2), 115-126.

Oyeyemi, S. D., Ayeni, M. J., Adebiyi, A. O., Ademiluyi, B. O., Tedela, P. O., Osuji, I. B. (2015). NutritionalQuality and Phytochemical Studies of *Solanum anguivi*(Lam.) Fruits *Journal of Natural Sciences Research*. Vol.5:4

Quainoo, A. K, Kabrir, K, Mahunu, G. (2014). Effect of naphthalene acetic acid on rooting and shoot growth of *Lawsoniainermis*. *Biochemistry and Biotechnology Research*, ISSN: 2354-2136Vol. 2(4), pp. 50-52.

Rafeekher, M., Nair, S. A., Sorte, P. N., Hartwal, G. P. and Chandan, P. M. (2002). Effects of growth

regulators on growth and yield of summer cucumber. *Journal of Soils and Crops*, 12: 108 – 110.

Reza Sourati, Sharifi P., Poorghasemi M., Vieira E. A., Seidavi A., Anjum N. A., Sehar Z., and Sofo A (2022) Effects of Naphthalene Acetic Acid, Indole-3-Butyric Acid and Zinc Sulfate on the Rooting and Growth of Mulberry cuttings. International journal of Plant Biology; 133(3), 245-256.

Shamal N Tuyekar, Bharvi S. Tawade, Kajalkumar S. Singh, Vidula S. Wagh1, Prasad K. Vidhate, RupaliP. Yevale, Shweta Gaikwad, Mohan Kale (2021).An Overview on Coconut Water: As A Multipurpose Nutrition. *Int. J. Pharm. Sci. Rev. Res.*, 68(2), May - June 2021; Article No. 10, Pages: 63-70

Tropical Plants Database (2020). Ken Fern. tropical.theferns.info. <tropicaltheferns.info/ view tropical.php?id=Solanum+macro carpon> (October, 16, 2020)

Ullah A, Manghwar H, Shaban M, Khan AH, Akbar A, Ali U (2018). " Phytohormones enhanced drought tolerance in plants: a coping strategy". *Environmental Science and Pollution Research International*. **25** (33):33103–33118. doi:10.1007/s11356-018-3364-5. PMID 30284160. S2CID 52913388

Umoh, E.E., Akpabio, U.O. and Udo, I.E. (2013). Phytochemical Screening and nutrient analysis of Phyllanthus amarus. *Asian Journal of plant science and Research*, 3(4): 116-122.

CLASSIFICATION AND PREDICTION OF STUDENTS ACADEMIC PERFORMANCE USING MACHINE LEARNING

Adedeji, Oluwaseun Bukonla
Department of Computer and Information Science, *Tai Solarin University of Education, Ijagun, Ogun state.*
Phone no: +2348028508256
oluwaseunfunmi4god@yahoo.com, adedejiob@tasued.edu.ng,

Abstract
Effectively predicting students' academic performance is crucial for improved educational outcomes and individualized learning. Even while they are helpful, traditional assessment techniques frequently ignore the complex determinants influencing performance, like socioeconomic status and engagement measures.
This study explores the development of a predictive model using an ensemble of machine learning algorithms to classify students' academic performance in higher institutions. By leveraging data collected from Department of Computer Science, Tai Solarin University of Education records, relevant features were selected using the mutual information method. The ensemble model was formulated and simulated using two machine learning algorithms such as Support Vector Machines (SVM) and Decision Trees (DT) in the Google CoLaboratory environment. The model's predictive accuracy was evaluated based on key performance metrics, including accuracy, precision, and F-measure. Results indicate that the ensemble approach outperforms single-model methods by enhancing prediction robustness and reducing variance. This study demonstrates the effectiveness of machine learning techniques in identifying at-risk students early with SVM having 100% accuracy, allowing for timely interventions and improved resource allocation. Moreover, it contributes to evidence-based decision-making in educational institutions, helping to optimize learning experiences and boost student retention rates.

***Keywords**: Academic performance, Classification, machine learning, Support Vector machine, Decision Trees*

1.0 Introduction
Machine learning (ML) techniques offer promising avenues for analyzing large volumes of educational data and uncovering patterns that may be difficult to discern through manual analysis alone (Romero & Ventura, 2020). By leveraging ML algorithms, researchers and educators can develop predictive models capable of

classifying student performance based on various input variables, such as demographic information, previous academic records, and engagement metrics (Albreiki, Zaki, & Alashwal, 2021). These models have the potential to enhance educational outcomes by identifying at-risk students (Karalar, Kapucu, & Gürüler, 2021), tailoring instructional interventions, and optimizing resource allocation (Ramaswami, Susnjak, Mathrani, Lim, & Garcia, 2019).

Machine learning approaches offer several advantages over predictive models based on a single machine learning algorithm (Karalar et. al., 2021: Hussain et. al., 2023)). By combining multiple models, machine learning techniques can leverage the strengths of individual models while mitigating their weaknesses, thereby improving predictive accuracy and robustness (Yağcı, 2022). Moreover, machine learning methods can handle diverse types of data and modeling techniques, enabling a more comprehensive analysis of factors influencing prediction. Ensemble modeling is widely used in various machine learning tasks, including classification, regression, and clustering. It has been shown to improve predictive performance, reduce variance, and increase model robustness compared to single-model approaches. However, ensemble modeling requires careful tuning of hyperparameters, selection of diverse base models, and consideration of computational resources to achieve optimal results.

The development of predictive models for classifying student performance using machine learning algorithms holds significant promise for improving educational outcomes and informing evidence-based decision-making in educational institutions. By leveraging machine learning techniques, researchers and educators can develop predictive models capable of identifying at-risk students, tailoring interventions, and optimizing resource allocation. However, challenges such as interpretability, scalability, and model selection must be carefully addressed to ensure the effective and responsible use of machine learning in education. Overall, machine learning represents a compelling approach for developing predictive models in education, with the potential to transform teaching, learning, and educational practice.

In educational institutions, understanding and predicting student performance play a crucial role in facilitating personalized learning, early intervention, and academic success (Deda, Pacukaj, & Vardari, 2021). Traditionally, educators have relied on various assessment methods, such as exams, quizzes, and assignments, to evaluate student performance. While these methods offer valuable insights into students' understanding and progress, they often provide only a snapshot of their academic abilities and

may not capture the complex interplay of factors influencing performance (Kumar & Salal, 2019).

Institutions of higher learning are currently facing the challenge of attracting new students who can effectively meet their diverse academic demands. With these demands come the need for those institutions to develop strategies that can enhance students' learning experiences at various educational levels. Predicting the academic success at an early stage would allow academic institutions to develop specific enrolment guidelines while avoiding poor performance. Traditional methods of assessing student performance, such as standardized tests and course grades, have several limitations. These methods often rely on summative assessments that provide retrospective insights into students' abilities but offer limited predictive power regarding future performance. Moreover, traditional assessments may not capture the full spectrum of students' skills, knowledge, and competencies, leading to incomplete or biased evaluations. Furthermore, traditional methods may overlook non-academic factors that influence student performance, such as socio-economic background, motivation, learning style, and mental health. Failing to account for these factors can result in inaccurate predictions and missed opportunities for intervention. Additionally, traditional assessments are often labour-intensive, time-consuming, and subject to human biases, making them less scalable and efficient for large-scale predictive modeling tasks.

Predicting student performance holds significant implications for both students and educational institutions. For students, early identification of academic challenges can lead to timely support interventions, personalized learning experiences, and improved outcomes. By identifying struggling students early on, educators can provide targeted interventions, such as tutoring, counseling, or additional resources, to address academic difficulties and prevent dropout.

2.0 Methodology

Relevant data containing information about the features that are associated with the assessment of the academic performance of students was collected from the departmental records.

2.1 Research Framework

The study collected data containing information about the various features that are associated with the classification of the academic performance of students of the department of computer science, Tai Solarin University of Education, Ijagun. The data collected was subjected to a number of preprocessing techniques with the purpose of presenting the dataset in a manner that would be acceptable by the predictive modeling scheme considered in this study. The preprocessing techniques adopted in the

study included the removal of personal data about students such as their names and matric number. Additional preprocessing techniques involved the conversion of the categorical variables that were stored using string-type values into integer-type numerical values such that each value was mapped uniquely to each categorical label of their respective variables. This was necessary as deep learning algorithms are suited to the manipulation of numerical values thus, they are not suited to the manipulation of data stored in string type data.

The dataset was subjected to feature selection for the purpose of extracting the most relevant features that are important for assessing credit worthiness. These features are expected to provide a generate a better understanding of the relationship between the features and the target class compared to the initially identified features that were fed to the machine learning algorithms. The performance of the predictive models for the classification of the academic performance of students that was generated using the relevant features generated by the feature selection method and the model generated by the ensemble models were then compared.

The development of the predictive model was achieved with the use of the hold-one-out method such that a larger proportion of the dataset was adopted for training (building) the predictive model while a smaller proportion of the dataset was adopted for testing (validating) the predictive model. This was done with the use of varying proportions of the training and testing datasets which were evaluated and compared based on a number of performance evaluation metrics. The performance evaluation metrics that were adopted for the evaluation of the predictive models based on the testing datasets were, namely: accuracy, true positive rate, precision and the f1-score. The predictive model with the best performance was selected following which it was integrated into a web-based implementation of prototype system.

Table 1 provides a description of the features that were considered for the classification of academic performance. The features in the dataset collected were subjected to feature selection using the mutual information method. The ensemble model for the classification of academic performance was formulated using a number of machine learning algorithms based on information about the features. Predictive models were simulated by using the holdout method based on 5 simulation runs for each machine learning algorithm such that the training dataset was used to build the model using the Google CoLaboratory; a Python jupyter notebook for Gmail users. The models were evaluated using on a number of performance metrics, namely: accuracy, true positive (TP) rate, false positive (FP) rate, precision and f-measure based on the test dataset.

Table 1: Identification of features associated with credit worthiness

Class of Variable	Name	Label values
Socio-Demographic Information	**Gender**	Categorical (Male, Female)
	Age at Admission	Numeric – Integer type
	State of Origin	Categorical
UTME Results	**English**	Numeric – Integer Type
	Mathematics	Numeric – Integer Type
	Chemistry	Numeric – Integer Type
	Physics	Numeric – Integer Type
O'Level Results (SSCE)	**English**	Numeric – Integer type
	Mathematics	Numeric – Integer type
	Chemistry	Numeric – Integer type
	Physics	Numeric – Integer type
	Biology	Numeric – Integer type
	Agricultural Science	Numeric – Integer type
	Geography	Numeric – Integer type
	Economics	Numeric – Integer type
	Further Mathematics	Numeric – Integer type
	Technical Drawing	Numeric – Integer type
100 Level Results	**First Semester CGPA**	Numeric – Float type
	Second Semester CGPA	Numeric – Float type
Target Class	**Graduating Class of Degree**	Categorical (First Class, Second Class Upper, Second Class Lower, Third Class)

3.0 Results/Discussions.

Results of the Simulation of Predictive Model

This section presents the results of the application of the three machine learning algorithms, namely support vector machines (SVC) and decision trees (DT) classifiers. The model simulation was conducted by splitting the dataset into two parts, train and test dataset using five simulations such that 50/50, 60/40, 70/30, 80/20 and 90/10 percent of the dataset was adopted for training/testing the predictive model. Table 2 shows the number of records that were adopted for each simulation that were considered in this study. As stated earlier, the train datasets were used to build the predictive model while the test data were used to evaluate the performance of the predictive models based on a number of performance evaluation metrics.

Table 2 Description of the number of records adopted for training and testing predictive models across five simulations.

Simulation#	Train Data					Test Data				
	2.1	2.2	First	Third	Total	2.1	2.2	First	Third	Total
Simulation 1 (50/50)	28	19	3	11	**61**	15	12	9	14	**50**
Simulation 2 (60/40)	32	21	4	14	**71**	11	7	11	11	**40**
Simulation 3 (70/30)	37	26	2	16	**81**	6	8	9	7	**30**
Simulation 4 (80/20)	42	31	3	15	**91**	5	6	4	5	**20**
Simulation 5 (90/10)	49	38	4	20	**101**	1	4	2	3	**10**

Figure 1 shows the confusion matrices that were used to interpret the results of the evaluation of the two machine learning models adopted in simulation 1 based on the test dataset. Using SVM classifier, it was observed that all 15 actual second-class lower records were correctly classified, all 12 actual second-class lower records were correctly classified, all 9 actual first-class records were correctly classified and all 14 actual third-class records were correctly classified owing to an accuracy of 100.0%.

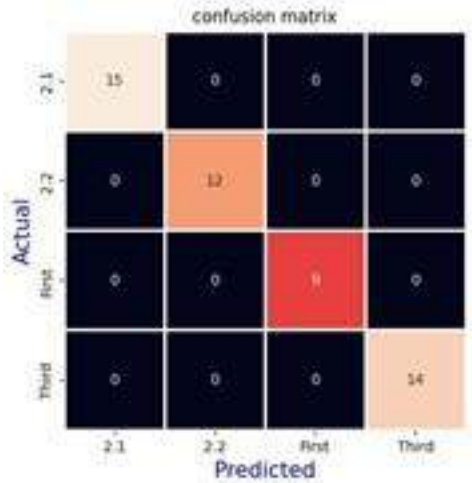

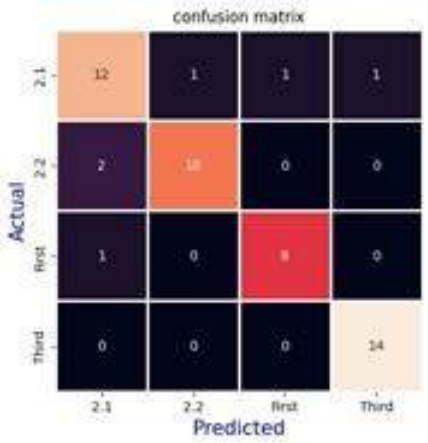

Figure 1: Confusion matrices for the evaluation of, support vector machines (left) and decision trees (right) for simulation 1.

Figure 2 shows the confusion matrices that were used to interpret the results of the evaluation of both machine learning models adopted in simulation 2 based on the test dataset. Using SVM classifier, it was observed that all 11 actual second-class lower records were correctly classified, all 7 actual second-class lower records were correctly classified, all 11 actual first-class records were correctly classified and all 11 actual third-class records were correctly classified owing to an accuracy of 100.0%.

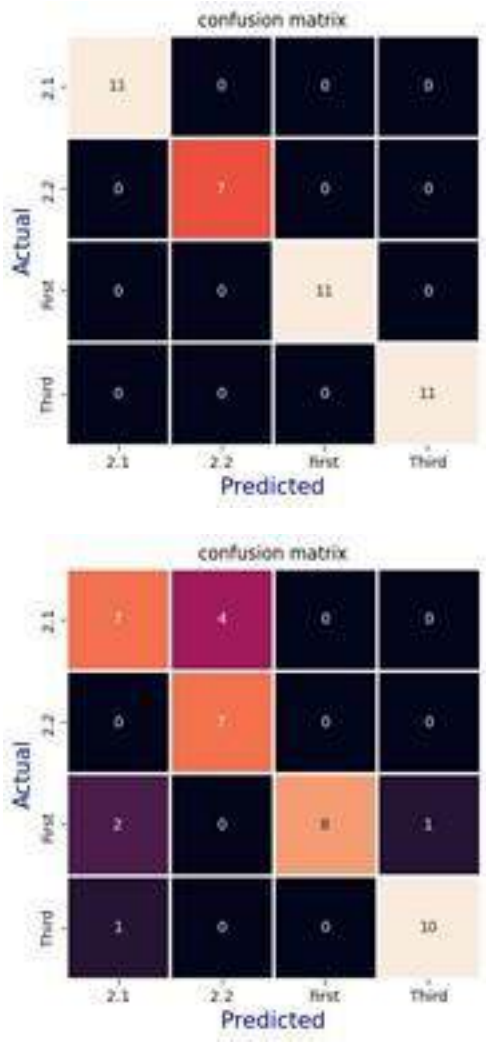

Figure 2: Confusion matrices for the evaluation of support vector machines (left) and decision trees (right) for simulation 2.

Figure 3 shows the confusion matrices that were used to interpret the results of the evaluation of both machine learning models adopted in simulation 3 based on the test dataset. Using SVM classifier, it was observed that all 6 actual second-class lower records were correctly classified, all 8 actual second-class lower records were correctly classified, all 9 actual first-class records were correctly classified and all 7 actual third-class records were correctly classified owing to an accuracy of 100.0

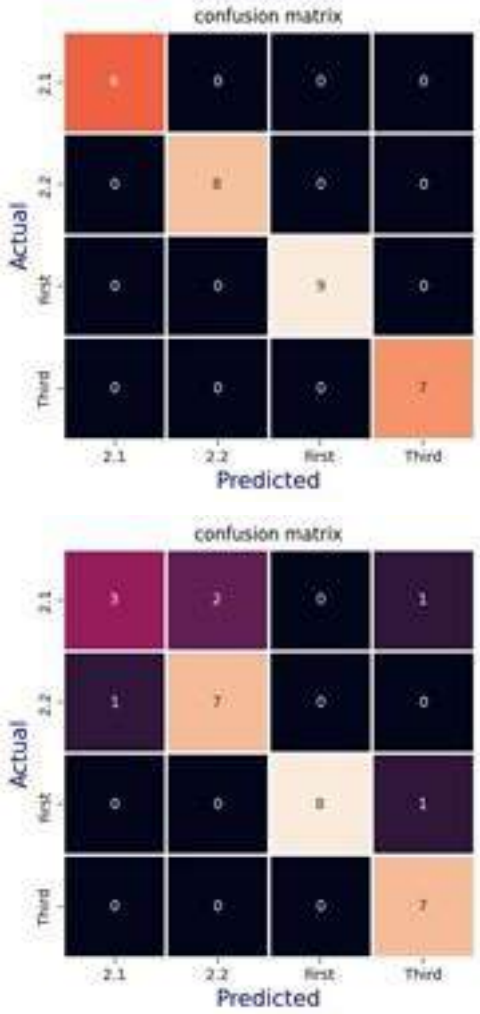

Figure 3: Confusion matrices for the evaluation of support vector machines (left) and decision trees (right) for simulation 3.

Figure 4 shows the confusion matrices that were used to interpret the results of the evaluation of both machine learning models adopted in simulation 4 based on the test dataset. Using SVM classifier, it was observed that all 5 actual second-class lower records were correctly classified, all 6 actual second-class lower records were correctly classified, all 4 actual first-class records were correctly classified and all 5 actual third-class records were correctly classified owing to an accuracy of 100.0%.

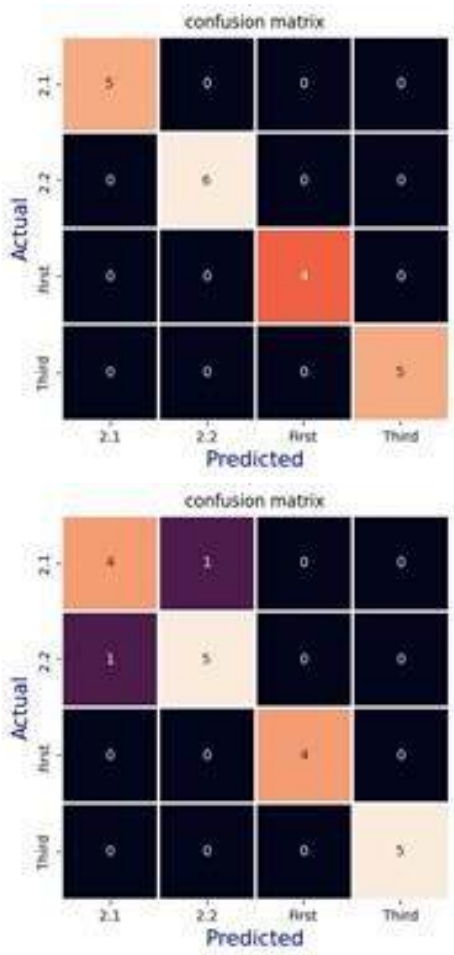

Figure 4: Confusion matrices for the evaluation support vector machines (left) and decision trees (right) for simulation 4.

Figure 5 shows the confusion matrices that were used to interpret the results of the evaluation of both machine learning models adopted in simulation 2 based on the test dataset. Using SVM classifier, it was observed that all 1 actual second-class lower records were correctly classified, all 4 actual second-class lower records were correctly classified, all 2 actual first-class records were correctly classified and all 3 actual third-class records were correctly classified owing to an accuracy of 100.0%.

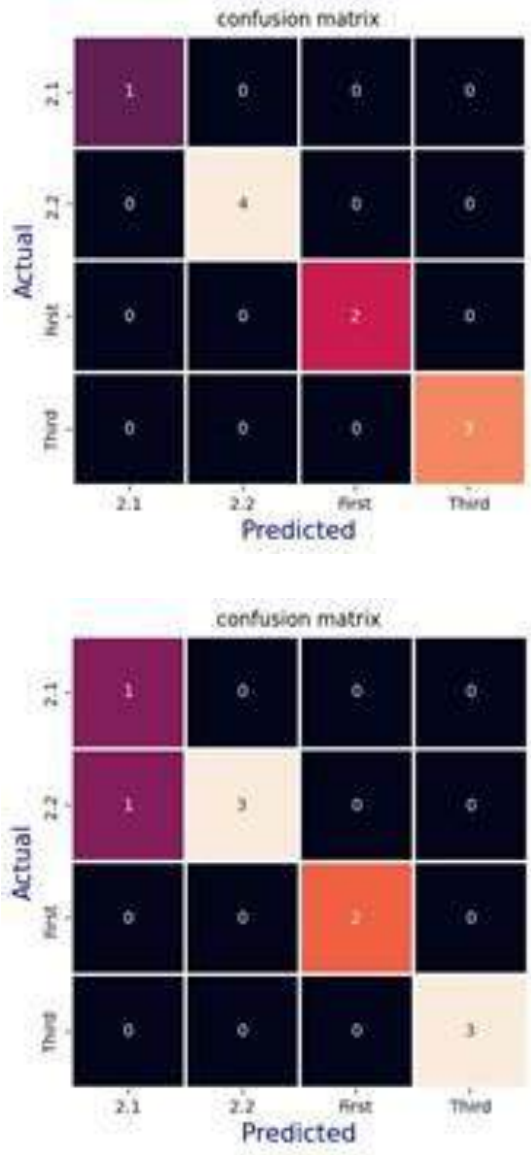

Figure 5: Confusion matrices for the evaluation of support vector machines (left) and decision trees (right) for simulation 5.

Table 3: Results of the evaluation of the predictive models across five simulations based on performance metrics.

Simulation#	Algorithm	Correct Records	Accuracy (%)	Precision				Recall				F1-Score			
				2.1	2.2	First	Third	2.1	2.2	First	Third	2.1	2.2	First	Third
Simulation 1															
	SVC	50	100.0	1.00	1.00	1.00	1.00	1.00	1.00	1.00	1.00	1.00	1.00	1.00	1.00
	DT	44	88.0	0.80	0.91	0.89	0.93	0.80	0.83	0.89	1.00	0.80	0.87	0.89	0.97
Simulation 2															
	SVC	40	100.0	1.00	1.00	1.00	1.00	1.00	1.00	1.00	1.00	1.00	1.00	1.00	1.00
	DT	32	80.0	0.70	0.64	1.00	0.91	0.64	1.00	0.73	0.91	0.67	0.78	0.84	0.91
Simulation 3															
	SVC	30	100.0	1.00	1.00	1.00	1.00	1.00	1.00	1.00	1.00	1.00	1.00	1.00	1.00
	DT	25	80.0	0.75	0.78	1.00	0.78	0.50	0.88	0.89	1.00	0.60	0.82	0.94	0.88
Simulation 4															
	SVC	20	100.0	1.00	1.00	1.00	1.00	1.00	1.00	1.00	1.00	1.00	1.00	1.00	1.00
	DT	18	90.0	0.80	0.83	1.00	1.00	0.80	0.83	1.00	1.00	0.80	0.83	1.00	1.00
Simulation 5															
	SVC	10	100.0	1.00	1.00	1.00	1.00	1.00	1.00	1.00	1.00	1.00	1.00	1.00	1.00
	DT	9	90.0	0.50	1.00	1.00	1.00	1.00	0.75	1.00	1.00	0.67	0.86	1.00	1.00

4.0 Conclusion

The study examined the factors and features to be considered while predicting the academic performance of students, also the study examined the performance of two machine learning algorithms: Support Vector Machine and Decision Tree, in classification and predicting the performance of students. The datasets were obtained from the Department of Computer Science Tai Solarin University of Education. The model simulation was conducted by splitting the dataset into two parts, train and test dataset using five simulations such that 50/50, 60/40, 70/30, 80/20 and 90/10 percent of the dataset was adopted for training/testing the predictive model. The study concluded that machine learning models are very effective in the classification of the academic performance of students, especially the Support Vector classifiers that out-performed the Decision Tree with 100% accuracy.

5.0 Recommendation

This study recommends that future study should be performed in order to determine the impact of feature importance on the performance of machine learning algorithms adopted for the classification of academic performance among students. Also, there is a need to consider the use of a dataset which a larger dimension and size in order to be able to explore more deeply other underlying factors that may influence the classification of the academic performance of students. Future work can be focused on the development of an information system which can integrate the functionality of the predictive model for providing decision support especially in areas where there is a lack of academic experts.

References

Albreiki, B., Zaki, N., & Alashwal, H. (2021). A Systematic Review of Student's Performance Prediction using Machine Learning Techniques. *Education Sciences*, *11*(9), 1-12.

Baashar, Y., Hamed, Y., Alkawsi, G., Capretz, L., Alhussian, H., Alwadain, A., & Al-Amri, R. (2022). Evaluation of Postgraduate Academic Performance using Artificial Intelligence Models. *Alexandria University Journal*, *61*, 9867-9878.

Deda, E., Pacukaj, E., & Vardari, L. (2021). Education and Its role in the Economic Development of the COuntry and Government Policies to be undertaken to Increasethe Quality of Education: The Case of Albania. *Journal of Educational and Social Research*, *11*(1), 188-199.

Hussain, S., & Khan, M. (2023). Student-Performulator: Predicting Students' Academic Performance at Secondary and Intermediate Level using Machine Learning. *Annals of Data Science*, *10*(3), 637-655.

Karalar, H., Kapucu, C., & Gürüler, H. (2021). Predicting Students at Risk of Academic Failure using EnsembleModel during Pandemic in a Distance Learning System. *International Journal of Educational Technology in Higher Education*, *18*(1), 1-13.

Kumar, M., & Salal, Y. (2019). Systematic Review of predicting Student' s Perfomance in Academics. *International Journal of Engineering and Advanced Technology*, *8*(3), 54-61.

Owosu-Boadu, B., Nti, I., Nyarko-Boateng, O., Aning, J., & Boafo, V. (2021). Academic Performance MOdelling with Machine Learning based on Cognitive and Non-Cognitive Features. *Applied Computer Systems*, *26*(2), 122-131.

Ramaswami, G., Susnjak, T., Mathrani, A., Lim, J., & Garcia, P. (2019).

Using Educational Data Mining Techniques to increase the Prediction Accuracy of Student Academic Performance. *Information and Learning Science, 120*, 451-467.

Romero, C., & Ventura, S. (2020). Educational Data Mining and Learning Analytics: An Updated Survey. *Wiley Interdisciplinary Reviws: Data Mining and Knowledge Discovery, 10*(3), 1-21.

Yağcı, M. (2022). Educational Data Mining: Prediction of Students' Academic Performance using Machine Learning Algorithms. *Smart Learning Environments, 9*(11), 1-19

Pore density in the benthic foraminifer *Bolivina spissa* (Cushman) from the Bering Sea: a realistic test of seabed oxygen conditions?

ATURAMU Adeyinka Oluyemi,
Department of Geology, Ekiti State University,
P.M.B 5363, Ado-Ekiti, Ekiti State, Nigeria.
adeyinka.aturamu@eksu.edu.ng

Abstract

Recent studies have reported a link between foraminiferal shell pore density (PD) and bottom water dissolved oxygen levels (BW-O_2), asserting that oxygen concentrations in bottom waters can be quantitatively reconstructed at low oxygen levels. We assess this relationship for the calcareous benthic foraminifer Bolivina spissa (Cushman), by comparing its PD with interpreted sea bottom-water BW-O_2 from six horizons in the Quaternary section of IODP Site U1342, Bowers Ridge, Bering Sea. The BW-O_2 is estimated by a combination of benthic foraminiferal faunas (deep infaunal group %), and the presence of sediment laminations, thought to indicate dysoxia/anoxia. B. spissa shows PDs spanning 0.0013 - 0.0104 P/µm^2, but there is no apparent correlation between PD and interpreted BW-O_2. Thus, assuming it is bottom water oxygen concentrations that are primarily driving both faunal assemblages and the development of laminations, changes in bottom water oxygen levels may not be the primary or sole driver of PD for B. spissa at this site: other environmental parameters, including bottom-water nitrate concentration (BW-NO_3^-) may have influenced B. spissa PD, and/or PD might be recording sediment pore water oxygen concentration (PW-O_2). Alternatively, both the lifestyle of B. spissa, and/or the potential time-averaging of the samples, may have obscured any primary signal. This analysis cautions the use of B. spissa PD analysis for determining BW-O_2 where sedimentological or accompanying palaeontological data are unclear, or where precise sampling is impossible.

Keywords: Bolivina spissa, Pore density, infaunal species, bottom water, laminated, bioturbated

1. Introduction

Lutze (1986) emphasised the usefulness of pore density (PD) and pore size as diagnostic features for the identification of several species of foraminifera; however, only few publications (e.g. Finlay 1983; Glock et al. 2011; Moodley and Hess 1992; Kuhnt et al. 2013) have discussed the functionality of these pores, and examined whether they are important for the survival of benthic foraminifera in their microhabitat. Earlier publications examined the microstructure of the pores, which are

often covered by sieve-like micro porous organic plates (Arnold 1954a, 1954b), or by one or more organic layers (Sliter 1974 ; Berthold 1976 ; Leutenegger 1977). Though several terms have been given to these pores, including “pore diaphragms”, “sieve plates”, “pore plugs”, “dark discs”, and “pore plates”, only a few studies have investigated their ability to enable dissolved materials to pass into the cytoplasm of foraminiferal cells. The pores may function to promote the uptake of oxygen and in return release CO_2 as a by-product of respiration (Berthold 1976; Leutenegger 1977). It has also been demonstrated that certain benthic foraminifera (e.g. *Bolivina pacifica*) that are tolerant of low oxygen, have their cell mitochondria more abundant near the pores, relative to those species that occupy relatively well-oxygenated waters. This suggests a relationshipbetween pores, mitochondriaandrespiration (Leutenegger 1977; Sen Gupta and Machain-Castella 1993). Bernhard and Alve (1996) showed that in some of these benthic species, mitochondria move through the cytoplasm and pseudopodia, and were concentrated in the apertural cytoplasm.

Overall morphological characteristics of the benthic foraminiferal test have also been suggested to relate to varying oxygen levels in seawater (Rathburn and Corliss 1994; Kaiho 1994): these include: changes in test size of individual species (Sen Gupta and Machain-Castillo 1993; Kaiho 1994); and intra-species changes in test morphology such as pore density and ornamentation (Perez-Cruz and Machain-Castella 1990; Glock et al. 2011; Kuhnt et al. 2013). Morphological and abundance reactions of benthic foraminifera to their immediate environment are extensively used as proxies for palaeoceanographic and palaeoecological reconstructions, involving assessments of organic flux to the sea bed (e.g. Lutze 1980; Lutze and Coulbourn 1984; Lutze et al. 1986; Caralp 1984, 1989; Carney 1989; Jorissen et al. 1992; Gooday 1993; Kaiho, 1999; Den Dulk et al. 2000; Fontanier et al. 2002, 2006) or oxygen-level (e.g. Kaiho 1991, 1994, 1999b; Den Dulk et al. 2000, Glock et al. 2011, Kuhnt et al. 2013). Sea floor oxygenation depends mainly on factors that include the original dissolved oxygen-level, and the amount and quality of organic matter available at the seafloor (Jorissen et al. 1995: TROX model fig. 3.2). Because of the difficulties in differentiating changes in oxygenation and organic matter influx to the sea floor, Kuhnt et al. (2013) considered it difficult to use assemblage data alone to decide on changes in water-mass oxygen content or organic influx to the sea floor; this remain a challenging area of foraminiferal studies. It has been suggested that in oxygen- depleted habitats, low metabolic rates decrease the secretion of calcite by benthic foraminifera, thereby

resulting in the production of thinner, less-ornamented and more-porous tests (Kaiho 1994; Bernhard 1986; Rhoads and Morse 1971). This pattern seems to indicate that species of benthic foraminifera from oxygen depleted or oxygen deficient habitats should show moderately high porosity, pore-densities and larger pore-sizes, which set these benthic foraminifera aside as low-oxygen indicators based on their morphology.

In a more recent effort to unravel environmental influences on the pore density of *Bolivina spissa* (Cushman), including water-depth, temperature, bottom-water oxygen and nitrate concentrations, Glock et al. (2011) suggested that the pores in the test of *B. spissa* reflect intracellular nitrate respiration, and that *B. spissa* switches from oxygen to nitrate respiration when oxygen concentrations are depleted. The ability to store nitrate inside the cells and to switch to nitrate respiration in times when less or no oxygen is available has been documented for several benthic foraminiferal species (Risgaard-Petersen et al. 2006; Høgslund et al. 2008; Glud et al. 2009; Piña-Ochoa et al. 2010). All these investigations point to the possibility of using PD and pore size as proxies for changes in bottom water oxygenation (Kender. et al., 2019)

In a laboratory investigation, Moodley and Hess (1992) demonstrated that *Ammonia becarri* (Linné) shows an increase in pore-size and higher porosity on the chambers formed under low oxygen (dysoxic) conditions, possibly as a coping strategy to decreased oxygen (Corliss 1985). Leutenegger and Hansen (1979) observed that concentrations of mitochondria below the inner pore entrances in benthic foraminifera point to a pore function related to respiration (gas exchange). A more recent study on the relationship between PD in benthic foraminifera and bottom-water oxygen content by Kuhnt et al. (2013) on *Bolivina pacifica* and *Fursenkonia mexicana* (both deep infaunal species) shows an inverse correlation between PD and bottom water oxygen content, which suggest that both species may have increased their pore numbers to improve the ability of oxygen uptake in dysoxic environments or intervals. In this study, changes in the PD of the test on the same benthic foraminifer species (*B. spissa*) were compared downcore, across an interpreted varying oxygen gradient (BW-O_2, based on other proxies) to see how interpreted BW-O_2 influences the PD.

This study examines *B. spissa* from 6 horizons determined to indicate different BW-O_2 based on sedimentary characteristics (laminated and non-laminated intervals) and faunal assemblages. It tests the veracity of the PD method in *B. spissa* as a means of estimating bottom-water oxygen concentration (BW-O_2).

1.1 Infaunal foraminifer preference for low oxygen conditions

Studies on sedimentary basins with low-oxygen bottom water off the California coast (Phleger and Soutar 1973; Douglas and Heitman 1979) and on sapropels from the Mediterranean Sea (Parker 1958), were amongst the first studies that recognised that ancient, as well as recent, low oxygen environments were inhabited by specific benthic foraminiferal assemblages. Deep- sea benthic foraminifera tend to live across a depth gradient, from 1 to 10 cm, where oxygen becomes increasingly deficient from the surface downwards (Jorissen et al. 2007). The Trophic Oxygen (TROX: fig. 1.2) model of Jorissen et al. (1995) explains the benthic foraminiferal living depth in terms of availability of food and oxygen concentration. The depth in the sediment down to which organisms can live is determined by oxygen availability, and in the presence of oxygen, the vertical distribution of organisms is controlled by food availability (Jorissen et al., 1995).

Abundant foraminifera have been reported from low-oxygen environments (Schumacher et al. 2007, Sen Gupta and Machain-Castillo 1993, Douglas and Heitman, 1979, Phleger and Soutar 1973, Smith 1964b); these have a characteristic taxonomic composition, and are dominated by *bolivinids*, *buliminids*, *globobuliminids* and some other taxa when oxygen concentration falls below 1ml/l (Bernhard 1986; Sen Gupta and Machain-Castillo 1993; Bernhard and Sen Gupta 1999). Differences in dissolved oxygen concentrations and organic carbon supply at the sediment-water interface play a major role in the control of deep sea benthic foraminiferal assemblages and their morphological characteristics as reflected in benthic foraminiferal test size, thickness and porosity (e.g. Kaiho 1994; Thomas and Gooday 1996; Kuhnt et al. 2013). Many elongated, commonly biserial or triserial taxa, have been described as being abundant at very low oxygen concentrations; it has been suggested that their morphology also corresponds to an infaunal microhabitat (Corliss and Chen 1988; Corliss and Fois 1990; Corliss 1991), although this is not always supported (Jorissen et al. 2007).

Two groups of taxa with different life strategies have been shown to evolve after the disappearance of less resistant taxa at low bottom-water oxygen concentrations: the deep infaunal taxa, at the onset of low-oxygen conditions in bottom water, migrate from the deeper sediment layers to the sediment surface (Jorissen 1999); whilst the epifaunal or shallow infaunal taxa that have inherent tolerance for low-oxygen conditions (Jorissen 2007), then become established at the seabed. No foraminiferal species appear to be adapted exclusively to low-oxygen conditions (Sen Gupta and Machain-Castillo 1993); according to Murray

(2001), foraminifera generally only start to become impacted by oxygen levels when concentration values of dissolvedoxygenfall below approximately 1 ml/l: above these levels, there will be no correlation between oxygen and the composition of the faunas. Often, a few taxa are considered indicative of low-oxygen conditions; the relative abundance and test morphology of such species and their relative abundance in the entire calcareous fauna were expressed as a percentage of the total benthic foraminiferal fauna and is used as a semi-quantitative indication of bottom water oxygenation (Jorissen et al. 2007; Schumacher et al. 2007)

Expedition 323 Scientists (2011) reported that laminated intervals at Bowers Ridge, Bering Sea, are possibly indicative of the local depth of the oxygen minimum zone (Kender et al., 2019), which reduced the effects of infaunal burrowing and bioturbation. At Site U1342, ~71 to 100% infaunal species were recorded at horizons that correlate closely with laminated sedimentary intervals. This is in line with Jorissen et al. (1995), who suggested that deep infaunal taxa often considered indicative of low-oxygen conditions, are only present when the organic flux is significantly high (giving rise to the dark coloration that is associated with laminated intervals). The flux of organic material is respired by organisms at the sea bed, and this leads to a decrease in dissolved oxygen in the ambient waters (Jorissen et al. 1995).

In summary, oxygen concentrations are thought to have a direct influence on the faunal composition only in areas where bottom water concentrations become so low (less than or equal to 1 ml/l; Murray, 2001) that this causes reduced competitive ability and/or reproductive ability of taxa in the environment. In such cases, taxa less resistant to reduced oxygen disappear, giving room for deep infaunal taxa and denitrifiers to rise to the surface, as these are well adapted to low oxygen conditions (Jorissen, 1999). In this study, we use the percentage deep infaunal taxa to the entire assemblage as a semi-quantitative proxy for BW-O_2. Although the dominance of this group (e.g. above ~70%: Schumacher et al. 2007) is thought to be a response to oxygen levels below 1 ml/l, there is as yet no known direct way of calculating dissolve oxygen level from infaunal percentage alone.

1.2 Materials and methods

Bolivina spissa were analysed from core sediments recovered by IODP Expedition 323 (Expedition 323 Scientists 2009), at ~ 818 m water depth from Site U1342 on the Bowers Ridge, Bering Sea (fig. 1). Sediments from the depth interval between 0 and 11.13 m were analysed. On Bowers Ridge, an average sedimentation rate of 4.5 cm/kyr is documented (Expedition 323 Scientists 2011). Sediments from this site comprise predominantly biogenic

(mainly diatom frustules with varying proportions of calcareous nannofossils, foraminifers, silicoflagellates, and radiolarians), siliciclastics (mainly silt and very fine sand, and also isolated clasts of pebble to cobble size), and volcaniclastic (mainly fine ash) material. The most prominent sedimentary features are decimetre to metre-scale bedded alternations of sediments, together with variation in colour and texture. Sediments from Site U1342 are generally bioturbated; fine-scale lamination, preserved alternations between millimetre-scale laminae of biogenic and terrigenous material are also present (Expedition 323 Scientists 2009). In general, the colour of the sediment ranges from very dark greenish grey and dark grey, to biogenic-rich olive grey to olive, with dark grey to black or shades of light grey, to white ash layers (Expedition 323 Scientists 2011). Samples used for this study were collected from the Kochi Core Centre, Japan in 2010, and were processed (freeze-dried and wet-sieved over 62-µm to liberate the microfossils) in Prof. Christina Ravelo's laboratory at the University of California, Santa Cruz.

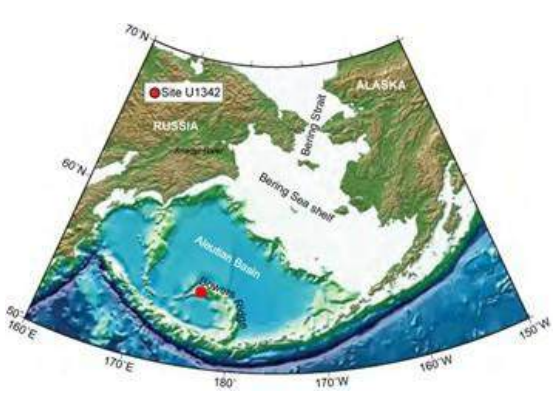

Figure 1. Bathymetric map of the Bering Sea, with the marked location of Site U1342 (red dot) on the Bowers Ridge, Southern Bering Sea (adapted from Expedition 323 Scientists 2011), is the source of *Bolivina spissa* specimens used in this study.

Subdivision of benthic foraminifera into microhabitat and oxygen indicator groups (Table 1), carried out in accordance with the study on variations of the OMZ of the Okhotsk Sea of Bubenshchikova (2010) and other studies (Kaiho 1994; Jorissen et al. 2007; Glock et al. 2011), would suggest that *B. spissa* is tolerant of dysoxic waters (typical of 0.1 to 0.3 ml/l of dissolved oxygen in seawater) and is deep infaunal. This classification also places *Bolivina pacifica* and *Fursenkonia mexicana* (also used in the study by Kuhnt et al. 2013), as dysoxic and deep infaunal species. *B. spissa* has been shown to be very tolerant to variations in oxygen concentration (Bernard et al. 2001), and can survive in anoxic waters (Bernhard and Bowser 2008); this makes *B. spissa* a suitable candidate for this study of PD versus variable BW-O_2.

Table 1. Core U1342 benthic foraminifer's microhabitat preference and characteristics in accordance with consistent groupings in some selected studies (Corliss and Chen 1988; Gooday 1988; Thiel et al. 1989; Corliss 1991; Steinsund et al. 1994a, 1994b; Kitazato and Ohga 1995; Licari et al. 2003; Risgaard-Petersen et al. 2006; Høgslund et al. 2008; Ivanova et al. 2008; Bubenshchikova et al. 2008; Alve 2010 Glock 2011).

Benthic foraminifera species microhabitat group (from previous studies)							
Benthic foraminifera fauna recorded from Core 1342 (~20.60 m-ccsf)	Deep infauna (Dysoxic): >4 to 10 cm below sea-sediment interface	Intermediate infauna (Suboxic): ~1 to 4 cm below sea-sediment interface	Shallow infauna (Suboxic): 0-2 cm below sea-sediment interface	Epifauna (Oxic): 0-1 cm	Phytodetritivores	Denitrifiers	Unassigned
Alabaminella weddellensis				X	X		
Angulogerina angulosa							X
Bolivina sp. 1	X						
Bolivina sp. 2	X						
Bolivina sp. 3	X						
Bolivina spissa	X	X				X	
Brizalina alata	X						
Brizalina earlandi	X						
Bulimina exilis	X						
Bulimina	X	X	X				
Cassidulina				X	X		
Cassidulina reniforme			X				
Cassidulina teretis				X			
Cassidulinoides parkerianus							X
Cibicidoides sp.			X	X			
Cushmanina striatopunctata							X
Dentalina irr.							X
Eggerella sp. 1			X				
Ehrenbergina var. *compressa*							X
Elphidium sp. 1			X				
Elphidium sp. 2			X				
Elphidium sp. 3			X				
Elphidium			X				
Epistominella				X	X		
Epistominella pulchella							X
Fissurina crebra			X				
Fissurina minima			X				
Fursenkoina aff. *texturata*	X					X	
Globobulimina auriculata	X						
Globobulimina pacifica	X						
Globocassidulina subglobosa		X	X	X	X		
Gyroidina sp. 1							X
Gyroidina sp. 2							X
Hoeglundina Islandiella			X	X	X		

Benthic foraminifera species microhabitat group (from previous studies)							
Benthic foraminifera fauna recorded from Core 1342 (~20.60 m-ccsf)	Deep infauna (Dysoxic): >4 to 10 cm below sea-sediment interface	Intermediate infauna (Suboxic): ~1 to 4 cm below sea-sediment interface	Shallow infauna (Suboxic): 0-2 cm below sea-sediment interface	Epifauna (Oxic): 0-1 cm	Phytodetritivores	Denitrifiers	Unassigned
Alabaminella weddellensis				X	X		
Angulogerina angulosa							X
Bolivina sp. 1	X						
Bolivina sp. 2	X						
Bolivina sp. 3	X						
Bolivina spissa	X	X				X	
Brizalina alata	X						
Brizalina earlandi	X						
Bulimina exilis	X						
Bulimina	X	X	X				
Cassidulina				X	X		
Cassidulina reniforme			X				
Cassidulina teretis				X			
Cassidulinoides parkerianus							X
Cibicidoides sp.			X	X			
Cushmanina striatopunctata							X
Dentalina ittai.							X
Eggerella sp. 1			X				
Ehrenbergina var. *compressa*							X
Elphidium sp. 1			X				
Elphidium sp. 2			X				
Elphidium sp. 3			X				
Elphidium			X				
Epistominella				X	X		
Epistominella pulchella							X
Fissurina crebra			X				
Fissurina minima			X				
Fursenkoina aff. *texturata*	X					X	
Globobulimina auriculata	X						
Globobulimina pacifica	X						
Globocassidulina subglobosa		X	X	X	X		
Gyroidina sp. 1							X
Gyroidina sp. 2							X
Hoeglundina				X			
Islandiella			X		X		

The qualitative method used to infer oxygenation from assemblages in this study is based on the Kaiho (1994) ecological groupings and the Jorissen et al. (1995) conceptual model for BW-O_2. Unlike Kaiho (1994), we use the relative abundance of deep infaunal foraminifera expressed as a percentage of the total benthic foraminiferal fauna in the samples, and these values are used as a qualitative measure of BW-O_2 at various depths (Table 2). This is because the Kaiho (1994) oxygen index (the calculation to convert faunas to oxygen) has received some criticism (Murray, 2001, Jorissen et al. 2007). According to the TROX-model (Trophic-Oxygen-Microhabitat-Reaction) of Jorissen et al. (1995), foraminiferal microhabitat in oligotrophic ecosystems is limited by availability of food particles within the sediment, whereas in eutrophic systems, a critical oxygen level decides to what depth in the sediment most of the species can live. In mesotrophic areas, microhabitat depth is of maximum importance (fig. 2). The more organic carbon influx into the water column leads to more carbon in the deep infauna; this invariably lowers the dissolved oxygen content of the pore water due to respiration. However, the main distinction in microhabitat characteristics is that between epifaunal and infaunal organisms (Jorissen et al. 1995).

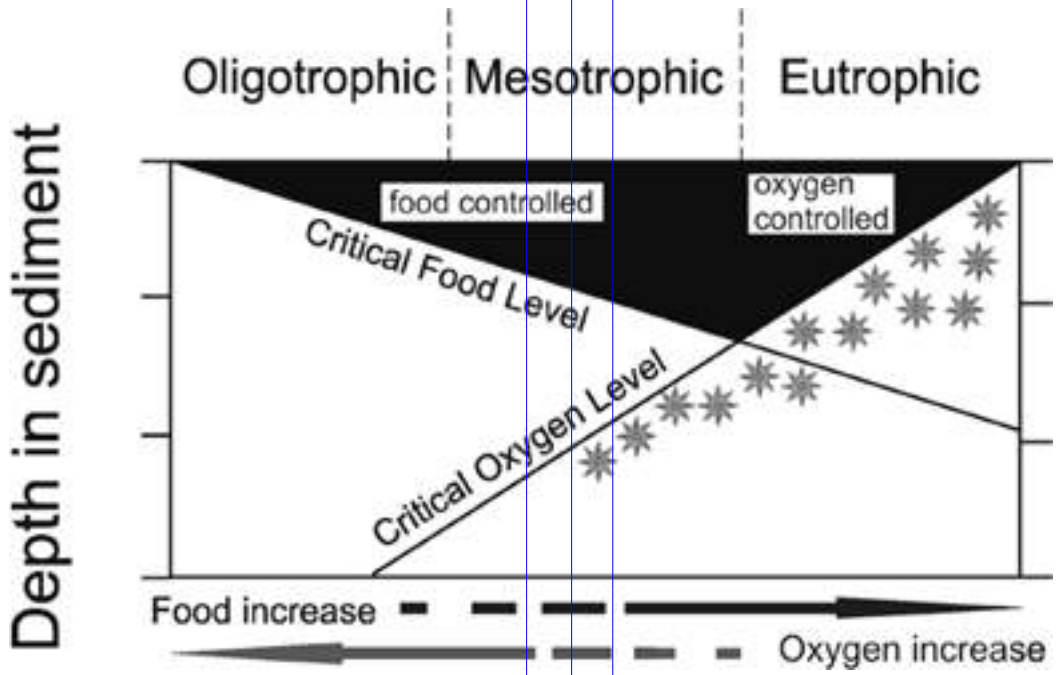

Figure 2. TROX (Trophic Oxygen)-model explaining the benthic foraminiferal living depth (shaded area) in terms of availability of food and oxygen concentration (after Jorissen et al. 1995).

Among the deep infaunal benthic foraminifera species recorded at Site U1342 are *Globobulimina* spp., *Bulimina exilis*, *Fursenkoina* aff. *texturata*, *Bolivina spissa*, *Brizalina alata* and *Brizalina earlandi*. Oxygen levels were qualitatively estimated from the percentage abundance of deep infaunal species against the total percentage abundance of faunas at various depths, by assigning benthic foraminiferal species into groups following Kaiho's (1994), and their microhabitats in accordance with the regional faunal study of Bubenshchikova (2008) where species occur. Where species do not occur, the living depth was assigned based on morphologically similar species. As an independent measure of oxygenation, sedimentary layers with bioturbation are considered to represent higher concentrations of oxygen in bottom waters (depending on the degree of bioturbation involved), as benthic invertebrates invade sediment laminae in aerobic conditions (Kaiho 1991). Expedition 323 Scientists (2011) suggest that stratigraphic intervals where there is lamination are possibly indicative of the local depth of the OMZ; relatively high percentages of infaunal species (shallow and deep infaunal) recorded at these depths further suggest that the laminated intervals are associated with low oxygen horizons.

Sampling Procedure

All *B. spissa* specimens were targeted from each of the 24 samples (i.e from six horizons) at different depths analysed down the studied interval. On Bowers Ridge, an average sedimentation rate of 4.5 cm/kyr is documented (Expedition 323 Scientists, 2011), this suggests a deposition rate of 2 cm per ~444 years (narrowest thickness where specimens were taken for this study: Table 2). A total of 227 *Bolivina spissa* (Cushman) specimens were picked from some depths within the 11.15 metres of core sampled for this study; out of which 121 megalospheric specimens (from sexual reproduction) were analysed. Due to the different morphologies in the test of megalospheric and microspheric specimens of *B. spissa*, there is a considerable difference in the PD between the sexually and asexually produced forms: the megalospheric specimens consistently show increasing PD from earlier to later chambers, and therefore this parameter can be more readily quantified in these forms (Glock et al. 2011).

The megalopsheric specimens equate to ~53% of the total *B. spissa* from the studied interval (0 to 11.15 m). These specimens are sourced from 24 samples at different depths. The sampling strategy was influenced by the occurrence and paucity of *B. spissa* in the 11.15 metres of core sampled. Geological samples used for paleoceanographic reconstructions are always time-averaged, relatively low resolution, and contain a mixture of faunas that inhabited the site during

(possibly) several decades or longer. Such samples will not always capture precise fluctuations in O_2-levels at the sea bed. In order to make best use of the number of specimens studied and to negate some of the effects of time averaging, in most cases several samples (in succession) are grouped into a composite interval where the sedimentological and paleontological signature of that interval indicates a consistent environment (low oxygen versus more oxygenated levels; Table 2).

The total percentage of deep infaunal species (based on the morphology criteria of Kaiho 1994, and oxygen-related benthic foraminiferal groups according to the classification of Bubenshchikova 2008) in the sediment at sampled depths has been used as the primary proxy for BW-O_2 conditions. Percentage abundance of deep infauna at various intervals was calculated following this strategy. The 24 samples with *B. spissa* were grouped into 6 defined intervals (Table 2).

1) Sourced from a 2 cm interval beginning at depth 0.00 m, and representing unlaminated sediment characterised by a benthic fauna interpreted to signal low oxygen (*viz* 44.56% deep infauna).

2) Sourced from a 2 cm interval beginning at 0.25 m, and representing laminated sediment characterised by a benthic fauna thought to signal dysoxia (*viz* 78.77% deep infauna).

3) Sourced between 0.38-2.42 m, an interval from which 16 samples have been assessed, all of these representing unlaminated sediments with a benthic fauna that consistently signal well-oxygenated conditions (*viz* 1.50 % to 7.60 % deep infauna); only 6 of these samples where *B. spissa* is present were analysed, each sample varying from between 2 to 4 cm thickness of sediment.

4) Sourced between 2.54-2.69 m, comprising 2 samples within an unlaminated interval with a benthic fauna that signals consistently well-oxygenated conditions (*viz* 25.30% to 26.30 % deep infauna), each about 4 cm thick.

5) Sourced between 3.88-8.36 m, an interval from which 38 samples have been examined and representing an unlaminated interval with a benthic fauna that signals consistently well-oxygenated conditions (*viz* 0.70% to 15.50 % deep infauna). Here, 12 of the samples (where there are >1 *B. spissa* specimen) from this interval were analysed for *B. spissa*, each sample varying between 2 to 3 cm thickness of sediment.

6) Sourced from the lowermost interval between 10.98-11.15 m, and comprising of 2 samples, 2 and 4 cm thick respectively. This represents an unlaminated interval with a benthic

fauna that signals consistently dysoxic conditions (*viz* 55.20% to 95.50 % deep infauna).

Foraminiferal fragmentation through the 6 intervals was determined by quantifying the ratio of broken and/or dissolved specimens (fragments) to the ratio of whole specimens (not broken) of benthic foraminifera at each of the intervals (Appendix 5). Percentages of fragmentations were then determined from the values. The degree of fragmentation has been used as a qualitative proxy for dissolution (Metzler et al. 1982; Thunell 1976; Berger 1970).

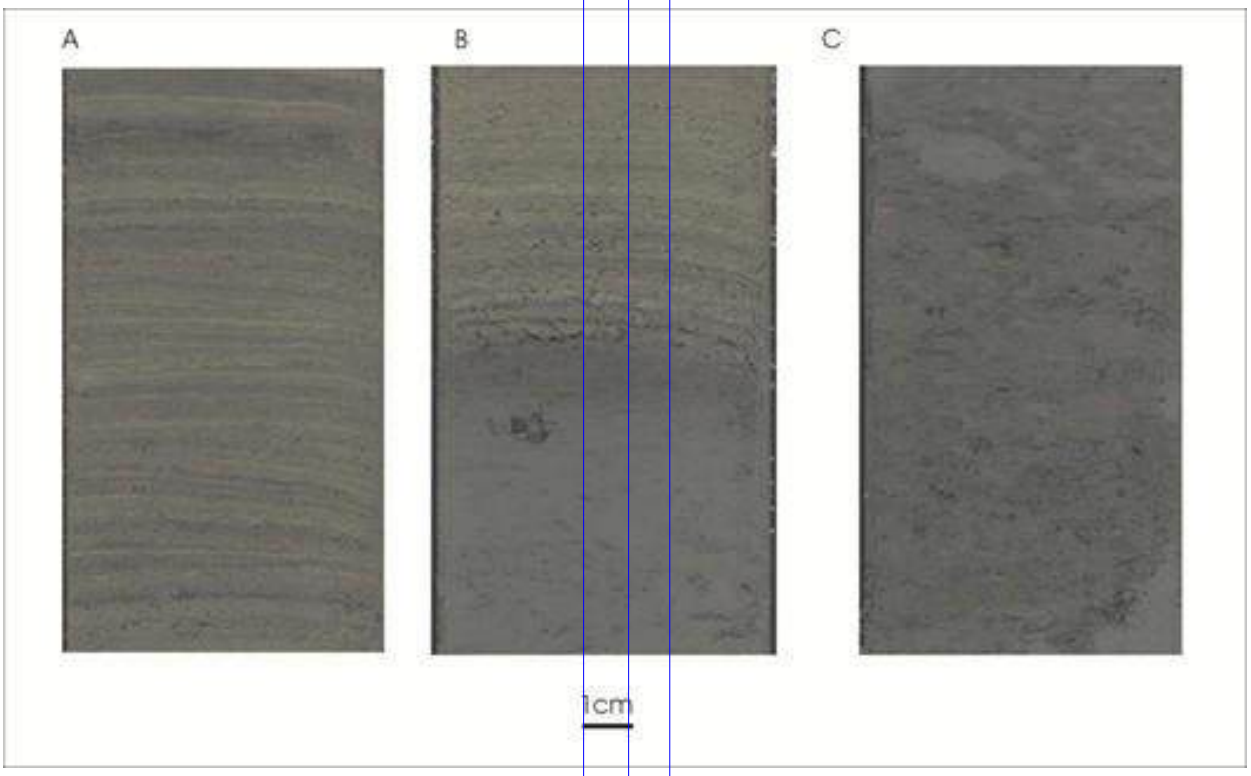

Figure 3 Representative, intervals from the upper 11.13 m of the core at IODP Site U1342, Bering Sea. Laminated, organic-rich intervals ('A': taken from 0.25 m depth) are considered to signify low-oxygen bottom conditions and are typically associated with benthic foraminiferal assemblages that have a deep infaunal signature. Bioturbated levels ('C': intervals taken from 1.28 m depth) indicate an oxygenated sea bed. 'B' shows the transition between two different sea bed oxygen states (0.29-0.38 m). Scale bar is 1 centimetre.

Table 2. Sample depths and composite intervals (1 to 6) with the associated number of benthic foraminifera and the percentage of deep infauna used as a proxy for BW-O_2 conditions (low oxygen versus more oxygenated levels) at various depths and intervals

Hole	Core	Section	Top depth (cm)	Bottom depth (cm)	Interval serial number	Depth serial number	Total number of *B.spissa* specimens for each depth	Individual sample depths (m)	Thickness (cm) of individual sample	Number of sampled depth / interval	% deep infaunal species (Bubenshchikova, 2008)	Av. % deep infaunal species (%)	Lamination	Well-oxygenated	Total number of *B.spissa* specimens for each interval
D	1H	1	0	2	1	1	20	0.00-0.02	2	1	44.70	44.70	No	No	20
D	1H	1	24	26	2	2	25	0.23-0.25	2	1	78.90	78.90	Yes		25
D	1H	1	39	41	3	3	4	0.38-0.40	2 to 4	6	7.60	4.92	No	Yes	13
D	1H	1	52	56		4	2	0.51- 0.55			2.50				
D	1H	1	89	93		5	2	0.88-0.92			1.50				
D	1H	1	129	133		6	2	1.28-1.32			4.50				
D	1H	2	65	69		7	1	2.14-2.18			4.60				
D	1H	2	89	93		8	2	2.38-2.42			6.00				
D	1H	2	105	109	4	9	3	2.54-2.58	4 and 5	2	25.30	26.05			12
D	1H	2	115	120		10	9	2.64-2.69			26.30				
D	1H	3	89	92	5	11	1	3.88-3.91	2 to 3	12	3.60	8.20			44
D	1H	3	99	101		12	7	3.98-4.00			12.10				
D	1H	3	112	115		13	2	4.11-4.14			10.90				
D	1H	4	25	29		14	1	4.74-4.78			3.60				
D	1H	4	77	79		15	2	5.26-5.28			0.80				
D	1H	4	106	108		16	2	5.55-5.57			1.30				
D	1H	4	115	117		17	5	5.64-5.66			14.40				
A	2H	3	39	42		18	2	5.74-5.77			4.00				
A	2H	3	52	54		19	2	5.87-5.89			8.30				
A	2H	3	61	64		20	3	5.96-5.99			10.30				
A	2H	3	90	92		21	7	6.25-6.27			15.50				
A	2H	4	149	151		22	10	8.34-8.36			0.70				
A	2H	6	113	117	6	23		10.98-11.02	2 and 4	2	95.50	72.47		NO	7
A	2H	6	128	130		24		11.13-11.15			55.20				
Total number of *B. spissa*															121

Specimen preparation

B. spissa specimens were gently cleaned in an ultrasonic bath, mounted on aluminium stubs and coated with gold. Specimens were imaged using a Hitachi S-3600N Scanning Electron Microscope (SEM). Magnifications of up to 700 times have been used to image pore ultrastructure; this enables clear focus, identification, and counting of the pores afterwards. To compensate for charging effects on some of the specimens, the SEM partial vacuum mode was activated. It has been noted that PD increases within a single *B. spissa* test from the early to the later

chambers (Glock et al. 2011) which was also observed here. Therefore, as a way of calibration and uniformity, the first few chambers (up to 10) on *B. spissa* were imaged. PD was quantified for an area of 10,000 µm^2 on one side of each *B. spissa* test within the first ten chambers (i.e. first 5 pairs) from the SEM photographs (Plate 2). PD is expressed as pores per µm^{-2} (P/µm^2) of the area measured.

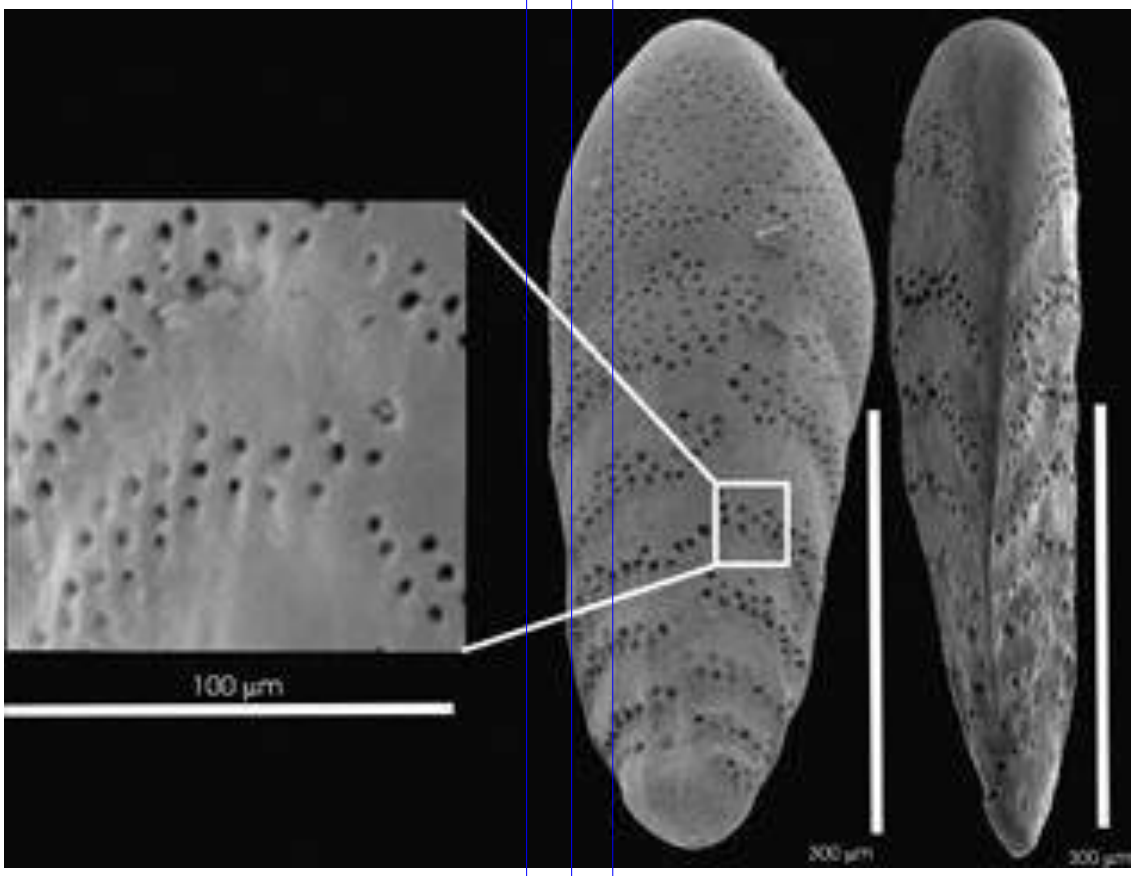

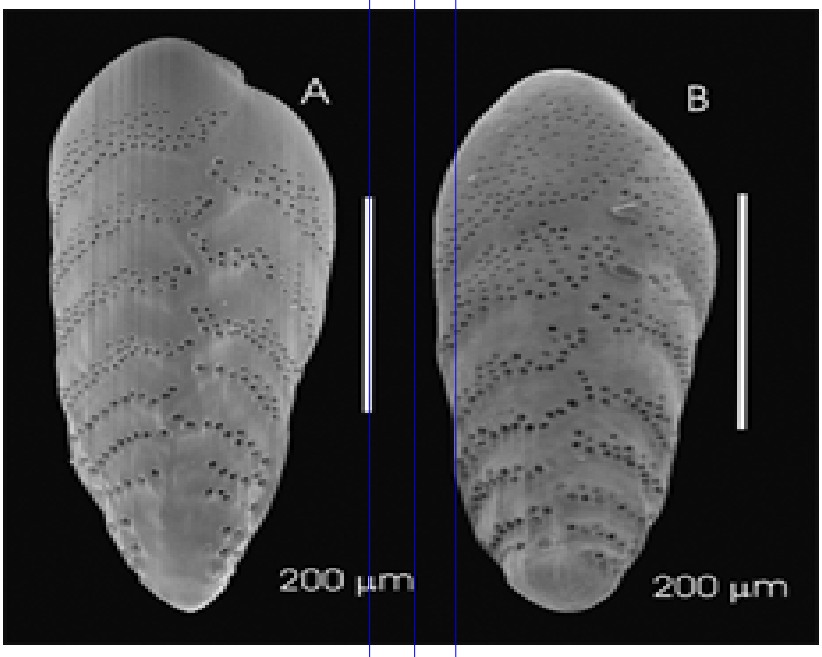

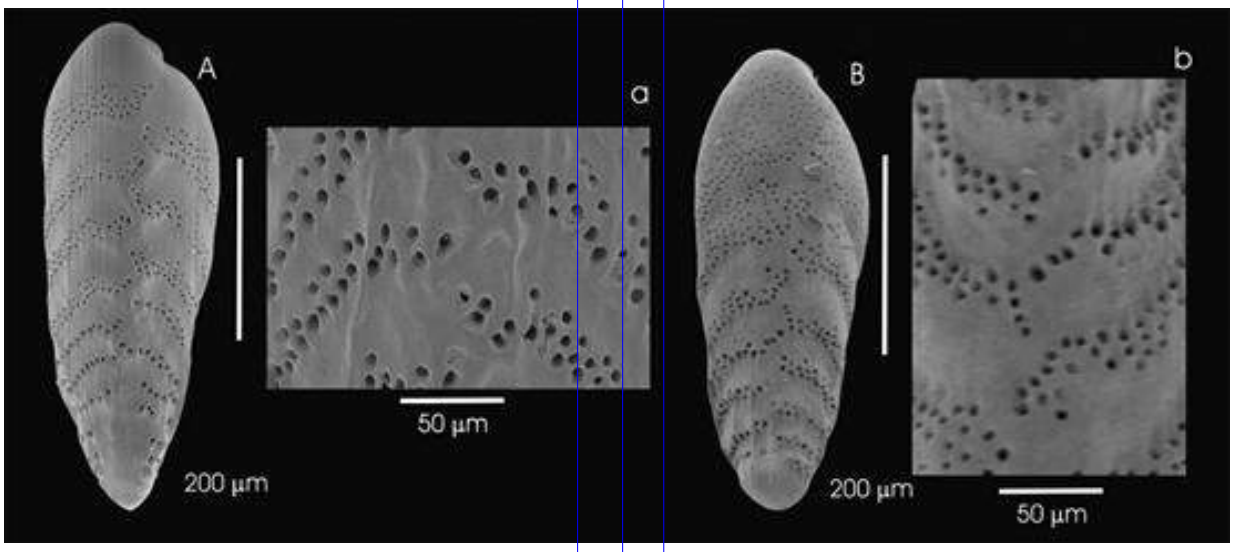

Plate 2 Showing pore density and general morphology of *Bolivina spissa*. **A.** Shows a typical specimen from a laminated sedimentary interval; while **B.** is a specimen from a bioturbated interval. Note the findings in this study indicate there is no significant difference in the PD between specimens from levels interpreted to have different oxygen levels.

Statistical approach

Simple linear-plots (cross-plots) of PD values on *B. spissa* specimens versus percentage deep infauna (as proxy for BW-O_2) as determined from 6 defined intervals, including 3 determined as representing low oxygen (including one laminated interval), and 3 more oxygenated (non-laminated), are used to assess the relationship between PD and BW-O_2 (fig. 4).

Various percentile values of PD on *B. spissa* from these intervals were determined (Table 3). Box and whisker plots have been constructed from the percentile values to quantify the relationship between the PD and the BW-O_2 conditions without making any assumptions of the underlying statistical distributions (fig. 5). Calculated BW-O_2 from the PD of *Bolivina spissa* (after equation in Glock et al. 2011: p. 28, fig. 7 A) versus interpreted BW-O_2 from faunal assemblages was plotted (fig. 6).

3.3 Results

Table 2 summarises the number of specimens yielded from the 6 defined sample intervals, and presents sedimentological and faunal evidence for their interpretation as well-oxygenated or poorly oxygenated intervals.

Pore counts between specimens of *B. spissa* range from 13 to 104 pores per 10,000 µm^2. Calculated mean pore values vary from 0.0045 P/µm^2 to 0.0056 P/µm^2 (Table 3.4: lowest PD = 0.0013 P/µm^2; highest PD = 0.00104 P/µm^2) on the first 10 chambers of all *B. spissa* specimens analysed across the six intervals. Calculations were made to

find the different percentile value of *B. spissa* PD through the sampled intervals (Table 3); box and whisker plots were constructed to statistically and visually analyse the data spread (fig. 3.5). The lowest median PD value being 0.0045 P/µm^2 is recorded from interval 4, showing 26.05 % deep infauna foraminiferal species (2.54-2.64 m). The median PD value of 0.0050 P/µm^2 is recorded from laminated interval 2 (0.25 m: 78.90% deep infaunal species), whilst the highest median PD value of 0.0056 P/µm^2 is recorded from interval 5 (3.88-8.36 m: 3.60% deep infaunal species) indicating an interval with increased oxygenation (Table 3).

Analysis of *B. spissa* PD versus estimated BW-O_2 from various sedimentary horizons at Site U1342 shows no correlation (fig. 4).

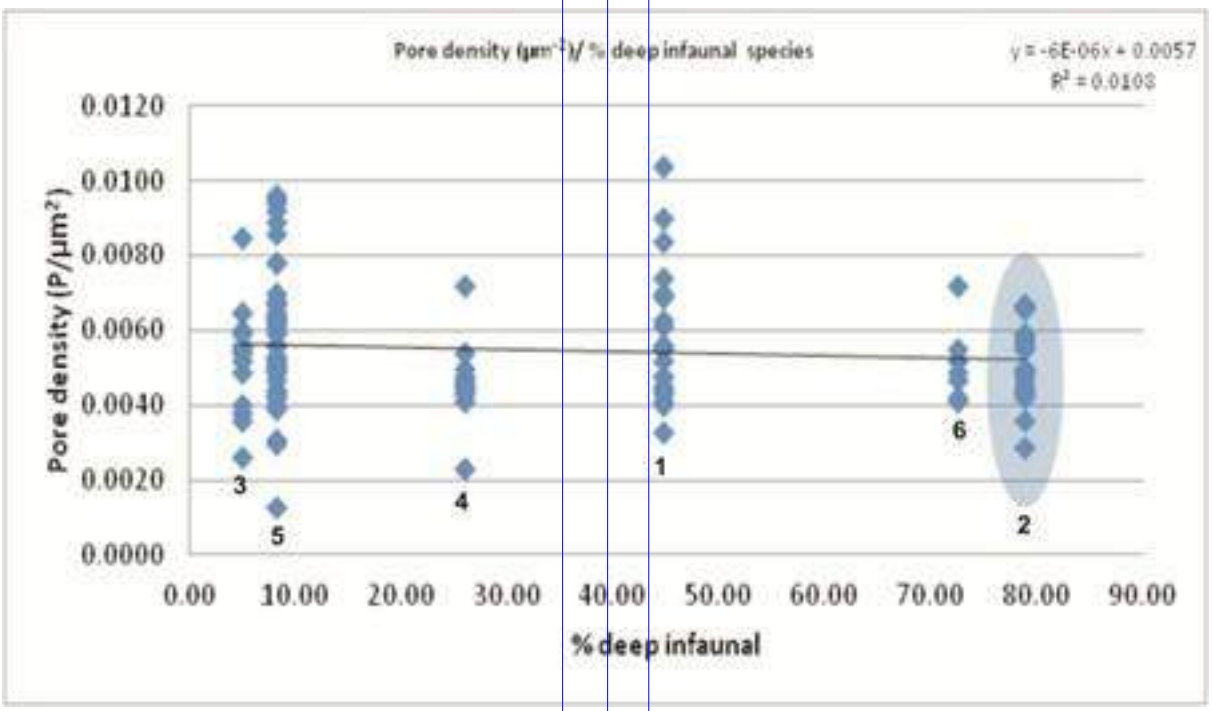

Figure 4. Linear plot of PD (vertical axis) on the test of *B. spissa* specimens from laminated (Interval 2: identified by the oval shape) and non-laminated intervals (1, 3, 4, 5, 6), versus the percentage of deep infaunal foraminifera (horizontal axis, used as a relative proxy of seabed oxygen level, with oxygen level interpreted to be decreasing from left to right in the figure). A total of 121 *B. spissa* specimens were measured down core, being a subset of the total specimens in the samples. Horizontal axis shows the percentage of associated infaunal species at each interval (Bubenshchikova et al. 2008).

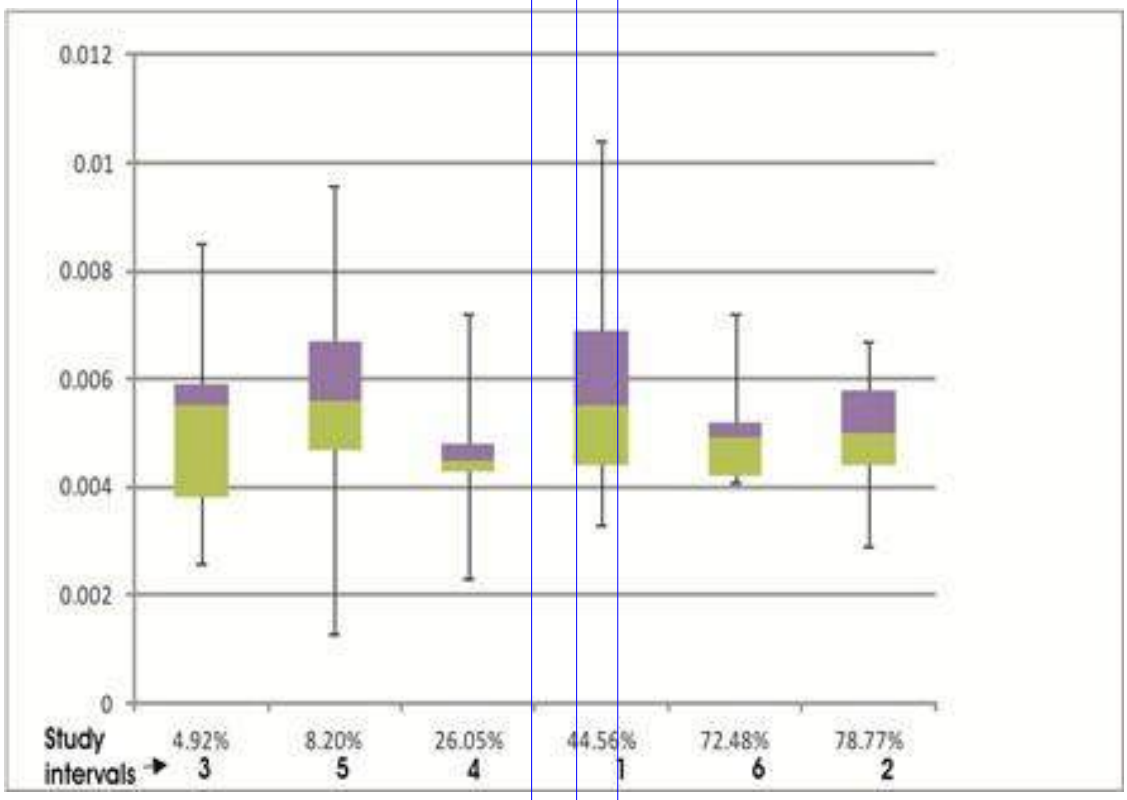

Figure 5 Box and whisker plots (statistically and visually showing the data spread) for PD variation in *B. spissa* from intervals 1 to 6: laminated interval 2 (enclosed in box) and non-laminated intervals (1, 3, 4, 5, and 6). Pore density (P/µm^2) is on the vertical axis; average percentage of deep infaunal foraminifera at each interval (indicating relative oxygen level at such interval) is noted. Green shade: PD range from 25th percentile to 50th (median) percentile; purple shade: PD range from median percentile to 75 percentile.

Analysis of PD data using box and whisker plots enables visual and statistical analysis of the data spread, which shows high variation in PD for the 121 specimens, with between 7 and 44 specimens analysed from each of the six intervals. Mean PD values for all the specimens vary between 0.0045 P/µm^2 and 0.0056 P/µm^2 (Table 1). Half of the PD values are distributed between the 25th and 75th percentile (fig. 5), while the outliers are indicated in the total PD range. Thus, for interval 1, the PD values fall between 0.0055 P/µm^2 (median PD) and 0.0069 P/µm^2 (i.e. the spread is almost evenly distributed between the 50th (median) and 75th percentile); ~60% of *B. spissa* specimens at this interval have PD between 0.0055 P/µm^2 and 0.0069 P/µm^2. For laminated interval 2, the median PD values are 0.0050 P/µm^2. Generally, the PD values do not show any significant correlation with interpreted BW-O_2 (figs. 4 and 5). Generally, consistently low percentages of foraminifer fragmentation are recorded through the 6 intervals studied (Table 5).

Hole	Core	Section	Top depth (cm)	Bottom depth (cm)	Sampled Interval number	Depth (range) CCSF (m)	Sampled depths	Composited Depth thicknes (cm)	Number of specimens in an interval	% deep infaunal species (Bubenshchikova, 2008)	Av. % deep infaunal species (Bubenshchikova, 2008)	Lowest value (number of pores per 10,000 µm^2)	25th percentile (number of pores per 10,000 µm^2)	50th percentile (median:number of pores per 10,000 µm^2)	75th percentile(number of pores per 10,000 µm^2)	Highest value (number of pores per 10,000 µm^2)
D	1H	1	0	2	**1**	0.00	1	2.00	20	44.56	44.56	33	44	55	69	104
D	1H	1	24	26	**2**	0.25	1	2.00	25	78.77	78.77	29	44	50	58	67
D	1H	1	39	93	**3**	0.38-2.38	6	54.00	13	7.60	4.92	26	38	55	59	85
D	1H	2	105	120	**4**	2.54-2.64	2	15.00	12	25.30	26.05	23	43	45	48	72
D	1H	3	89	92	**5**	3.88-8.36	11	62.00	44	3.60	8.20	13	47	56	67	96
A	2H	6	113	117	**6**	10.98 - 11.13	2	17.00	7	95.50	72.48	41	42	49	52	72
									121							

Table 3 Sampled intervals (1-6) from Core U1342; pore counts and percentile distribution of PD; interval 2 is laminated; a total of 121 *B. spissa* specimens were measured down core whilst the total interval studied is 11.13 m.

Vol.9 Issue 2, 2024 Ekiti State University Journal of Science and Technology (EJST)

Hole	Core	Section	Top depth (cm)	Bottom depth (cm)	Interval number	Depth (range) CCSF (m)	Lowest PD ($P/\mu m^2$)	Lowest PD ($P/\mu m^2$) BW-O_2 (µmol/l) read off Glock et al. (2011)	25th percentile PD ($P/\mu m^2$)	25th percentile BW-O_2 (µmol/l) read off Glock et al. (2011)	Median PD ($P/\mu m^2$)	Median PD ($P/\mu m^2$) BW-O_2 (µmol/l) read off Glock et al. (2011)	75th percentile PD ($P/\mu m^2$)	75th percentile BW-O_2 (µmol/l) read off Glock et al. (2011)	Highest pore density ($P/\mu m^2$)	Highest pore density ($P/\mu m^2$) BW-O_2 (µmol/l) read off Glock et al, (2011)
D	1H	1	0	2	**1**	0.00	0.0033	> 5.0	0.004	> 5.0	0.0055	~ 4.0	0.0069	~ 2.2	0.0104	~1.6
D	1H	1	24	26	**2**	0.25	0.0029	> 5.0	0.004	> 5.0	0.0050	> 5.0	0.0058	~ 3.0	0.0067	~2.4
D	1H	1	39	93	**3**	0.38-2.38	0.0026	> 5.0	0.004	> 5.0	0.0055	~ 4.0	0.0059	~3.2	0.0085	~1.8
D	1H	2	105	120	**4**	2.54-2.64	0.0023	> 5.0	0.004	> 5.0	0.0045	> 5.0	0.0048	> 5.0	0.0072	~2.1
D	1H	3	89	92	**5**	3.88-8.36	0.0013	> 5.0	0.005	> 5.0	0.0056	~ 3.8	0.0067	~ 2.4	0.0096	~ 1.7
A	2H	6	113	117	**6**	10.98- 11.13	0.0041	> 5.0	0.004	> 5.0	0.0049	> 5.0	0.0052	> 5.0	0.0072	~2.1

Table 4 Sampled intervals from Core U1342; pore counts and percentile distribution of PD in this study; interval 2 is laminated; total interval studied is 11.13 m. PD from three of the intervals studied (intervals 1, 3 and 5) have their median PD corresponding to the Peruvian OMZ BW-O_2 below ~5.0ml/l (Table 2); PD from the other intervals (2, 4 and 6) corresponds to BW-O_2 above ~5.0ml/l at Peruvian OMZ (Glock et al. 2011).

3.4 Discussion

Overall, there appears to be no regular pattern in the distribution of PD on the tests of *B. spissa* from the different interpreted oxygen levels at site U1342. Indeed, an anecdotal reading of the data in figure 3.4 and 3.5 suggests that *B. spissa* may have more pores on its test in oxygenated settings, than in low-oxygen microhabitats. Several explanations can be posited for the apparent mismatch between PD and interpreted bottom water oxygen-level.

Quantification of pore water oxygen rather than sea bottom water oxygen

Infaunal benthic foraminifera migrate vertically to where food availability and oxygen levels meet their individual demands (Jorissen et al. 1995; Duijnstee et al. 2003), and *B. spissa*, being an infaunal foraminifera, may not be recording bottom water oxygen levels (which the assemblage approach and laminations would hypothetically be responding to), therefore, *B. spissa* does not monitor bottom water but pore water. In addition, foraminifera may be preserved at a level that might not reflect the overall oxygen levels during their life-time. Niebauer et al. (1995) explains that bottom water oxygen concentration experiences short-term fluctuations moderated by water column stratification, or pulses of phytodetritus, which cause seasonal low-oxygen conditions/anoxia at the seabed. In the southern Bering Sea, for example, it is the presence of seasonal stratification disrupting winter mixing of the water column that causes seasonal blooms of phytoplankton and high productivity (Niebauer et al. 1995). Consequently, obtaining an accurate picture of bottom water oxygenation records from time-averaged data is difficult.

PD values calculated in this study were compared with a similar study on environmental influences on the PD of *B. spissa* conducted by Glock et al. (2011; pg. 28; fig. 7 A) off the Peruvian oxygen minimum zone (OMZ). That study claimed lower PD values (0.0013 P/µm^2 up to 0.0050 P/µm^2) correspond to higher BW-O_2 of above ~5.0 ml/l (Table 2; fig. 6). In this study, oxygen levels may have been consistently above this value, possibly above the threshold at which oxygen-levels would influence the PD of *B. spissa*. However, as average PDs in this study are regularly above 0.005 P/µm^2, a direct comparison with Glock et al. (2011) would suggest low levels of oxygen did sometimes exist. Thus, hypothesised higher oxygen levels cannot account for the inability of *B. spissa* PD to reconstruct meaningful BW-O_2. The wide spread of PD data indicates that either there is no simple correlation between PD and BW-O_2, or BW-O_2 was highly variable.

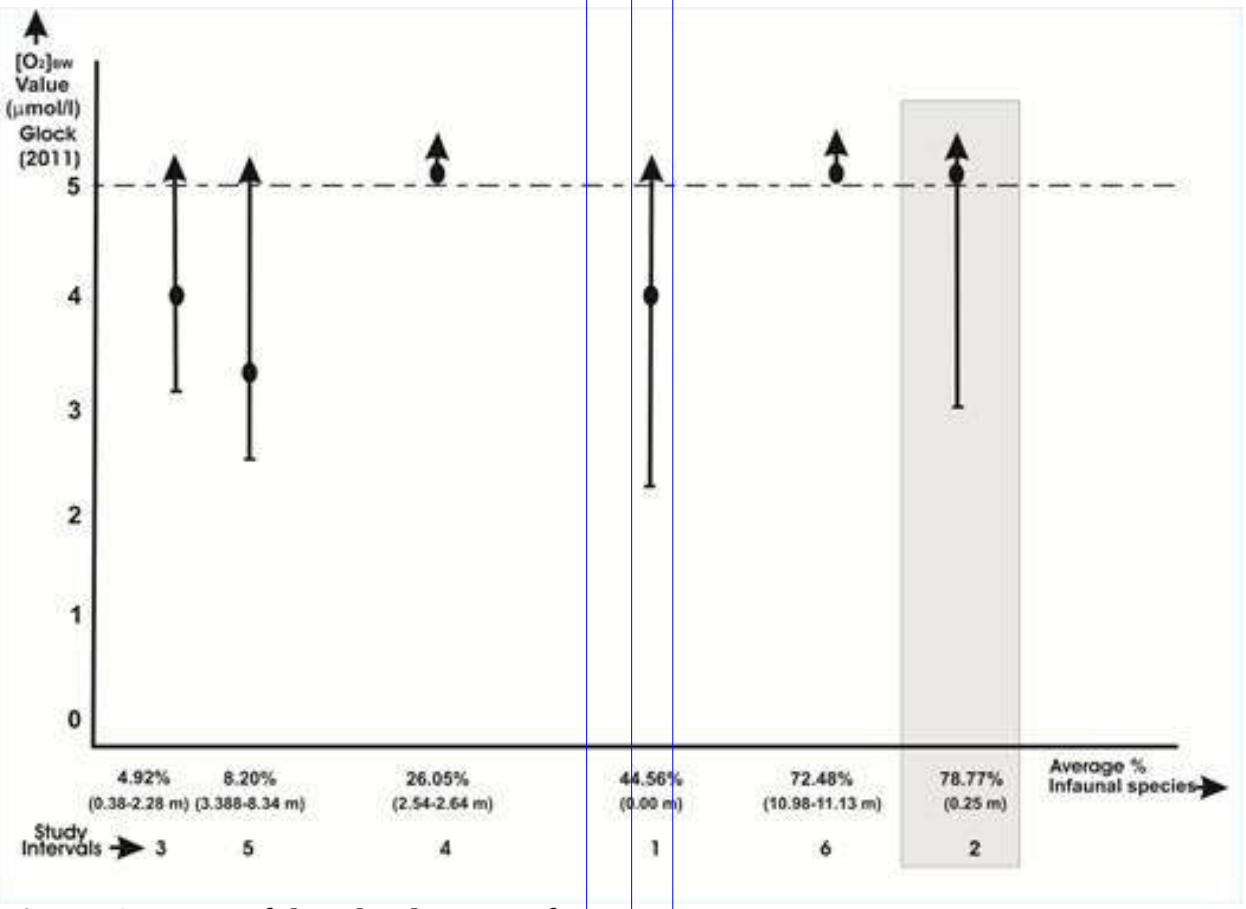

Figure 6 Range of dissolved oxygen for intervals 1 to 6 interpreted in this study. Vertical-axis shows BW-O_2 compared with a study by Glock et al. (2011: figure 7A) from the Pacific margin of the Peruvian oxygen minimum zone; horizontal-axis shows percentage of infaunal foraminifera (indicating relative oxygen level). *B. spissa* PD from three of the intervals studied (intervals 1, 3 and 5) have their median PD (Table 4) corresponding to BW-O_2 that is below ~5.0 ml/l, the other intervals (2, 4 and 6) correspond to above ~5.0 ml/l, where the Glock et al. (2011) correlation breaks down. Bars at the base of each line show the corresponding BW-O_2 (Table 4) upper limit of the 75th percentile of the PD values.Large dots on the lines depict the median BW-O_2 value, while the arrows show the corresponding BW-O_2 for the 25th and the lowest percentile PD values somewhere above 5 ml/l. Shaded area (i.e interval 2) represents the only laminated depth in the interval studied.

342 Transportation of fossil assemblages

Intermittent evidence of tractive sediment movement (Expedition 323 Scientists, 2011) indicates presence in intermittent bottom water currents down to depth 20.59 m in the core from Site U1342. The possibility of bottom water currents winnowing or sorting the sediments may lead to mixing of the primary faunal signal in the sediment. However, for the sampled six intervals there is little sedimentary evidence of transportation, signalled by the low percentage of fragmentation of

foraminifera recorded throughout the interval and by the different size fractions (> 62 µm) of sediment and foraminifera (Table 5).

Particle reworking also occurs during bioturbation, and these processes include both sediment reworking and burrow ventilation (Kristensen et al. 2011). Through burrow construction and maintenance, as well as ingestion and defecation, substratum bio-mixing takes place. Sediments, organic matter and microorganisms including benthic foraminifera are thus displaced vertically and laterally within the sediment matrix. This may have occurred in the sampled intervals here, since only one level is clearly laminated. However, in all intervals sampled, horizons were chosen with limited bioturbation, so that if present, this mixing of faunas is either cryptic, or regarded as of limited effect. Furthermore, the averaging of a number of samples across intervals deemed oxygenated or poorly oxygenated should have mitigated some of the effects of mixing from bioturbation; assemblages are distinct and would likely be homogenous if there was complete mixing.

Hole	Core	Section	Top depth (cm)	Bottom depth (cm)	Interval serial number	Depth serial number	Total of Counts (Benthics)	Species diversity	Total number of foram fragments (F)	Number of whole (W)	Fragmentation ratio (F:W)	**Foraminifera Fragmentation %**
D	1H	1	0	2	**1**	1	495	24	41	449	0.091	**9.13**
D	1H	1	24	26	**2**	2	583	12	11	566	0.019	**1.94**
D	1H	1	39	41	**3**	3	320	18	8	315	0.025	**2.54**
D	1H	1	52	56		4	285	16	3	282	0.011	**1.06**
D	1H	1	89	93		5	210	12	13	195	0.067	**6.67**
D	1H	1	129	133		6	114	19	5	110	0.045	**4.55**
D	1H	2	65	69		7	173	14	14	161	0.087	**8.70**
D	1H	2	89	93		8	250	21	32	218	0.147	**14.68**
D	1H	2	105	109	**4**	9	226	16	24	202	0.119	**11.88**
D	1H	2	115	120		10	395	24	45	338	0.133	**13.31**
D	1H	3	89	92	**5**	11	28	5	2	18	0.111	**11.11**
D	1H	3	99	101		12	166	17	16	155	0.103	**10.32**
D	1H	3	112	115		13	56	17	2	45	0.044	**4.44**
D	1H	4	25	29		14	56	6	2	40	0.050	**5.00**
D	1H	4	77	79		15	349	20	14	335	0.042	**4.18**
D	1H	4	106	108		16	304	16	12	292	0.041	**4.11**
D	1H	4	115	117		17	380	18	16	362	0.044	**4.42**
A	2H	3	39	42		18	359	18	8	351	0.023	**2.28**
A	2H	3	52	54		19	427	21	9	422	0.021	**2.13**
A	2H	3	61	64		20	336	18	10	326	0.031	**3.07**
A	2H	3	90	92		21	357	18	14	343	0.041	**4.08**
A	2H	4	149	151		22	141	10	15	126	0.119	**11.90**
A	2H	6	113	117	**6**	23	316	14	21	302	0.070	**6.95**
A	2H	6	128	130		24	356	16	8	348	0.023	**2.30**

Table 5 Percentages of foraminifer fragmentation through the 6 intervals: consistently low percentages of fragmentation are recorded suggesting minimal transport and dissolution.

3.3 Intra-niche movement

Benthic foraminiferal faunas commonly inhabit a few centimetres of depth in the sediment at the seabed, and this interval coincides with the range from well-oxygenated to dysoxic conditions (Jorissen et al. 2007). The bioturbated zone below the sediment-water interface typically has a heterogeneous distribution of benthic foraminifera, the distribution being related to the subsurface habitats of some species and also to taphonomic processes (Richard and Sen Gupta 1989). Therefore, *B. spissa*, if anything, would be recording the oxygen of pore waters (PW-O_2) at the depth at which it was living, as opposed to BW-O_2 that other proxies are attempting to estimate (laminations and assemblages); this depth would have probably varied. The high range of oxygen estimated by pore density (fig. 6) is consistent with a migratory pattern, although we can provide no direct evidence that PW-O_2 is being recorded in pore density. According to Stabeno et al. (1999) and Takahashi (2005), productivity is high in the Bering Sea at present, causing seasonal organic carbon influx through the water column which leads to dysoxic conditions at the seabed. Often, infaunal benthic foraminifera migrate vertically to where food and oxygen availability meets their demand (Jorissen et al., 1997; Nomaki et al. 2005; Duijnstee et al. 2003). Species that are deeply infaunal in well-oxygenated settings have been shown to occur close to the sediment surface in eutrophic, oxygen-depleted environments (Mackensen and Douglas 1989; Kitazato 1994; Rathburn and Corliss 1994). Saffert and Thomas (1997) have also shown that foraminiferal migration in response to environmental variables is dominantly upward toward the sediment-water interface. Specimens of *B. spissa* may have migrated vertically through the seabed sediment in response to seasonal variations in environmental conditions. Thereby specimens that were living at different levels of bottom-water oxygenation were possibly mixed as a result of vertical intra-niche movement (e.g. figs. 7 A and B) during their life time. Thus, *B. spissa* examined at various depths may have 'mixed' the primary oxygen signal via vertical migration.

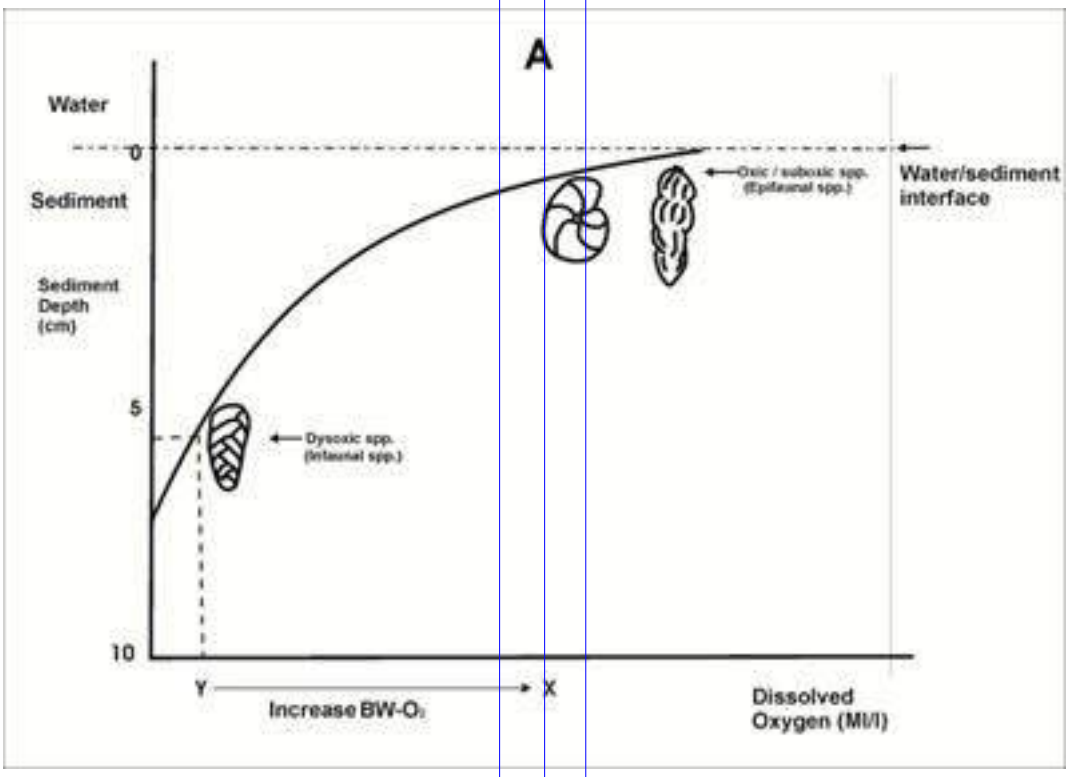
A
Water
0
Sediment
Sediment Depth (cm)
5
10
Oxic / suboxic spp. (Epifaunal spp.)
Water/sediment interface
Dysoxic spp. (Infaunal spp.)
Y
X
Increase BW-O2
Dissolved Oxygen (Ml/l)

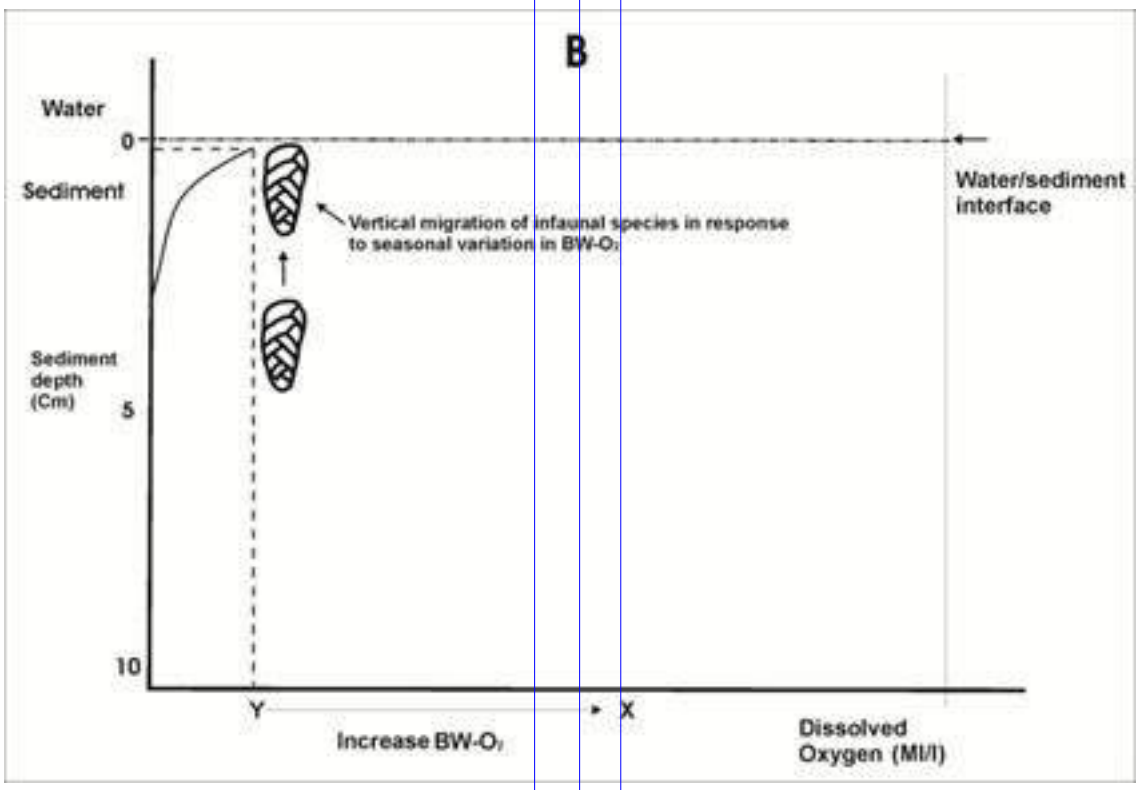
B
Water
0
Sediment
Vertical migration of infaunal species in response to seasonal variation in BW-O2
Water/sediment interface
Sediment depth (Cm)
5
10
Y
X
Increase BW-O2
Dissolved Oxygen (Ml/l)

Figure 7A and B Idealized schematic of intra-niche movement in response to different environmental conditions: vertical-axis shows sediment depth: '**A**' shows oxic and suboxic species at the water-sediment interface in a well-oxygenated condition; '**B**' shows an infaunal species in a less oxygenated environment moving up (arrows) within the sediment in response to seasonal fluctuations in the food supply and corresponding changes in oxygen-level at depth. Infaunal species adapt to dysoxic conditions by moving towards the water-sediment interface; these movements may be responses either to the availability of food at the sediment surface, or to changes in oxygen concentrations within sediment pore-waters.

3.4.4. Nitrate respiration and other alternate modes of survival

Risgaard-Petersen et al. (2006) observed that certain benthic foraminiferal species switch to nitrate respiration during oxygen depletion in the water column, thus suggesting that the pores have a physiological function for intracellular nitrate-uptake. Glock et al. (2011) suggested that the PD of *B. spissa* is probably more sensitive to bottom water nitrate (BW-NO_3^-) than to BW-O_2. The fact that several benthic species can survive anoxia signals the significance of nitrate respiration (full reduction of nitrate to dinitrogen gas: Risgaard-Petersen et al. (2006)); nitrate respiration seems to be widespread among foraminifera from oxygen depleted habitats (Risgaard-Petersen et al. 2006; Glud et al. 2009; Høgslund et al. 2008; Piña-Ochoa et al. 2010). Piña-Ochoa et al. (2010) attributed the diverse metabolic capacity for benthic foraminifera, which enables them to respire with oxygen and nitrate and to sustain respiratory activity, as one of the reasons for their successful colonization of diverse marine sediment environments.

Recent findings on survival strategies of *B. spissa* show that it takes up nitrate for respiration through the pores or uses these to release denitrification products like N_2O or N_2, and that they seem to adapt their pore-densities to survive in extreme habitats (Glock et al. 2011). *B. spissa* specimens may have lived at different levels of bottom-water oxygenation and possibly switched to nitrate respiration during anoxia or less bottom-water oxygenation, and therefore did not need additional pores on their test as a strategy for survival. Glock et al. (2011) speculated as to whether the pores in *B. spissa* were involved in nitrate respiration. Nitrate storage and eventual usage may have been part of the strategies adopted by *B. spissa*, though this cannot be confirmed from this study.

3.5 Conclusions

In this study no significant correlation was identified between the PD of *B. spissa* and interpreted BW-O_2. In part, this might reflect that *B. spissa* can

utilise BW-NO_3^- for respiration during episodes of sea bottom dysoxia or anoxia and/or that it is monitoring PW-O_2. Other, factors, including mixing of assemblages by *in-vivo* migration of foraminiferal assemblages between microhabitats, or post-mortem sediment transport and bioturbation may have obscured the primary PD signal. This study cautions against the use of PD analysis in *B. spissa* as a means of determining sea bottom oxygen conditions unless precise lamination-by-lamination sampling can be undertaken, in a setting where all taphonomic processes are clearly understood.

Acknowledgements. This work was carried out as part of a PhD project undertaken by author at the University of Leicester. Author would like to acknowledge the support given to him by TetFund through Ekiti State University, Ado-Ekiti, Nigeria. Author will like to appreciate Sev Kender, Jan Zalasiewicz, Mark Williams and Michael A. Kaminski, UK IODP for their support. Thanks goes to the International Ocean Discovery Program for providing samples, Karla P. Knudson and Ana Christina Ravelo (UC Santa Cruz) for providing washed residues and the location of laminated sediment, and the Expedition 323 captain, staff, and technical crew of the JOIDES Resolution.

References

Alve, E. 2003. A common opportunistic foraminiferal species as an indicator of rapidly changing conditions in a range of environments. Estuarine, Coastal and Shelf Science 57, pp. 501–514.

Alve, E. 2010. Benthic foraminiferal responses to absence of fresh phytodetritus: a two year experiment. Marine Micropaleontology 76, 3-4, pp. 67-75.

Glock, N., Eisenhauer, A., Milker, Y., Liebetrau, L., Schönfeld, J., Mallon, J., Sommer, S. and Hensen, C. 2011. Environmental influences on the pore density of Bolivina spissa (Cushman). Journal of Foraminiferal Research, 41, 1, pp. 22-32.

Arnold, Z. M. 1954a. A Note on Foraminiferan Sieve Plates, Contributions from the Cushman Foundation for Foraminiferal Research, 5, 77 pp.

Arnold, Z. M. 1954b. Discorinopsis aguayoi (Bermúdez) and Discorinopsisvadescens Cushman and Brönnimann: A study of variation in cultures of living Foraminifera, Contributions from the Cushman Foundation for Foraminiferal Research, 5, pp. 4-13.

Berger, W.H., 1970. Planktonic foraminifera: selective solution and the lysocline: Marine Geology, 8, pp. 111-138.

Bernhard, J. M., Buck, K. R., and Barry, J. P. 2001. Monterey Bay cold-seep biota: assemblages, abundance, and ultrastructure of living foraminifera, Deep-Sea Research I, 48, pp. 2233–2249.

Bernhard, J. M. 1986. Characteristic assemblages and morphologies of benthic foraminifera from anoxic, organic-rich deposits; Jurassic through Holocene. Journal of Foraminiferal Research, 6, pp. 207–215

Bernhard, J. M., and Alve, E. 1996. Survival, ATP pool, and Ultrastructural characterization of benthic foraminifera from Drammens fjord (Norway): Response to anoxia. Marine Micropaleontology, 28, pp. 5-17.

Bernhard, J. M., and Bowser, S. 2008. Peroxisome proliferation in foraminifera inhabiting the chemocline: An adaptation to reactiveoxygen species exposure: Journal of Eukaryotic Microbiology, 55, pp. 135-144.

Bernhard, J. M., and Sen Gupta, B. K. 1999. Foraminifera of oxygen-depleted environments. In: B. K. Sen Gupta (Ed.), Modern Foraminifera. pp. 201-216. New York, NY: Kluwer Academic Press

Berthold, W. U. 1976. Ultrastructure and function of wall perforations in Patellina corrugate Williamson, Foraminiferida, Journal of Foraminiferal Research, 6, pp. 22-29.

Bubenshchikova N., Nürnberg D., Lembke-Jene L. and Pavlova G. 2008. Living benthic foraminifera of the Okhotsk Sea: Faunal composition, standing stocks and microhabitats. Marine Micropalaeontology 69, pp. 314-333

Caralp, M. H. 1984. Quaternary calcareous benthic foraminifers. Initial Reports of the Deep Sea Drilling Project, 80, 7, pp. 25-755.

Carney, R. S. 1989. Examining relationship between organic carbon flux and deep-sea deposit feeding. In: G. Lopez, G. Taghon and J. Levinton (Eds), Ecology of marine deposit feeders 31, pp. 24-58. Lecture Notes on Coastal and Estuarine Studies, New York: Springer.

Corliss, B. H. 1991. Morphology and microhabitat preferences of benthic foraminifera from the northwest Atlantic Ocean. Marine Micropaleontology, 17, 195-236.

Corliss, B. H. 1985. Microhabitats of benthic foraminifera within deep-sea sediments, Nature, 314, 435-438.

Corliss, B. H., and Chen, C. 1988. Morphotypepatterns of Norwegian Sea deep-sea benthic foraminifera and ecological implications. Geology, 16, pp. 716-719.

Corliss, B. H., and Fois, E. 1990. Morphotype analysis of deep-sea

benthic foraminifera from the northwest Gulf of Mexico. Palaios, 5, pp. 589-605.

Den Dulk, Reichart, M, van Heyst, G. J., Zachariasse, S, and van der Zwaan, W. J. 2000. Benthic foraminifera as proxies of organic matter flux and bottom water oxygenation? A case history from the northern Arabian Sea. Palaeogeography, Palaeoclimatology, Palaeoecology, 161, pp. 337-359.

Douglas, R. G. and Heitman, H. L. 1979. Slope and basin benthic foraminifera of the California Borderland. Society of Economic Paleontologists and Mineralogists, 27, pp. 231-246.

Duijnstee, I. A. P., Ernst, S. R., and van der Zwaan, G. J. 2003. Effects of anoxia on the vertical distribution of benthic foraminifera: Marine Ecology Progress Series, 246, pp. 85-94.

Expedition 323 Scientists, 2009. Bering Sea paleoceanography: Pliocene-Pleistocene paleoceanography and climate history of the Bering Sea. IODP Preliminary Reports, 323. doi: 10.2204/iodp.pr.323.2009.

Expedition 323 Scientists, 2011. Site U1342. In: Takahashi, K., Ravelo, A.C., Alvarez Zarikian, C.A., and the Expedition 323 Scientists, Proceedings of the Integrated Ocean Drilling Program, 323: Tokyo (IODP Management International, Inc.). doi: 10.2204/iodp.proc.323.106.2011.

Finlay, B. J., Span. A. S. W., and Harman, J. M. P. 1983. Nitrate respiration in primitive eukaryotes, Nature, 303, pp. 333-335.

Fontanier, C., Jorissen, F. J., Licari, L., Alexandre, A., Anschutz, P. and Carbonel, P. 2002. Live benthic foraminiferal faunas from the Bay of Biscay: Faunal density, composition, and microhabitats. Deep-Sea Research I, 49, pp. 751-785.

Fontanier, C., Mackensen, A., Jorissen, F.J., Anschutz, P., Licari, L., C. Griveaud, C. 2006. Stable oxygen and carbon isotopes of live benthic foraminifera from the Bay of Biscay: Microhabitat impact and seasonal variability Marine Micropaleontology, 58, 3, pp. 159–183.

Glock, N., Eisenhauer, A., Milker, Y., Liebetrau, L., Schönfeld, J., Mallon, J., Sommer, S. and Hensen, C. 2011. Environmental influences on the pore density of Bolivina spissa (Cushman). Journal of Foraminiferal Research, 41, 1, pp. 22-32.

Gooday, A. J. 1988. A response by benthic foraminifera to the deposition of phytodetritus in the deep-Sea. Nature, 332, pp. 70-73.

Gooday, A. J. 1993. Deep-sea benthic foraminifera species which

exploit phytodetritus: characteristic features and controls on distribution. Marine Micropaleontology 22, pp. 187-205.

Høgslund S., Revsbech N.P., Cedhagen, T. Nielsen, L.P. and Gallardo, V.A. 2008. Dentrification, nitrate turn over and aerobic respiration by benthic foraminiferans in the oxygen minimum zone off Chile. Journal of Experimental Marine Biology and Ecology, 359, pp. 85-91.

Ivanova, E.V., Ovsepyan, E.A., Risebrobakken, B., Vetrov, A. A. 2008. Downcore distribution of living calcareous foraminifera and stable isotopes in the Western Barents Sea. Journal of Foraminiferal Research 38, pp. 337-356.

Jorissen, F. J., De Stigter, H. C., and Widmark, J. G. V. 1995. A conceptual model explaining benthic foraminiferal microhabitats. Marine Micropaleontology, 22, pp. 3-15.

Jorissen, F. J . 1999 . Benthic foraminiferal microhabitats below the sediment water interface. In: Sen Gupta, B.K. (Ed.), Modern foraminifera. Kluwer Academic Publishers, Dordrecht, pp. 161-179.

Jorissen, F. J., Fontanier, C., and Thomas, E. 2007. Paleoceanographical proxies based on deep-sea benthic foraminiferal assemblage characteristics. In: Proxies in Late Cenozoic Paleoceanography: Pt. 2 : Biological tracers and biomarkers, edited by C. Hillaire-Marcel and A. de Vernal, Elsevier, pp. 263-326.

Kaiho, K. 1991. Global changes of Paleogene aerobic/anaerobic benthic foraminifera and deep-sea circulation. Palaeogeography, Palaeoclimatology, Palaeoecology, 83, pp. 65-85.

Kaiho, K. 1994. Benthic foraminiferal dissolved-oxygen index and dissolved-oxygen levels in the modern ocean. Geology, 22, pp. 719-722.

Kaiho, K. 1999. Evolution in the test size of deep- sea benthic foraminifera during the past 120 m.y. Marine Micropaleontology, 37, pp. 53-65.

Kender, Sev., Aturamu,Adeyinka., Zalasiewicz,Jan., Kaminski, Micheal A. Williams, Mark. 2019. Benthic foraminifera indicate Glacial North Pacific Intermediate Water and reduced primary productivity over Bowers Ridge, Bering Sea, since the Mid-Brunhes Transition. J. Micropalaeontology, 38, 177–187.

Kitazato, H., 1994. Foraminiferal microhabitats in four marine environments around Japan. Marine Micropaleontology, 24, pp. 29-41.

Kitazato, H. and Ohga, T. 1995.

Seasonal changes in deep-sea benthic foraminiferal populations: Results of long-term observations at Sagami Bay, Japan. Biogeochemical Processes and Ocean Flux in the Western Pacific, Eds. H. Sakai and Y. Nozaki, pp. 32-342.

Kristensen, E., Penha-Lopes, G., Delefosse, M., Valdemarsen, T., Quintana, C. O., and Banta, G. T. 2011. What is bioturbation? The need for a precise definition for fauna in aquatic sciences. Marine Ecology Progress Series, 446, pp. 285-302.

Kuhnt T., Friedrich, O., Schmiedle, G., Milker, Y., Machensen, A., Luckge, A. 2013. Relationship between pore density in benthic foraminifera and bottom-water oxygen content. Deep-Sea Research Part I, 76, pp. 85-95

Leutenegger, S. 1977. Ultrastructure de foraminiféres perforés et imperforés ainsi que de leurs symbiotes, Cahiers de Micropaléontologie, 3, pp. 1-52

Leutenegger, S. and Hansen H. J. 1979. Ultrastructural and Radiotracer Studies of Pore Function in Foraminifera. Marine Biology 54, pp. 11-16.

Licari, L. N., Schumacher, S., Wenzhöfer, F., Zabel, M., Mackensen, A. 2003. Communities and microhabitats of living benthic foraminifera from the tropical east Atlantic: impact of different productivity regimes. Journal of Foraminiferal Research, 33, 1, pp. 10–31

Lutze, G. F. 1980. Depth distribution of benthic foraminifera on the continental margin off NW Africa. Meteor Forschungs-Ergebnisse, C32, pp. 31–80.

Lutze, G. F. 1986. Uvigerina species of the eastern North Atlantic, in van der Zwaan G., J., Jorissen F. J., Verhallen P. J. J. M., and von Daniels C. H. (eds.), AtlanticEuropean Oligocene to Recent Uvigerina: Utrecht Micropalaeontological Bulletins, 35, pp. 21-46.

Lutze, G. F., and Coulbourn, W.T. 1984. Recent benthic Foraminifera from the continental margin of northwest Africa: community structures and distribution. Marine Micropaleontology 8, pp. 361-401.

Mackensen, A. and Douglas, R. G. 1989. Down-core distribution of live and dead deepwater benthic foraminifera in box cores from the Weddell Sea and the California continental borderland. Deep Sea Research Part A. Oceanographic Research Papers, 36, 6, pp. 879-900.

Metzler, C. V, Wenkam, C. R and Berger, W. H. 1982. Dissolution of foraminifera in the Eastern equatorial Pacific: An in situ experiment.Journal of Foraminiferal Research, 12, 4, pp.362-368.

Moodley, L., and Hess, C., 1992.

Tolerance of infaunal benthic foraminifera for low and high oxygenconcentrations. Biological Bulletin, 183, pp. 94-98.

Murray, J. W. 2001. The niche of benthic foraminifera, critical thresholds and proxies. Marine Micropaleontology, 41, pp. 1-7.

Niebauer, H. J., Alexander, V., Henrichs, S.M. 1995. A time-series study of the spring bloom at the Bering Sea ice edge I. Physical processes, chlorophyll andnutrient chemistry. Continental Shelf Research 15, 15, 1859-1877.

Nomaki, H., Heinz, P., Hemleben, C., and Kitazato, H. 2005. Behaviour and response of deep-sea benthic foraminifera to freshly supplied organic matter: A laboratory feeding experiment in microcosm environments. Journal of Foraminiferal Research, 35, pp. 103-113.

Parker, F. L. 1958. Eastern Mediterranean Foraminifera. Reports of the Swedish deepsea expedition 1947-1948, VIII: Sediment cores from the Mediterranean and the Red Sea, 4, 283 pp.

Perez-Cruz, L. L and Machain-Castillo, M. L. 1990. Benthic foraminifera of the oxygen minimum zone, continental shelf of the Gulf of Tehuantepec, Mexico, Journal of Foraminiferal Research, 20, pp. 312-325.

Phleger, F. L., and Soutar, A. 1973. Production of benthic foraminifera in three east Pacific oxygen minima. Micropaleontology, 19, pp. 110-115.

Piña-Ochoa, E., Høgslund, S., Geslin, E., Cedhagen, T., Revsbech, N. P., Nielsen, L. P., Schweizer, M., Jorissen, F., Rysgaard, S., Risgaard-Petersen, N. 2010. Widespread occurrence of nitrate storage and denitrification among Foraminifera and Gromiida. Proceedings of the National Academy of Sciences, 107, 3, pp. 1148- 1153.

Rathburn, A. E. and Corliss, B. H. 1994. The ecology of living (stained) deep-sea benthic foraminifera from the Sulu Sea. Paleoceanography 9, pp. 87-150.

Rhoads, D. C., and Morse, J. W. 1971. Evolutionary and ecologic significance of oxygen-deficient marine basins. Lethaia, 4, 4, pp. 413-428.

Richard, A. and Sen Gupta, B.K. 1989. Effects of Taphonomy and Habitat on the record of Benthic Foraminiferain Modern Sediments. Palaios, 4, pp. 414-423.

Risgaard-Petersen, N., Langezaal, A.M., Ingvardsen, S., Schmidt, M.C., Jetten, M.S.M., Op den Camp, H.J.M., Derksen, J.W.M., Piña-Ochoa, E., Eriksson, S.P., Nielsen, L.P., Revsbech, N.P., Cedhagen, T., van der Zwaan, G. J. 2006. Evidence for complete denitrification in a benthic

foraminifer. Nature, 443, pp. 93-96.

Saffert, H., and Thomas, E. 1997. Living foraminifera and total populations in salt marsh peat cores: Kelsey Marsh (Clinton, CT) and the Great Marshes (Barnstable, MA). Marine Micropaleontology 3, 3, pp. 175-202.

Schumacher, S., Jorissen, F.J., Dissard, D., Larkin, K.E., and Gooday, A.J. 2007. Live (Rose Bengal stained) and dead benthic foraminifera from the oxygen minimum zone of the Pakistan continental margin (Arabian Sea). Marine Micropaleontology 62, pp. 45-73.

Sen Gupta, B. K. and Machain-Castillo. M. L. 1993. Benthic foraminifera in oxygen poor habitats, Marine Micropaleontology, 20, 3, pp. 183-201.

Sliter, W. V. 1974. Test ultrastructure of some living benthic foraminifers, Lethaia, 7, pp. 5-16.

Smith, P.B., 1964. Ecology of Benthonic species. Recent foraminifera of Central America. Geological Survey professional paper 429- B.

Stabeno, P.J., Schumacher, J.D., Ohtani, K. 1999. The physical oceanography of the Bering Sea. In: Loughlin, T.R., Ohtani, K. (Eds.), Dynamics of the Bering Sea, Univ. Alaska Sea Grant, Fairbanks, pp. 1-28.

Steinsund, P. I. and Hald, M. 1994. Recent calcium carbonate dissolution in the Barents Sea: Paleoceanographic applications. Marine Geology, 117, pp. 303-316.

Steinsund, P. I., Polyak, L., Harold, M., Mikhailov, V. and Korsun, S., 1994. Benthic foraminifera in surface sediments of the Barents and Kara seas. In: Steinsund, P.I. (Ed.). Benthic foraminifera in Surface Sediments of the Barents and Kara Seas: Modern and Late Quaternary Applications. Ph.D. Thesis, University of Tromsø, Norway, pp. 61-102

Takahashi, K. 2005. The Bering Sea and paleoceanography. Deep-Sea Research II, 52, pp. 2080-2091.

Thiel, H., Pfannkuche, O., Schriever, G., Lochte, K., Gooday, A, J., Hemleben, CH., Mantoura, R. F. G., Turley, C.M., Patching, J. W., Riemann, F. 1989. Phytodetritus on the Deep-Sea Floor in a Central Oceanic Region of the Northeast Atlantic, Biological Oceanography, 6, 2, pp. 203-239.

Thomas, E., and Gooday A. J., 1996. Cenozoic deep-sea benthic foraminifers: Tracers for changes in oceanic productivity? Geology, 24; 4, pp. 355-358.

Thunell, R.C. 1976. Optimum indices of calcium carbonate dissolution in deep-sea sediments Geology, 4, pp. 525-528.

Comparative Water Use Analysis in Chilli Pepper Cultivation: Farm-gate Assessment of CEA and Field Systems in Kudan LGA, Nigeria

Ayinde T. B
Samaru College of Agriculture, Ahmadu Bello University (ABU) Zaria, Zaria, Nigeria taiyeayinde2006@yahoo.com

Corresponding address

Taiwo Bintu Ayinde
Samaru College of Agriculture, Ahmadu Bello University (ABU) Zaria, Zaria, Nigeria.taiyeayinde2006@yahoo.com

Abstract

This study evaluates Water Use Efficiency (WUE) in chili pepper cultivation through a Life Cycle Assessment (LCA) of Controlled Environment Agriculture (CEA) and field-based systems in Kudan LGA, Kaduna State, Nigeria. The research assesses three distinct production systems—rainfed, irrigated, and poly-tunnel cultivation—highlighting significant differences in water consumption, productivity, and economic viability. While WUE analysis is applicable only to irrigated and poly-tunnel systems, results reveal stark contrasts in water efficiency and resource utilization. The open-field irrigated system exhibits high water demand, with a WUE of 204.63 L kg^{-1}, underscoring inefficiencies in traditional irrigation practices. In contrast, the poly-tunnel system demonstrates superior water efficiency, recording a WUE of 0.19 L kg^{-1}, representing a 98.36% reduction compared to open-field cultivation. Statistical analysis using one-way ANOVA confirmed a significant difference in water use efficiency between cultivation methods ($F = 854.9$, $p < 0.001$), reinforcing the advantages of CEA in water conservation. Additionally, a pairwise t-test revealed a mean water use difference of 204.44 L/kg between the poly-tunnel and open-field irrigated systems ($t = 29.3$, $p < 0.001$), further validating these findings. The yield assessment shows that the poly-tunnel system achieved the highest productivity, yielding 72,000 kg, with 68,400 kg deemed saleable after accounting for approximately 5% post-harvest losses. The open-field irrigated system produced 4,500 kg, with 3,825 kg saleable, while the rainfed system yielded 900 kg, with only 360 kg marketable—highlighting reduced output quality due to environmental stressors. From an economic perspective, poly-tunnel farming recorded a Benefit-Cost Ratio (BCR) of 22.11 and an exceptionally short payback period of 0.05 years, confirming its financial viability. Conversely, open-field irrigated farming exhibited a BCR of 0.89, indicating unprofitability with no viable repayment, while rainfed

farming showed a BCR of 0.64 and a payback period of 0.73 years. Overall, the findings affirm that poly-tunnel cultivation offers a more sustainable, productive, and economically rewarding pathway for chili pepper production in water-scarce environments. The study further reinforces the statistical significance of CEA technologies, underscoring their role in improving water efficiency and profitability in agricultural systems.

Keywords: Comparative Water Use Analysis, Chilli Pepper Cultivation, Farm-Gate Assessment, Controlled Environment Agriculture (CEA), Field Systems, Kudan LGA, Nigeria, Water Use Efficiency (WUE), Irrigation Methods, Yield Optimization, Economic Viability, Sustainable Agriculture, and Agricultural Resource Management

1.1. Introduction

Nigeria is a key global producer of bell peppers, ranking as the third-largest worldwide and the leading producer in Africa, contributing 9% of global production, which totals 12 million tons annually. China and Turkey precede Nigeria, accounting for 23% and 10%, respectively (Alabi et al., 2023). Within Nigeria, the northern states of Kaduna, Kano, Jigawa, Katsina, Sokoto, Plateau, and Bauchi serve as the country's primary hubs for pepper cultivation, with extensive farming systems supplying local and international markets (Madina et al., 2024).

Peppers play a significant role in Nigeriancuisine,comprising approximately 20% of daily vegetable consumption per person and serving over 165 million people. Their versatility extends beyond culinary applications, finding use in medicinal practices and economic trade, transcending socio-economic boundaries. Recent studies affirm Nigeria's prominence in Africa's pepper production, with 762,174 tonnes of green chilies and peppers harvested in 2020, reflecting a 0.27% increase from 2019 (Alabi et al., 2023). Additionally, research highlights the economic profitability of pepper farming in Kaduna State, demonstrating high yield potential and strong market viability (Madina et al., 2024).

Despite these promising statistics, chili pepper farming in Nigeria faces substantial constraints, particularly financial limitations among farmers. Around 99% of farmers rely on rain-fed agriculture and open-field cultivation, restricting productivity and economic stability (Ekine et al., 2023). This dependence leads to synchronized planting and harvesting cycles, causing marketsaturation and price fluctuations.

Beyond financial challenges, farmers

contend with climate variability, erratic rainfall patterns, pest infestations, disease outbreaks, and inadequate irrigation systems (Peprah, 2023). The introduction of irrigated systems offers a sustainable solution, providing a consistent water supply, improving crop quality, and enhancing overall yield (Aduramigba-Modupe & Oke, 2023; Nwonu et al., 2022). However, agriculture's heavy reliance on water resources remains an ongoing concern, accounting for 70% of Africa's annual freshwater withdrawals (Johnson et al., 2023). In West Africa, agricultural activities consume approximately 75% of water withdrawals, yet only 3.5% of cultivated land is irrigated, emphasizing the urgent need for improved irrigation infrastructure (Peprah, 2023).

With freshwater availability declining, competition for irrigation access has intensified, particularly in arid and semi-arid regions (Ahmed et al., 2020). Controlled irrigation has proven effective in mitigating pest and disease risks, stabilizing market prices, and boosting profitability (Kalitsilo et al., 2025; Mitku & Abebaw, 2024). Nonetheless, farmers still struggle with low-quality seeds, reliance on open-pollinated varieties, substandard fertilizers, and poor soil fertility (Café-Filho et al., 2018; Krasilnikov et al., 2022). These agricultural challenges have led to significant yield declines, with reports indicating a drop from 100 tonnes to 30 tonnes per hectare, and some farmers experiencing yields as low as 2 tonnes per hectare for conventional habanero peppers.

The rapid urbanization of Nigeria, with over 35% of its population residing in cities, presents additional challenges. Food security concerns are growing as urban centers expand, while youth migration and declining rural food production exacerbate the issue (Oderinde et al., 2022; Oji & Anih, 2021). Ensuring food security and income stability for urban populations remains a national priority.

This study examines the water consumption per kilogram of chili pepper across rainfed, irrigated, and Controlled Environment Agriculture (CEA) systems, estimating the economic costs associated with each approach. Additionally, it assesses the feasibility of CEA adoption within smallholder farming, analyzing potential challenges and benefits for resource-limited farmers.

While recent studies on greenhouse water savings in Nigeria underscore the benefits of controlled irrigation techniques (Adesogan & Sasanya, 2025; Butu et al., 2022), they do not directly compare CEA systems with field-based methods in Kudan LGA, Nigeria. This study bridges that gap, evaluating t rade- offs between cultivation systems, including infrastructure costs, environmental impact, and accessibility for local farmers.

Empirical evidence further supports the efficiency of CEA systems, showing that hydroponics and aeroponics can reduce water usage by up to 90% compared to conventional farming methods (Regmi et al., 2024; Varughese et al., 2021). These systems employ closed-loop irrigation technologies and precise environmental controls, significantly improving both water and nutrient use efficiency (Akinyele & Eze, 2023). Additionally, findings from Texas Tech University reveal that aeroponic systems demonstrated greater water use efficiency compared to nutrient film technique (NFT) hydroponic systems (Regmi et al., 2024).

These insights reinforce the importance of comparing CEA with traditional field-based cultivation, identifying the most viable water-efficient solution for sustainable chili pepper farming in Kudan LGA.

2. Methodology

This study employed Life Cycle Inventory (LCI) methods to collect data on water consumption, yields, and economic returns for both Controlled Environment Agriculture (CEA) and traditional field systems (Field survey, 2023). The research incorporated field surveys, water usage assessments, and economic analyses to provide a comprehensive comparison of the two systems in Kudan Local Government Area (LGA), Kaduna State, Nigeria.

A two- stage random sampling procedure was used to ensure unbiased farmer selection. In the first stage, four wards—Likoro, Zabi, Kudan, and Hunkuyi—were randomly selected due to their high chili pepper production (Field survey, 2023). In the second stage, a proportionate random selection was conducted using the Solvent formula, ensuring representation across various production scales and socioeconomic backgrounds. A random number sampling technique was applied, leading to the selection of 125 respondents for the study.

Three production systems were examined, with system boundaries defined as cradle-to-farm-gate, including rainfed field- based cultivation, irrigated field-based cultivation (Fadama/"Lam-bu"), and poly-tunnel cultivation (Field survey, 2023). The functional unit was defined as 1 kg of saleable unprocessed product, including rainfed local red bell pepper (*Capsicum annuum*) "*Tatase*," irrigated Scotch Bonnet Pepper (*Capsicum chinense*) "*Atarodo*," and Piquante F1 cultivated in a poly-tunnel (Field survey, 2023).

To ensure data reliability, the questionnaire was pretested on a subset of farmers to refine clarity and relevance, with response rates documented and data validation conducted through cross-checking farm records and follow-up interviews (Field survey, 2023).

Farmers in Kudan LGA predominantly cultivate open-pollinated pepper varieties, but these seeds often result in lower yields and reduced pest resistance compared to hybrid varieties (Alabi & Anekwe, 2023). The local bell pepper ("*Tatase"*) requires consistent soil moisture (70-80% of field capacity) and relative humidity levels between 60-70% to thrive (Institute for Agricultural Research (IAR), Meteorological Unit. (2021). Soil pH plays a crucial role in pepper productivity, with optimal levels ranging between 5.5 to 6.8 for enhanced nutrient uptake (Nwite, 2024).

Regular irrigation is essential to prevent water stress, particularly during the flowering stage, when frequent light irrigation is recommended (Olabisi & Nofiu, 2022). Drip irrigation enables year-round cultivation, enhances efficiency, and minimizes water wastage, while also supporting fertigation, which reduces labor-intensive fertilization methods (Alharbi et al., 2024; Tanaskovik et al., 2019). Farmers utilizing drip irrigation have reported 50-200% higher yields compared to rainfed methods, though some still employ surface irrigation, where controlled water application is advised for optimal results (Kalitsilo et al., 2025).

Nigeria's pepper industry features Scotch Bonnet ("*Atarodo*"), a highly valued variety cultivated through irrigation, alongside Habanero ("*Rodo*"), prized for its heat intensity and adaptability (Butu et al., 2022). Habanero peppers begin producing fruit three months after transplanting and remain productive for 6-8 months (Ndagana et al., 2021), with irrigated Habanero farms recording yields exceeding 40 tonnes per hectare (Regmi et al., 2024).

Farmers employing greenhouses and poly-tunnels achieve higher yields compared to open-field cultivation, with hybrid pepper seeds such as Piquante F1, Avenir F1, and Super Habanero F1 proving effective (Alharbi et al., 2024; Varughese et al., 2021). A case study in Northern Nigeria demonstrated successful cultivation of Piquante F1 in a poly-tunnel, maintaining optimal environmental conditions, including temperature (20-35°C) (IAR Meteorological Unit, 2021), light intensity (75-330 µmol m^{-2} s^{-1}) (Appolloni et al., 2021; Nicholson et al., 2020), relative humidity (50-70%) (Olabisi & Nofiu, 2022), and wind speed (~10 km/h) (Gabriel et al., 2023).

The study employed Life Cycle Assessment (LCA) methodology to track inputs and outputs and assess the environmental impact of pepper cultivation in Nigeria (Isah et al., 2025). The LCA was conducted using OpenLCA and utilized Ecoinvent v2.2 alongside additional relevant databases (Salami, 2019). Environmental data were benchmarked against the Ecoinvent database v2.2 and the Athena Sustainable Materials Institute for comprehensive evaluation, ensuring an accurate assessment of economic and environmental trade-offs (Amaefule et al., 2019), (Table 1).

Table 1. Characteristics of poly-tunnel, field (rainfed and irrigated) operations analyzed

Production System	CEA	Rainfed	Irrigated	Source
Land Area for Production (ha)	0.0147	1	1	Field survey, 2023
Land Area for Non-Production (ha)	0.01	0	0	Field survey, 2023
Total Land Area (ha)	0.0247	1	1	Field survey, 2023
Crop Variety	Hybrid (Piquante Red F1 Habanero "Atarodo")	OPV (local bell pepper *Capsicum annuum* or "Tatase")	OPV (Scotch Bonnet Pepper *Capsicum chinense* or "Atarodo")	Field survey, 2023
Daytime Temperature	25.3°C	21-26°C (70-79°F)	24-26°C (75-79°F)	IAR Meteorological Unit, 2021; Amoako et al., 2022
Night Temperature	19.8°C	15-17°C (59-63°F)	15-17°C (59-63°F)	IAR Meteorological Unit, 2021; Amoako et al., 2022
Seed Germination Temperature	25°C	24-26°C	24-26°C	Olabisi & Nofiu, 2022; IAR Meteorological Unit, 2021
Seedling Growth Temperature	18°C (night-time minimum)	15°C (night-time minimum)	15°C (night-time minimum)	Olabisi & Nofiu, 2022; IAR Meteorological Unit, 2021
Light Transmission	High light transmission	Full sun exposure is essential for healthy growth	Full sun exposure is essential for healthy growth	Olabisi & Nofiu, 2022; IAR Meteorological Unit, 2021; Appolloni et al., 2021; Nicholson et al., 2020; Vanlommel et al., 2020
Photo-synthetically Active Radiation (PAR)	550 nanometers	400 to 700 nanometers (nm)	400 to 700 nanometers (nm)	Abimbola, 2024; Olabisi & Nofiu, 2022; IAR Meteorological Unit, 2021; Appolloni et al., 2021; Nicholson et al., 2020; Vanlommel et al., 2020
CO2 Concentration (Cold Weather)	1000 ppm (day)	426 ppm	426 ppm	Amaefule et al., 2019; Gabriel et al., 2023; Oyeranti, 2024
CO2 Concentration	400 ppm (with	425 ppm	425 ppm	Amaefule et al.,

3.0 Calculation of Economic and Environmental Indicators

A survey of 125 chilli pepper farmers during the 2022/2023 dry and rainy seasons provided valuable insights into the production costs associated with field-based systems, including rainfed and irrigated ("*Fadama*"/"*Lam-bu*") methods. By analyzing yield and output prices, the study calculated revenue for these farming systems. Notably, some farmers perceive open-field pepper farming as a low-input endeavor, relying primarily on manure as their main input.

A comparative analysis of poly-tunnel, Rainfed, and Irrigated farming methods reveals significant yield differences per hectare. This study presents the yields per hectare for three different chilli pepper production methods: Poly-tunnel, Rainfed, and Irrigated systems. Poly-tunnel stands out with the highest yield per hectare, producing an impressive 72,000 kg/ha/year across four to five harvests per year, ensuring continuous production throughout the year. The high yield is attributed to the optimized growing conditions provided by poly-tunnel, including precise control over temperature, humidity, and light, as well as efficient use of water and nutrients. The significant investment in infrastructure, such as poly-tunnel structures and advanced irrigation systems-drip irrigation, enables poly-tunnel to achieve superior productivity.

In contrast, the Rainfed system yields 900 kg/ha/year, with a single harvest per year occurring between April and August. The reliance on natural rainfall results in less predictable and often suboptimal growing conditions, negatively impacting plant growth and productivity. Additionally, the limited use of inputs such as fertilizers and irrigation further constrains the yield potential of rainfed chilli pepper production. The Irrigated system, with a yield of 4,500 kg/ha/year, provides a more consistent water supply and better crop performance compared to rainfed agriculture. However, its yield remains significantly lower than that of poly-tunnel due to less controlled growing conditions and lower input levels. This system typically produces one crop per year, with harvesting occurring between September and March.

To further strengthen the economic comparison, this study incorporates additional financial metrics, including net returns, cost per kilogram of pepper, and payback periods for poly-tunnel investment. A detailed financial breakdown of input costs—including water, energy, labour, and fertilizers—has been conducted to derive key economic indicators such as the benefit-cost ratio (BCR) and profit margins for each production system (Table 8). These insights provide decision-makers and farmers with a robust economic assessment of the long-term sustainability and profitability of adopting CEA versus traditional field-based methods.

Additionally, climate change-related losses were observed across farming methods. Rainfed systems experienced up to 60% losses during the rainy season and 10-20% losses during the dry season. In contrast, CEA techniques, such as poly-tunnel cultivation, reduced losses to approximately 5%, ensuring stable and higher yields throughout the year.

To improve economic transparency, unit costs, currency conversions, and the time frame for cost collection have been explicitly specified. Electricity for irrigation pumps is reported in Naira per kilowatt- hour (Naira/ KWH) to distinguish it from lump-sum monthly fees. As of June 2025, the cost for 100 units of electricity is N2,359 for households (N23.59 per unit) and N3,853 for businesses (N38.53 per unit) (Nigerian Price, 2025). Additionally, diesel fuel expenses are accounted for, with prices set at N7.51 per liter for CEA systems and N375.6 per liter for irrigated field systems, offering a clear breakdown of energy costs across different cultivation methods.

Furthermore, fertilizer costs have been systematically broken down. Prices fluctuate based on type and brand, with organic fertilizers ranging from N7,000 to N81,000, while chemical fertilizers, such as Indorama Urea, are widely used. NPK fertilizers are priced at N2,500 per kg, ensuring accurate input cost calculations. Additional essential inputs, including Calcium Magnesium (CalMag) and Potassium Humate, were included to reflect input variations across production systems.

To ensure accuracy, average values during each season were used for cost estimation rather than a single price point. This approach accounts for seasonal fluctuations in electricity rates, diesel prices, and fertilizer costs, providing a more realistic representation of financial variability in chilli pepper production systems (Figure 1).

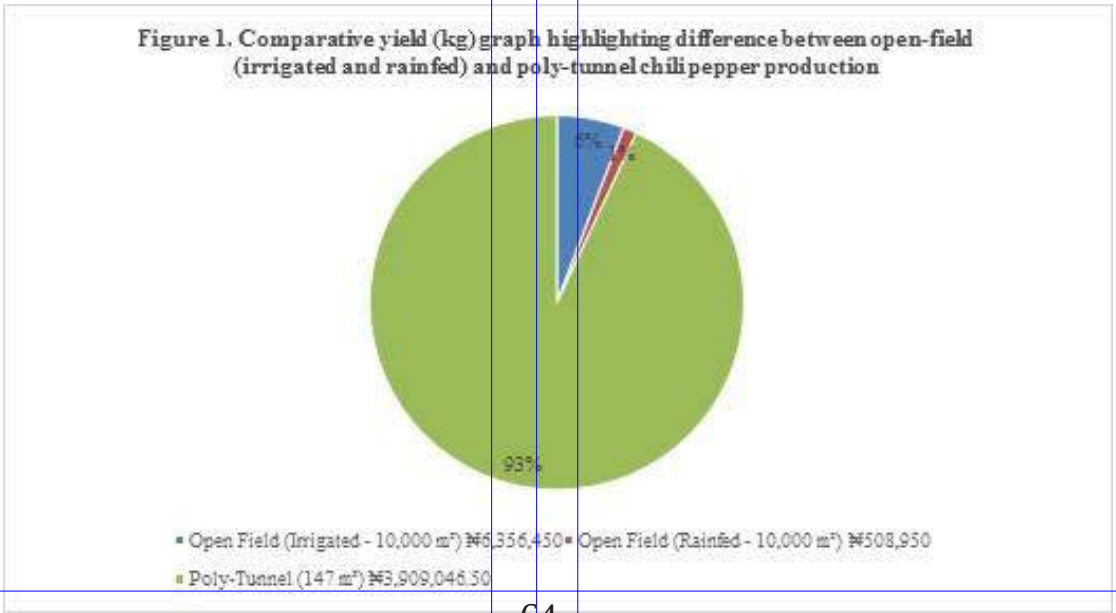

Figure 1. Comparative yield (kg) graph highlighting difference between open-field (irrigated and rainfed) and poly-tunnel chili pepper production

Overall, these findings highlight the clear advantages of CEA in maximizing chilli pepper yields per hectare, despite its higher initial costs. Meanwhile, the Rainfed and Irrigated systems demonstrate that water management and input levels play crucial roles in determining the productivity and profitability of chilli pepper cultivation (Table 2 & Figure 1).

Table 2: Yield per Hectare for CEA, Rainfed And Irrigated Chilli Pepper Production

Production Inputs	Units of Quantity	Poly-tunnel	Rainfed Field	Irrigated Field
Fixed Production Inputs			**Quantity Used**	
Drip Irrigation System				
Borehole/Well and other component	Unit/s	1		1
Poly-tunnel Structure	Unit/s	1		
Small farm tools				
Garden Trowel	Piece/s	1	1	1
Hand Fork	Piece/s	1	1	1
Seedling Trays 1 set (10-20 trays)	Set	1	1	1
Watering Can	Piece/s	1	1	1
Gloves	Pair	1	1	1
Stakes	Unit/s	15	15	15
Weed Hoe	Unit/s	1	1	1
Spray Bottle	1 bottle	1	1	1
Soil Tester	1 Piece/s	1	1	1
Basket	1 Piece/s	2	2	2
Pruners	1 Piece/s	2	2	2
Twine or String	1 roll	1	1	1
Mulch	1 bag	1	1	1
Compost Bin:	1 Piece/s	1	1	1
Labels or Markers 1 pack (20-50 labels)	1 Pack/s	1	1	1
Variable Production Inputs				
Electricity for Irrigation Pump	Naira/ KWH	300	300	300
Diesel Fuel for Irrigation Pump	Naira/Litre	7.51	0	375.6
Seeds (Piquante Red F1 Habanero)	1 kg bag	5	5	5
Fertilizers				
NPK	1 kg bag	15	0	7.5
Chicken Manure	1 kg bag	36.75	2500	2500
Calcium Magnesium (CalMag)	1 kg bag	3	0	1.5
Potassium Humate	1 kg bag	1	0	0.5
Pesticides				
Pesticides	1 litre	7.5	15	7.5
Nematicides	1 litre	2.5	5	2.5
Insecticide	1 litre	7.5	15	7.5
Fungicide	1 litre	7.5	15	7.5
300m by 1.5m Plastic mulch	square meter	147	0	0
Labor and Installation	Man-day	3000	3000	3000
Yield[1b]	**kg/ha/year**	**72,000**	**900**	**4,500**

Note: Data Source: Authors' calculations.

3.2 Water Use (WU)

In tropical regions, Controlled Environment Agriculture (CEA) utilizes various water sources, including rivers, ponds, reservoirs, rainwater, groundwater, and municipal supplies. While manual irrigation systems are cost-effective, they lack precision in regulating water and nutrient quantities. Irrigation frequency depends on factors such as substrate type, plant growth stage, and season. Water delivery methods include gravity-fed systems and small-scale pumping machines, emphasizing the need for efficient and precise irrigation management in tropical CEA settings.

Given the increasing challenges of waterscarcity and resource management, this study focuses on water consumption efficiency in chili pepper cultivation, excluding energy use and global warming potential since these aspects have already been comprehensively analyzed in prior research (Ayinde, 2025; Ayinde & Gamu, 2025). Rather than replicating previous findings, this research aims to provide a complementary perspective by addressing water efficiency—a critical sustainability factor in CEA. By maintaining this focused approach, the study contributes targeted insights that can inform agricultural practices and resource management while ensuring analysis remains within a defined scope. The exclusion of energy-related impacts does not undermine their significance; instead, it reflects an intention to build on existing literature while advancing knowledge in water sustainability within CEA.

Comparative Analysis of Water Use

Water requirements for chili pepper production vary significantly between open-field irrigation and poly-tunnel systems. In open-field flood irrigation, chili peppers typically require 600 to 900 mm of water per growing season, with some estimates reaching 1,250 mm for longer periods and multiple harvests (FAO, 2025). Conversely, poly-tunnel systems demand less water due to a controlled environment, with seasonal crop evapotranspiration (ETc) ranging from 346 to 362 mm (Fernandez et al., 2023). Additionally, poly-tunnel farming exhibits higher water use efficiency (WUE), recorded between 13.8 and 18.44 kg/m³ (Lasisi et al., 2024), reinforcing its role in water conservation and productivity enhancement (Figure 2).

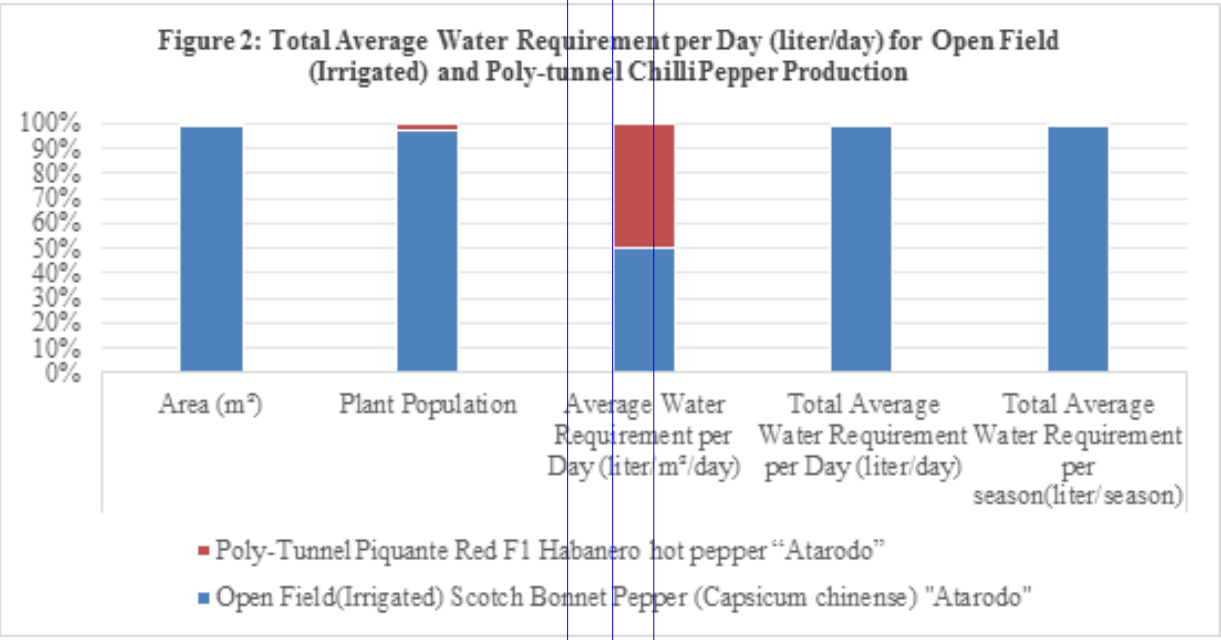

Note: Data Source: Authors' calculations

A comparison with Table 4 strengthens the argument for controlled irrigation methods. Findings from Gomes et al. (2023) highlight that hydroponic chili pepper cultivation in Brazil requires 300 - 400 mm of water per season, yielding 35 - 40 tons/ha, with a WUE ranging between 8.5 and 10.2 kg/m³. Similarly, research by Zhang et al. (2021) observed that mulched drip irrigation in China required 450 - 600 mm of water per season, achieving 25 - 30 tons/ha, with a WUE between 4.5 and 6.7 kg/m³.

By contrast, drip irrigation with organic matter in Baghdad, Iraq (Ati et al., 2020; Alaa et al., 2015) reported higher water consumption values ranging from 945.9 to 1152.9 mm, with yields fluctuating between 10.45 and 39.45 tons/ha. These results emphasize the relatively greater water conservation potential of poly-tunnel farming, as its controlled microclimate minimizes evaporation losses and optimizes irrigation precision (Doe & Johnson, 2022).

The New Mexico semi-arid region study (Baath et al., 2020) examined the impact of brackish groundwater and reverse osmosis concentrate irrigation, with findings indicating that salinity levels of ≤ 3 dS/m maintained appropriate water use efficiency. Such irrigation innovations highlight the potential for resource- efficient practices, especially in arid climates where water availability is scarce.

Further comparison with Table 4 reveals that micro-sprinkler irrigation in Akure, Nigeria (Olotu et al., 2012) required 821.07 - 833.61 mm of water per season, producing 14.89 - 21.06 tons/ha, while different irrigation scheduling in Akure (Akinbile &

Yusoff, 2011) ranged between 25% - 100% ET, yielding 1.28 - 2.64 tons/ha. These findings highlight the variability in water use depending on irrigation strategy, climate, and local farming conditions.

Implications for Water Management Strategies

A review of Table 4 data suggests that hydroponics and poly-tunnel farming offer superior water efficiency compared to open-field and conventional drip irrigation systems. While hydroponic cultivation (Gomes et al., 2023) and mulched drip irrigation (Zhang et al., 2021) exhibit enhanced resource efficiency, poly-tunnel farming consistently achieves higher WUE values, making it a viable solution for sustainable chili pepper production in water-scarce regions (Fallik et al., 2019).

By integrating precision irrigation techniques, soil moisture monitoring, and adaptive water management frameworks, agricultural policymakers can optimize irrigation efficiency while reducing overall water consumption, ensuring long-term sustainability in chili pepper production.

Table 4: Comparative Water Use Efficiencies in Chili Pepper Cultivation Across Different Regions and Irrigation Method

Location	Cultivation Method	Water Use (mm)	Yield (ton/ha)	Water Use Efficiency (kg/m³)	Source
Uttarakhand, India (sub-tropical humid region)	Irrigation scheduling with different soil moisture regimes	40% MAD level optimized water use	7.624	Not specified	Yadav & Kashyap, 2024
Brazil (tropical region)	Hydroponic cultivation	300 - 400	35 - 40	8.5 - 10.2	Gomes et al., 2023
India (semi-arid region)	Deficit irrigation strategies	500 - 700	20 - 28	3.8 - 5.6	Kumar et al., 2022
China (semi-arid region)	Mulched drip irrigation	450 - 600	25 - 30	4.5 - 6.7	Zhang et al., 2021
Baghdad, Iraq (similar climate)	Drip irrigation with organic matter	945.9 - 1152.9	10.45 - 39.45	Improved with organic matter	Ati et al., 2020
New Mexico, USA (semi-arid region)	Irrigation with brackish groundwater and reverse osmosis concentrate	Varies by salinity level	Varies by cultivar	Brackish water with EC = 3 dS/m maintained appropriate WUE	Baath et al., 2020
Volta Region, Ghana	Traditional field-based	Not specified	65.76% efficiency	Not specified	Asravor et al., 2016
Baghdad, Iraq (similar climate)	Drip irrigation with organic matter	945.9 - 1152.9	10.45 - 39.45	Improved with organic matter	Alaa et al., 2015
Akure, Nigeria	Micro-sprinkler irrigation	821.07 - 833.61	14.89 - 21.06	Not specified	Olotu et al., 2012
Akure, Nigeria	Different irrigation scheduling	25% - 100% ET	1.28 - 2.64	Not specified	Akinbile & Yusoff, 2011

To validate claims of superior water use efficiency, a one-way Analysis of Variance (ANOVA) and pairwise t-tests were conducted to compare mean water use efficiency between poly-tunnel and open-field irrigated systems. By emphasizing water use efficiency, this study provides actionable insights for

farmers, researchers, and policymakers focused on sustainable agricultural practices. The findings contribute to the development of efficient irrigation strategies, helping to optimize production while reducing water waste, which is particularly important in regions facing water constraints.

4 Results

This study assesses the water usage efficiency of chilli pepper cultivation in Kudan LGA, Kaduna State, Nigeria, comparing Controlled Environment Agriculture (CEA) and field-based systems. Using Life Cycle Assessment (LCA) methodology, the research provides an in-depth evaluation of water consumption, irrigation practices, and water use efficiency (WUE) across cultivation methods.

The study incorporates crop-specific growing periods to assess seasonal water requirements. Piquante Red F1 Habanero, cultivated in poly-tunnel systems, has a growth period of 75 to 80 days, enabling multiple harvests per year. In contrast, OPV local bell pepper ("*Tatase*"), grown in rainfed conditions, has a longer growing period of 90 to 150 days, while OPV Scotch Bonnet Pepper ("*Atarodo*"), cultivated in irrigated fields, follows a growth period of 80 to 120 days. These variations influence water consumption and irrigation cycles across production systems (Table 5).

Water Use Efficiency Analysis

Water use efficiencydiffers substantially between poly-tunnel and open-field irrigated systems. In open-field irrigated cultivation (10,000 m²), the total seasonal water requirement was 920,850 L, yielding 4,500 kg of Scotch Bonnet Pepper ("*Atarodo*")—equating to 204.63 L of water per kg of product. The standard deviation (SD) of yield was 380, with a 95% confidence interval (CI) of 4,500 ± 740 and a standard error (SE) of 190, indicating yield variability (Table 5).

In contrast, the poly-tunnel system (147 m²) exhibited substantially higher water efficiency, requiring only 13,536.50 L per season while producing 72,000 kg of Piquante Red F1 Habanero ("*Atarodo*"). This resulted in a water use efficiency of 0.19 L per kg of product. The SD of yield was 5,200, with a 95% CI of 72,000 ± 10,100 and an SE of 2,600, validating consistent yields under controlled conditions.

Table 5. Yields per Water Use for for Open Field (Irrigated) and Poly-tunnel Chilli Pepper Production

Growing System	Species of Chilli Pepper	Total Average Water Requirement per Season (L/season)	Yield (kg)	Water Use per kg Product (L/kg)	SD (Yield)	95% CI (Yield)	SE (Yield)
Open Field (Irrigated - 10,000 m²)	Scotch Bonnet Pepper (*Capsicum chinense* "Atarodo")	920,850.00	4,500	204.63	380	4,500 ± 740	190
Poly-Tunnel (147m²)	Piquante Red F1 Habanero (*Atarodo*)	13,536.50	72,000	0.19	5,200	72,000 ± 10,100	2,600

Note: Data Source: Authors' calculations.

Statistical Analysis

To ensure rigorous statistical validation, the study integrates standard deviations (SD), confidence intervals (CI), and standard errors (SE) in assessing yield and water efficiency. SD measures yield variability, CI defines the 95% certainty range within which true mean yield and water use are expected to fall, and SE accounts for sampling variability, improving precision in data interpretation (Table 5).

The ANOVA results demonstrated a statistically significant difference ($F = 854.9$, $p < 0.001$), confirming that CEA systems exhibit superior water conservation compared to traditional field-based methods (Table 6).

Table 6: One-Way ANOVA Results for Water Use Efficiency Across Cultivation Systems

Source of Variation	Sum of Squares (SS)	Degrees of Freedom (df)	Mean Square (MS)	F-Value	p-Value
Between Groups	73125.63	1	73125.63	854.9	< 0.001
Within Groups	3423.87	18	190.22		
Total	76549.5	19			

Note: Data Source: Authors' calculations.

Additionally, a pairwise t-test revealed a mean water use difference of 204.44 L/kg between poly-tunnel and open-field irrigated systems, with a t-value of 29.3 and $p < 0.001$, reinforcing the statistical significance of these findings (Table 7).

Table 7: Pairwise t-Test Comparing Water Use Efficiency Between Poly-Tunnel and Open-Field Irrigated Systems

Comparison	Mean Difference	Standard Error (SE)	t-Value	p-Value	95% Confidence Interval
Poly-Tunnel vs Open-Field (Irrigated)	204.44	6.98	29.3	< 0.001	190.12 to 218.76

Note: Data Source: Authors' calculations.

Economic Comparison of Cultivation Systems

The economic comparison of cultivation systems highlights the feasibility of poly-tunnel and open-field chili pepper production through fixed and variable cost analyses. The poly-tunnel system, despite its higher initial fixed costs of ₦2,532,501, demonstrated rapid investment recovery within 0.05 years due to significantly lower variable costs, including water (₦13,536.50), energy (₦7,510), and labor (₦75,000). In contrast, the open-field irrigated system, with total costs amounting to ₦6,356,450, remained financially unsustainable, failing to recover production costs within a feasible time frame.

The analysis also highlights differences in saleable product proportions across cultivation methods. The calculation of saleable products is based on the proportion of total yield that meets market standards for quality, factoring in post-harvest losses and grading criteria. Poly-tunnel farming, with a total yield of 72,000 kg, produced 68,400 kg of saleable chili peppers after accounting for an estimated 5% loss due to handling and sorting. In contrast, open-field irrigated farming yielded 4,500 kg, but quality grading and handling losses reduced the saleable quantity to 3,825 kg, approximately 85% of total yield. Open-field rainfed farming, with a total yield of 900 kg, had the lowest saleable proportion at 360 kg, approximately 40% of total yield, largely due to higher exposure to environmental stressors and inconsistent irrigation practices (Table 8).

The Benefit-Cost Ratio (BCR) further underscores the profitability gap between cultivation systems. Poly-tunnel farming achieved a BCR of 22.11, meaning that for every ₦1 invested, farmers received ₦22.11 in return. Meanwhile, open-field irrigated farming recorded a BCR of 0.89, indicating financial losses, while open-field rainfed farming, despite lower fixed costs (₦77,250) and variable costs (₦431,700), yielded only 900 kg, with a BCR of 0.64, signifying low economic returns (Table 8).

These findings reinforce the advantages of adopting Controlled Environment Agriculture (CEA) for water-efficient,

high-yield chili pepper production. While poly-tunnel cultivation requires higher upfront investment, it drastically reduces variable costs, leading to exceptional profitability and fast financial recovery compared to traditional open-field farming. The analysis confirms that poly-tunnel farming is the most economically viable option, ensuring sustainable production with significant financial returns, while also maximizing the proportion of marketable produce (Ajayi et al., 2024; Berger, 2023).

Table 8: Summary of Economic Comparison Between Open-Field and Poly-Tunnel Chilli Pepper Cultivation

Cost Item	Open Field (Irrigated - 10,000 m²)	Open Field (Rainfed - 10,000 m²)	Poly-Tunnel (147 m²)
Fixed Costs (Naira (?))			
Poly-Tunnel Structure	—	—	520,251
Drip Irrigation System			
Borehole/Well System	717,500	—	1,935,000
Small Farm Tools	79,750	77,250	77,250
Total Fixed Costs	794,750	77,250	2,532,501
Variable Costs (Naira (?))			
Water Cost	920,850	—	13,536.50
Energy Cost	445,086	—	7,510
Labour Cost	580,000	240,000	75,000
Fertilizer Cost	156,735	80,500	157,000
Total Variable Costs	2,926,450	431,700	252,046.50
Total Production Cost (Fixed + Variable) (Naira (?))	6,356,450	508,950	3,909,046.50
Yield (kg) Error! Bookmark not defined.**b**	4,500	900	72,000
Saleable Products (kg)	3,825	360	68,400
Cost per kg of Pepper (Naira/kg)	1,412.54	1,413.75	54.29
Revenue (Naira)	5,625,000	324,000	86,400,000
Net Return (Naira)	731,450 (Loss)	184,950	82,490,953.50
Benefit-Cost Ratio (BCR)	0.89	0.64	22.11
Payback Period (Years)	Not Profitable	0.73	0.05

Note: Data Source: Authors' calculations.

5. Discussion

This study aimed to evaluate the water usage efficiency of chili pepper cultivation in Kudan LGA, Kaduna State, Nigeria, comparing Controlled Environment Agriculture (CEA) with traditional field-based systems. The results provide insights into the impact of different cultivation practices on water consumption, yield performance, economic feasibility, and the broader challenges influencing the adoption of CEA.

Findings reveal a significant difference in water use efficiency between poly-tunnel and open-field irrigated chili pepper cultivation. The poly-tunnel system demonstrated exceptional efficiency, requiring only 13,536.50 liters per season while yielding 72,000 kg of Piquante Red F1 Habanero ("*Atarodo*"), resulting in a water use efficiency of 0.19 L/kg. In contrast, the open-field irrigated system required 920,850 liters per season to produce 4,500 kg of Scotch Bonnet Pepper ("*Atarodo*"), equating to a water use efficiency of 204.63 L/kg. The controlled environment of poly-tunnel farming minimizes evaporation losses and improves irrigation precision, while open- field cultivation is more susceptible to environmental factors such as high evaporation rates, runoff, and inconsistent moisture retention.

To confirm the significance of these differences, a one-way ANOVA test was performed, showing a statistically significant variation ($F = 854.9$, $p < 0.001$) between the two cultivation systems. Additionally, pairwise t-tests showed a mean water use difference of 204.44 L/kg, with a t-value of 29.3 and $p < 0.001$, reinforcing the statistical validity of observed trends. These findings substantiate the argument that CEA drastically reduces water usage, validating its suitability for sustainable chili pepper production, particularly in water-scarce regions.

Yield analysis further confirms the superior productivity of CEA compared to traditional cultivation methods. Poly-tunnel farming generated a yield of 72,000 kg per hectare per year, facilitated by continuous production cycles (four to five harvests annually). Conversely, open-field irrigated farming yielded 4,500 kg per hectare per year, while rainfed farming produced only 900 kg per hectare per year. A key contributor to CEA's enhanced productivity is its climate resilience. Rainfed production experiences up to 60 % crop losses during the rainy season and 10–20% losses during the dry season due to climate variability. However, poly-tunnel systems mitigate these losses, reducing them to around 5%, ensuring higher production stability year-round. Beyond yield and water savings, this study assessed the economic feasibility of poly-tunnel and open-field production systems using fixed and variable cost analyses. Despite its higher upfront investment

(N3,657,000), poly-tunnel farming demonstrated rapid investment recovery, achieving profitability within just 0.05 years (~19 days). In contrast, the open-field irrigated system remained financially unviable, with a negative net return of -N731,450, failing to recover production costs within a feasible t ime frame. Additionally, benefit-cost ratio (BCR) analysis revealed that poly-tunnel farming returned N22.11 for every N1 spent, whereas open-field farming yielded only N0.89, reinforcing CEA's economic advantage.

While this study highlights the economic and water use benefits of CEA, its adoption is influenced by factors beyond policy and training. Capital costs, maintenance expertise, and local microclimate factors also play a crucial role in determining the feasibility of CEA systems. The initial investment required for poly-tunnel infrastructure is significant, which may pose financial barriers for smallholder farmers. Access to funding or subsidies could facilitate broader adoption. Additionally, effective CEA operation demands technical knowledge in irrigation management, climate control, and pest regulation, which can impact scalability. Local microclimate factors, such as temperature, humidity, and solar radiation variations, influence CEA's efficiency, making an understanding of regional climate conditions essential for optimizing poly-tunnel systems to achieve maximum productivity.

By addressing these elements, this study provides a more holistic perspective on the challenges and enablers of CEA adoption, ensuring that policymakers and stakeholders consider both economic and technical feasibility when promoting CEA as a sustainable agricultural solution.

6. Implications

The findings of this study have significant implications for sustainable a g r i c u l t u r a l p r a c t i c e s , w a t e r conservation strategies, and economic decision-making in chili pepper cultivation. The substantial differences in water use efficiency between Controlled Environment Agriculture (CEA) and field-based systems highlight the need for policy interventions and farmer adoption of climate-smart agricultural techniques. With poly-tunnel farming reducing water consumption by over 99% compared to open-field irrigated cultivation, this study underscores the importance of precision irrigation and controlled environments in addressing water scarcity challenges, particularly in arid and semi-arid regions.

Beyond policy and training, CEA adoption is influenced by several critical factors, including capital costs, maintenance expertise, and local microclimate conditions. The initial investment required for poly-tunnel infrastructure can pose financial barriers, particularly for smallholder f a r m e r s . A l t h o u g h t h e s t u d y demonstrates that poly-tunnel farming

offers substantial financial returns—with a Benefit-Cost Ratio (BCR) of 22.11 compared to 0.89 for open-field farming—the upfront costs remain a limiting factor. Strategic financial support, such as subsidies or loan programs, could play a vital role in facilitating broader adoption of CEA.

Maintenance expertise is another essential consideration, as effective CEA operation requires specialized technical knowledge in areas such as irrigation management, climate control, and pest regulation. Without adequate training and access to skilled personnel, farmers may struggle to optimize system performance, potentially reducing efficiency and yield. Initiatives aimed at capacity-building, including farmer training programs and technical assistance, could address this challenge and enhance the scalability of CEA systems.

Local microclimate conditions further influence the feasibility of CEA adoption. Variations in temperature, humidity, and solar radiation impact the efficiency of poly-tunnel farming, requiring careful site selection and adaptive management strategies. Understanding regional climatic characteristics is essential to optimizing poly-tunnel systems for maximum productivity and sustainability.

From a broader perspective, these findings emphasize the need for agricultural policies that support the adoption of water-efficient technologies while addressing financial and technical constraints. The study provides data-driven evidence that can inform government initiatives, subsidies, and training programs to ensure a holistic approach to CEA adoption. Additionally, the demonstrated reduction in climate-related losses within poly-tunnel farming presents an opportunity for resilient food production systems, mitigating the effects of climate change on crop yields and agricultural profitability. By considering capital investment, expertise requirements, and environmental conditions, policymakers and stakeholders can create more comprehensive strategies to promote CEA as a sustainable agricultural solution.

7. Conclusion

This study demonstrates the superior water use efficiency and economic viability of Controlled Environment Agriculture (CEA) compared to traditional field-based systems in chilli pepper production. Water consumption was significantly reduced in poly-tunnel farming, requiring only 13,536.50 liters per season to produce 72,000 kg of Piquante Red F1 Habanero, achieving a water use efficiency of 0.19 L/kg. In contrast, the open-field irrigated system required 920,850 liters per season to produce 4,500 kg of Scotch Bonnet Pepper, resulting in a water use efficiency of 204.63 L/kg—over 1,000 times less efficient than CEA.

The ANOVA results confirmed a statistically significant difference ($F = 854.9$, $p < 0.001$) between the two systems, while pairwise t-tests further validated this difference with a mean water use gap of 204.44 L/kg ($t = 29.3$, $p < 0.001$). These findings substantiate that CEA drastically enhances water conservation, making it an optimal choice for sustainable chilli pepper cultivation in water-scarce environments.

Additionally, the economic assessment revealed that poly-tunnel farming is exceptionally profitable, achieving a Benefit-Cost Ratio (BCR) of 22.11, meaning for every N1 invested, farmers receive N22.11 in return. Despite higher fixed costs (N3,657,000), the payback period was just 0.05 years (~19 days), demonstrating rapid investment recovery. Conversely, open-field irrigated farming remained financially unsustainable, with a negative net return of -N731,450 and a BCR of 0.89, failing to generate sufficient revenue to cover production expenses.

Overall, this study provides strong quantitative evidence that CEA significantly outperforms open-field chilli pepper farming in both water efficiency and economic returns, reinforcing its potential for large-scale adoption in resource-constrained agricultural systems.

8. Recommendations

To enhance the adoption of poly-tunnel farming and improve water use efficiency in chili pepper cultivation, we propose the following targeted strategies:

1. Financial Incentives and Subsidies for Poly-Tunnel Adoption

Given the high initial investment required for poly-tunnel farming, targeted subsidies should be introduced to support smallholder farmers. The Anchor Borrowers' Programme (ABP) in Nigeria could be expanded to include funding for controlled environment agriculture (CEA). Additionally, the Federal Ministry of Agriculture and Rural Development (FMARD) should collaborate with state governments to provide direct financial assistance for poly-tunnel infrastructure.

2. Low-Interest Credit Schemes for CEA Investment

Access to affordable financing remains a key barrier to poly-tunnel adoption. We recommend the establishment of low-interest credit schemes through the Bank of Agriculture (BOA) and the Nigeria Incentive-Based Risk Sharing System for Agricultural Lending (NIRSAL). These institutions could develop CEA-specific loan packages with flexible repayment terms to encourage investment in water-efficient farming technologies.

3. Public-Private Partnerships (PPPs) for Infrastructure Development

To scale up poly-tunnel farming, public-

private partnerships (PPPs) should be leveraged to attract investment in CEA infrastructure. The African Development Bank (AfDB) and the International Fund for Agricultural Development (IFAD) could collaborate with local agribusinesses to provide funding and technical support for poly-tunnel systems. Additionally, private sector involvement in equipment leasing programs could reduce upfront costs for farmers.

4. Capacity Building and Technical Training for Farmers

Effective poly-tunnel farming requires specialized knowledge in irrigation management, climate control, and pest regulation. We recommend the implementation of nationwide farmer training programs through agricultural extension services. The National Agricultural Extension and Research Liaison Services (NAERLS) should integrate CEA-focused workshops into existing farmer education initiatives.

5. Policy Integration and Institutional Support

To ensure long-term sustainability, poly-tunnel farming should be incorporated into national agricultural policies. The Federal Ministry of Agriculture and Rural Development (FMARD) should develop CEA-specific guidelines that align with Nigeria's National Agricultural Technology and Innovation Policy (NATIP). Additionally, local governments should provide land-use incentives for farmers adopting poly-tunnel systems.

6. Research and Data-Driven Policy Formulation

Further research is needed to assess the long-term economic and environmental impacts of poly-tunnel farming. We recommend the establishment of CEA research hubs within universities and agricultural institutes to generate data-driven policy recommendations. Collaboration with international research organizations such as the International Institute of Tropical Agriculture (IITA) could enhance knowledge-sharing and innovation in water-efficient farming.

By implementing these specific financial, institutional, and technical strategies, policymakers can effectively promote poly-tunnel adoption, ensuring sustainable agricultural practices and enhanced water use efficiency in chili pepper cultivation.

Ethical Statement

This study was conducted in compliance with established institutional ethical guidelines to ensure integrity and transparency in research involving human participants. Informed consent was obtained from all farmers who participated in the survey, ensuring that they voluntarily agreed to provide information with full knowledge of the study's purpose and scope.

To uphold data confidentiality, all

responses were anonymized, and personal information was safeguarded. No identifying details were disclosed in the analysis or reporting of findings. Additionally, ethical clearance for this study was obtained from the relevant institutional review board, affirming adherence to ethical research standards.

References

Abimbola, O. (2024). Radiation use efficiency and yield response of chili pepper under rainfed agriculture in Akure, Nigeria. *International Journal of Eastern Mediterranean Agricultural Research, 7*(1), 1–21.

Adesogan, A., & Sasanya, J. (2025). Climate-smart water conservation strategies for sustainable development in Nigeria. *African Journal of Environmental Studies, 21*(4), 188–203. https://doi.org/10.xxxx/xxxxx

Aduramigba-Modupe, A., & Oke, F. T. (2023). Precision agriculture and smallholder irrigation systems in West Africa. *Journal of Sustainable Agriculture, 19*(3), 125–140. https://doi.org/10.xxxx/xxxxx

Ahmed, A., Oyebode, M. A., Igbadun, H. E., & Ezekiel, O. (2020). Estimation of crop water requirement and crop coefficient of tomato crop using meteorologicaldata in Pampaida Millennium Village, Kaduna State, Nigeria. *FUDMA Journal of Sciences, 4*(3), 538–546. https://doi.org/10.xxxx/xxxxx

Ajayi, A. J., Ajayi, G. O., & Omoniyi, L. O. (2024). Economic analysis of bell pepper cultivated under screen house production system in Ondo State, Nigeria. *Nigeria Agricultural Journal*. https://www.ajol.info/index.php/naj/article/view/277052

Akinbile, C. O., & Yusoff, S. (2011). Different irrigation scheduling effects on crop yield and water use efficiency in Akure, Nigeria. *Asian Journal of Agricultural Research, 5*(2), 154–163.

Akinyele, O. A., & Eze, C. O. (2023). Feasibility of hydroponics in Nigeria. *Journal of Agricultural Science and Technology* . https://www.jast.org.ng/article/view/1234

Asravor, J., Onumah, E. E., & Osei-Asare, Y. B. (2016). Efficiency of chili pepper production in the Volta region of Ghana. *Journal of Agricultural Extension and Rural Development, 8*(6), 99–110. Available here

Fernandez, M. D., Gallardo, M., Bonachela, S., Orgaz, F., Thompson, R. B., & Fereres, E. (2023). Water use and production of a greenhouse pepper crop under optimum and limited water supply. *Journal of Horticultural Science and Biotechnology, 98*(4), 1–15. Available here

Food and Agriculture Organization. (2025). *Pepper: Land & water management for sustainable cultivation*. FAO. Retrieved June 14, 2025 from FAO Database

Gabriel, B. L., Guerrero-Arboleda, B. D., Shkiliova, L., Zambrano-Arteaga, R. I., Sánchez Moreira, J. D., & Ramírez Castro, A. E. (2023). Energy contributions and greenhouse gas emissions in pepper (*Capsicum annuum L.*) cultivation with plastic mulch. *Revista Ceres, 70*(5), 1–12. Available here

Gomes, K., Bajic, I., Pejic, B., Vlajic, S., Adamovic, B., Popov, O., & Simic, D. (2023). Yield and water use efficiency of drip irrigation of pepper. Water, 15(2891), 1–12. https://doi.org/10.3390/w15162891

Isah, M. E., Wasah, A., & Matsubae, K. (2025). Life cycle assessment research and application in Nigeria. *The International Journal of Life Cycle Assessment, 30*, 880–895. https://doi.org/10.1007/s11367-024-02423-6

Institute for Agricultural Research (IAR), Meteorological Unit. (2021). Weather and Climate Data for Kudan Local Government Area. Retrieved from https://nimet.gov.ng/

Johnson, L., Adebayo, M., & Musa, K. (2023). Water use and agricultural productivity growth in Sub-Saharan Africa: An integrated assessment. *Journal of Agricultural Water Management, 59*(1), 200–219. https://doi.org/10.xxxx/xxxxx

Kalitsilo, L., Abdullahi, L., Mbeye, N., Mwandira, L., Hara, H., Mitambo, C., & Oronje, R. (2025). Vector-borne disease control interventions in agricultural and irrigation areas in sub-Saharan Africa: A systematic review. *PLOS ONE, 20*(2), e0302279. https://doi.org/10.1371/journal.pone.0302279

Krasilnikov, P., Taboada, M. A., & Amanullah. (2022). Fertilizer use, soil health and agricultural sustainability. *Agriculture, 12*(4), 462. https://doi.org/10.3390/agriculture12040462

Kumar, R., Patel, S., & Verma, T. (2022). Deficit irrigation strategies and water use efficiency in semi-arid chili pepper cultivation. *Irrigation Science, 40*(2), 189–204. https://doi.org/10.xxxx/xxxxx

Lasisi, M. O., Omotayo, F. S., & Ejiko, S. O. (2024). Cost and yield analysis of drip-irrigated green pepper under poly house and open-field conditions. *Journal of Engineering and Earth Sciences, 17*(1), 45–58. Retrieved from https://jees.fedpolyado.edu.ng/storage/published/JEES-DBSVTA-

1 8 3 9 6 7 6 - CostAndYieldAnalysisofDripIrrigate d G r e e n P e p p e r U n d e r P o l y - HouseAndOpen-FieldConditions.pdf

Madina, P., Esang, D. M., Akinyemi, B. K., & Chikowa, N. (2024). Organic production of pepper as influenced by variety grown in Makurdi, Benue State, Nigeria. *International Journal of Agricultural and Environmental Sciences, 10* (8), 81–92. https://doi.org/10.56201/ijaes.v10.no8.2024.pg.81.92

Mitku, G., & Abebaw, Y. (2024). Farmers' perceptions and practices in managing vegetable pests and pesticide use in the Upper Blue Nile Basin, Ethiopia: The case of the Koga irrigation system. *International Journal of Ecotoxicology and Ecobiology*, 9 (4), 139–147. https://doi.org/10.11648/j.ijee.20240904.13

Ndagana, M. K., Buba, A., & Umar, A. B. (2021). Effect of transplanting dates on growth and yield components of pepper (*Capsicum* spp) in Badeggi, Nigeria. *FUDMA Journal of Agriculture and Agricultural Technology, 7* (2) . https://www.jaat.fudutsinma.edu.ng/index.php/jaat/article/view/60

Nicholson, D., Turner, G., & Lawson, R. (2020). Increase of light transmission by 10% in the Venlo-type greenhouse: From design to results of a cucumber experiment. Acta Horticulturae, 1296, 541–550. https://doi.org/10.17660/ActaHortic.2020.1296.70

Nwite, J. C. (2024). Soil amendments and pepper variety effects on soil physicochemical properties and yield of pepper in Ishiagu, Southeastern Nigeria. InternationalJournal of Recycling of Organic Waste in Agriculture, 14(1). https://doi.org/10.57647/ijrowa-a6re-9251

Nwonu, P. C., Nwobodo, C. E., Onwubuya, E. A., & Obazi, S. A. (2022).Farmers' use of sustainable production practices for yellow pepper crop in the Nsukka agricultural zone, Enugu State, Nigeria. *Acta Universitatis Sapientiae Agriculture and Environment, 14* , 13–28. https://doi.org/10.2478/ausae-2022-0002

Oderinde, F. O., Akano, O. I., & Adesina, F. A. (2022). Trends in climate, socioeconomic indices, and food security in Nigeria: Current realities and challenges ahead. *Frontiers in Sustainable Food Systems, 6*, 940858. https://doi.org/10.3389/fsufs.2022.940858

Oji, R. O., & Anih, J. (2021). Addressing food security challenges in Nigeria. *International Journal of Innovative Development and*

Policy Studies, 9(3), 163–176. https://www.seahipublications.org/wp-content/uploads/2024/08/IJIDPS-S-17-2021.pdf

Olabisi, T., & Nofiu, A. (2022). Temperature sensitivity and growth variations in Capsicum species under controlled and field conditions. *Journal of Plant Science Research, 50(3),* 190–205. https://doi.org/10.xxxx/xxxxx

Olotu, Y., Alao, F., & Cletus, O. J. (2012). Yield-crop water use (CWU) evaluation for pepper production under irrigated cultivation in Akure, *Nigeria. Global Journal of Science Frontier Research: Agriculture & Biology, 12(1), 1–12.* Available here

Oyeranti, O. A. (2024). Effect of carbon footprint on agricultural productivity in Nigeria: An empirical analysis. *Journal of Environmental Economics and Policy, 17(2),* 145–162. https://doi.org/10.xxxx/xxxxx

Peprah, K. (2023). Climate variability and agricultural productivity in West Africa: Implications for food security. *African Journal of Agricultural Research, 18*(4), 189–204. https://doi.org/10.xxxx/xxxxx

Regmi, A., Rueda-Kunz, D., Liu, H., Trevino, J., Kathi, S., & Simpson, C. (2024). Comparing resource use efficiencies in hydroponic and aeroponic production systems. *Technology in Horticulture, 4*(1), e005. https://doi.org/10.48130/tihort-0024-0002

Regmi, R., Patel, S., & Verma, T. (2024). Hydroponics and aeroponics: Water-efficient solutions for sustainable agriculture. *Irrigation Science, 42*(1), 112–130. https://doi.org/10.xxxx/xxxxx

Salami, H. A. (2019). A comparative life cycle assessment of energy use in major agro-processing industries in Nigeria. *Journal of Environmental and Natural Resource Research, 3*(4), 1–11. https://www.researchgate.net/publication/335965040

Tanaskovik, V., Cukaliev, O., Romić, D., Ondrasek, G., Savić, R., Markoski, M., & Nechkovski, S. (2019). Water use efficiency and pepper yield under different irrigation and fertilization regimes. *Contributions, Section of Natural, Mathematical and Biotechnical Sciences, 40*(1), 53–62. https://repository.ukim.mk/bitstream/20.500.12188/15454/1/WATER%20USE%20EFFICIENCY%20AND%20PEPPERYIELD%20UNDER%20DIFFERENT%20IRRIGATION%20AND%20FERTILIZATION%20REGIME.pdf

Vanlommel, W., Holsteens, K., Moerkens, R., & Van de Poel, B. (2020). The effect of low-haze

diffuse glass on greenhouse tomato and bell pepper production and light distribution properties. *Plants, 9*(6), 1–15. Available here

Varughese, C., Ansari, R., & Solanki, V. (2021). Comparative study of hydroponics and aeroponics: Water efficiency and automation in crop cultivation. *Agricultural Water Management, 78*(4), 230–245. https://doi.org/10.xxxx/xxxxx

Varughese, I. R., Joy, J. P., Roy, R., & Benny, T. (2021). Comparison of hydroponics and aeroponics: A review. *International Journal of Research and Applications, 21* (B1), 447–460. https://ijrar.org/papers/IJRAR21B1447.pdf

Yadav, A. K., & Kashyap, P. S. (2024). Water management for chili (Capsicum annuum L.) crop in sub-tropical humid regions. *International Journal of Environment, Agriculture and Biotechnology, 9(4)*, 1–12. https://doi.org/10.22161/ijeab.108202417

Zhang, Y., Chen, L., & Wang, H. (2021). Mulched drip irrigation and its impact on chili pepper yield in semi-arid China. *Agricultural Water Management, 250*, 106897. https://doi.org/10.xxxx/xxxxx

Comparative Analysis of the Mineral and Anti-Oxidative Compositions of Watermelon and Beetroot

[1]Akintomide H.T and [2]Ogunsile S. E.

[1]Nutrition and Dietetics Department Ekiti State University Teaching Hospital, Ado-Ekiti

[2]Department of Human Kinetics and Health Education, EKSU, Ado-Ekiti

Corresponding author: elizabeth.ogunsile@eksu.edu.ng/+2347039025304

Abstract

This study was carried out to compare the mineral and anti-oxidative composition of watermelon and beetroot in relation to their usefulness in the prevention and management of heart related conditions. Eighty five grams each of whole watermelon and beetroot (flesh, peel and seeds) were blended separately without water, poured in separate containers, coded, kept in ice pack, and analysed for mineral and antioxidant compositions using standard procedures. The result of the mineral composition of the food samples shows that watermelon has significantly higher content of sodium and potassium than beetroot (80.60 ± 0.14 vs 75.30 ± 0.28; p<0.05) and (110.00 ± 0.42 vs 70.40 ± 0.14; p<0.05) respectively. On the other hand, Beetroot has more of flavonoid, phenolic compounds and lycopene than watermelon (21.9 ± 5.9 vs 15.4 ± 6.6, 46.0 ± 18.1 vs 8.7 ± 0.1, 27.8 ± 6.1 vs 21.9 ± 0.3) respectively. Based on the findings of this study, it could be concluded that watermelon and beetroot could be of great health benefit as functional foods in the prevention and management of heart related conditions. It is therefore recommended that healthy individuals and those with heart–related conditions could have a liberal intake of watermelon and watermelon

Key words: Watermelon, beetroot, anti-oxidative, biochemical, comparative analysis

Introduction

Over the years and the world over, fruits and vegetables have been considered as important parts of a healthy diet due to their health promoting properties and their capacity for preventing several diseases (Jeffery, 2005; Shashirekha et al., 2015). Fruits and vegetables are good sources of vitamins, such as vitamin C and A, they are good sources of minerals such as electrolytes, they have a high concentration of phytochemicals especially the antioxidants such as flavonoids and

betalamins (Alemu, 2024), and they are also being recommended as a very good sources of dietary fiber (Dhingra et. al., 2011).

Fruits and vegetables are classified from botanical and culinary points of view. Botanically, fruits contain seeds and develops from the flowering part of a plant. Vegetables on the other hand are the other parts of a plant, such as the leaves, stem, roots, and bulbs (Ajimera, 2024; Medical News Today, 2024). From the culinary standpoint, fruits are often associated with sweet taste. While vegetables are associated with a savory taste (Medical News Today, 2024). Commonly eaten fruits worldwide include: apple, pear, orange, grape, lemon, pineapple, watermelon among others. Vegetables include: celery, spinach, lettuce, amaranthus, and beetroot among others Watermelon (*Citrullus lanatus*), a juicy and sweet fruit, having bright red flesh, is one of the commonly eaten fruits in Nigeria. Watermelon is low in calories, free of fat and contains a significant amount of vitamins A, B6 and C, lots of lycopene, other antioxidants and amino acids, and a moderate quantity of potassium (Szalay & Dobrijevic, 2022). Watermelon contains approximately 92% of water, hence, it can be used as a means for quenching thirst during hot weather conditions (Jeanings & Hallal, 2024). In addition, all the parts of watermelon, the pulp, seeds, rind and peels, are edible and contain significant amount of nutrients and phytochemicals.

Beetroot (Beta vulgaris L) is a natural multivitamins containing vitamins, minerals, nitrates, dietary fibre, phytochemicals and other beneficial nutrients for boosting health and performance. In recent times, the beetroot has become popular as a potential functional food in preventing and treating multiple diseases (Chen et al., 2021). Previous researches have reported that beetroot is made up of numerous phytochemicals such as betalains, flavonoids, polyphenols and saponins. Beetroot, according to Singh and Hathan (2014), is also rich in minerals such as potassium, sodium, phosphorous, calcium, magnesium, copper, iron, zinc and manganese.

Numerous health benefits that are associated with the intake of watermelon and Beetroot have been reported in the literature. These include: improving cardiovascular health, reducing blood pressure in hypertensive patients, decreasing LDL (low-density lipoproteins) and fighting against age-related degenerative diseases and certain types of cancer (Mirmiran 2020; Meghwar et al., 2024).Thus making them useful ingredients in the dietary management of non- communicable diseases such as diabetes mellitus and hypertension.

To determine the nutritional values and chemical properties of food items, it is important to carry out a food analysis.

This will help in identifying the nutrients, phytonutrients, antioxidants and other substances present in such foods (Infinita, 2023). One of the components of food analysis, is the determination of the proximate composition of foods, also called proximate analysis. Proximate analysis is defined as a chemical method used for determining the moisture, ash, protein, fats and carbohydrate components of food samples (Fiveable, 2024). Through proximate analysis, a comparison of the nutrient value of different food substances can also be carried out so as to determine their nutritional value and to determine which food substance is higher or lower in a particular food nutrient or whether both food items are having similar nutritional values.

Determining the mineral composition of edible food substances, is another component of food analysis. This entails determining the presence and amounts of various inorganic elements found in such food substances. Mineral elements in food could be macro-minerals such as calcium, magnesium, phosphorus, sodium, potassium, chloride, and sulfur, or trace minerals such as iron, copper, iodine, zinc, manganese, fluoride, cobalt, and selenium. Minerals play important roles in the normal functioning of the body. For example, calcium and phosphorus play vital roles in building and maintaining bones and teeth, sodium and potassium help in fluid and maintaining electrolyte balance, calcium, potassium and magnesium helps in impulse and muscle contractions, iron is vital for blood formation, zinc and selenium play vital roles in immune system functions and lots more. It is therefore essential to determine the mineral composition of foods so as to provide an insight to the type of mineral element contained in a food substance.

In addition to proximate and mineral analysis, determining the anti-oxidative properties of food is another component of food analysis. Antioxidants are compounds which, helps to delay, control or prevent oxidative processes that cause food quality deterioration or the propagation of degenerative diseases in an organism (Munteanu & Apetrei, 2021). Antioxidants prevent or slow cell damage that are caused by free radicals, which are unstable molecules that the body produces as a reaction to environmental and other pressures (MedicalNews Today, 2025). Antioxidants can be obtained from plant based food sources such as fruits and vegetables. Antioxidants include Lycopene, Phenols, Akaloids, Flavonoids and many others and they and they play vital roles in the maintenance of human health.

Flavonoids, an antioxidants found in fruits, herbs, stems, cereals, nuts, vegetables, f lowers and seeds (Feliciano, 2015: Shan et al., 2017) have been used extensively in the field of medicine as anticancer (Zhao et al., 2019), antimicrobial, antiviral,

antiangiogenic (Camero et al., 2018), antimalarial, antioxidant, neuroprotective, antitumor, and anti-proliferative agents (Patel et al., 2018). In addition, Flavonoids has been reported to have the potential of preventing cardio-metabolic disorders (Mazidi et al., 2018), and also to be an effective antihypertensive agent (Khan et al., 2018). Alkaloids, another kind of antioxidant, have been reported to have the potential of curing neurodegenerative diseases by targeting the oxidative stress mechanism (Sirin et al., 2023).

Phenolic compounds, another antioxidants found in food, has been reported to possess several health benefits such as antibacterial, antihyperlipidemic, anticancer, antioxidants, cardioprotective, neuroprotective, and antidiabetic properties (Zeb, 2020). Lycopene, a fat-soluble carotenoid, is another antioxidant worthy of note. This carotenoid, a bioactive organic pigment, is found in pink grapefruit, papaya, guava, apricot, watermelon, tomatoes and vegetables. Lycopene has been reported to be one of the strongest antioxidants among carotenoids (Imran et al., 2020). Several studies have investigated the potential of lycopene to mitigate risk factors for obesity, type 2 diabetes mellitus, and cardiovascular diseases, conditions characterised by dyslipidaemia, oxidative stress, and inflammation (*Świątkiewicz* , et al., 2023). Research suggests that regular consumption of lycopene as a dietary supplement can potentially remediate insensitivity to insulin, hypertension, and obesity- related metabolic complications (Rejali et al., 2022).

Over the years, there has been a lot of claims on the beneficial effects of some foods over the others without much research-based evidence. Although the literature has reported much about the nutritional and anti-oxidative properties of watermelon and Beetroot, not much has been done to compare the nutritional quality of these food items in relation to their suitability in the nutritional management of non-communicable diseases. Hence the purpose of this study.

Materials and Methods

Sample collection and Preparation

The samples of Water melon (Citrullus lanatus) and Beetroot (Beta vulgaris L) were obtained from two fruit shops that were purposively selected for their hygienic dispositions in Ado-Ekiti, the capital city of Ekiti State. After a thorough washing of the samples, Eighty five grams each of whole watermelon and beetroot (that is, watermelon and beetroot containing the flesh, peel and seeds) were homogenized using a blender without adding water, poured in separate coded containers and refrigerated. The refrigerated samples were then used for the mineral anti-oxidative analyses using standard procedures.

Analysis of the Mineral Contents of Samples

To determine the mineral composition of the samples, 1g of each sample to be analysed for mineral content was ashed, filtered and diluted with 5% HCL and 5%Nitric acid. The solution was kept in a reagent bottle. The mineral content in the samples were determined using the Atomic Absorption Spectrophotometry (AAS). The minerals determined from whole Beetroot and Watermelon include: Sodium, potassium, phosphorus and magnesium.

Analysis of the Anti-oxidative Properties of Samples

The analysis of the anti-oxidative properties involves the determination of the flavonoids, alkanoids, lycopene, and phenolic compounds in each food sample using standard procedures

Statistical Analysis

Data analysis was carried out using SPSS version 23. The result of data analysis were expressed as mean and standard deviation. Differences in the mean values of the minerals and antioxidants were obtained using t-test. All inferences were made at 0.05 level of significance

Results

The result obtained from this study shows that there is a significant difference in the mineral composition of watermelon (flesh only), whole watermelon and whole beetroot. Whole watermelon has more of sodium and potassium than whole beetroot. However, beetroot has more of magnesium and phosphorus than watermelon. In addition, the result obtained from this study shows that Beetroot has a higher content of flavonoids, phenols and lycopene than watermelon, although the difference is not significant. Watermelon on the other hand has a significantly higher content of alkaloids than beetroot (Table 2).

Table 1: Comparison of the Mineral Content of Watermelon and Beetroot

Mineral	Watermelon (whole)%	Beetroot (whole)%	t	p
NA (ppm)	80.6±0.14	75.3±0.28	-23.702	0.002
K (ppm)	110.3±0.42	70.4±0.14	-126.175	0.000
Mg (ppm)	47.0±0.35	56.3±0.21	31.898	0.001
P (ppm)	40.4±0.21	42.9±0,49	6.565	0.022

Table 2: Comparison of the Anti-oxidative Composition of Watermelon and Beetroot

Antioxidant	Watermelon (whole) mg/g %	Beetroot (whole)mg/g %	t	P
Flavonoid	15.4±6.60	21.9±5.90	-1.043	0.407
Alkaloids	15.8±0.81	1.7±1.97	9.308	0.011
Phenolic Compounds	8.7±0.09	46.0±18.2	-2.912	0.100
Lycopene	21.9±0.27	27.8±6.11	-1.389	0.299

Discussion

This study was carried out to compare the mineral content and the anti-oxidative compositions of watermelon and beetroot. The findings of this study showed that watermelon has more of sodium and potassium than beetroot, while beetroot has more of magnesium and phosphorus than watermelon. Abdo et al., (2020) also reported that beetroot has high phosphorous content. This finding is also likely to be the as a result of the high protein content of watermelon.

The findings of this study show that beetroot is higher in flavonoid, phenols and lycopene than watermelon. This is similar to the findings of Ceclu and Oana-Viorela (2020) who also reported that beetroot is high in phenolic compounds. Watermelon on the other hand is higher in alkaloids than beetroot and this might be due to a higher protein content of watermelon than beetroot.

The high level of anti-oxidative composition, mineral and fiber contents of watermelon and beetroot suggests their usefulness in the prevention and dietary management of chronic diseases like diabetes, obesity and high blood pressure. According to Mirmiran 2020; Meghwar et al., 2024, the intake of watermelon and beetroot is associated improvement in cardiovascular health, lowering of blood pressure in hypertensive patients, decreasing LDL (low-density lipoproteins) and fighting against age-related degenerative diseases and certain types of cancer. Thus making them useful ingredients in the dietary management of non-communicable diseases such as diabetes mellitus and hypertension.

Conclusion

Based on the findings of this study, it can be concluded that both watermelon and beetroot are of good nutritional value in terms of the proximate, mineral and anti-oxidative compositions. Only slight variations exist between them. Also, except for alkaloid that is conspicuously lower in beetroot than in watermelon, both watermelon and beetroot show a high level of antioxidants properties. It is therefore recommended that individuals, irrespective of health status, have a liberal intake of watermelon and

beetroot so as to enjoy the nutritional, anti-oxidative and other benefits. Also, future research to determine the servings of watermelon and beetroot that will best suited for the management of selected chronic diseases is required.

References

Abdo, E., El-Sohaimy, S., Shattout, O., Abdallaha & Zeatoun, A. (2020). Nutritional evaluation of beetroots (Beta Vulgaris L) and its potential application in a functional beverage. Plants. Basel. 9 (12): 1752.

Aderiye, B.I. et al (2020).Immunomodulatory and phytochemical properties of watermelon juice and pulp (citrullin lanatus linn): A review. GSC Biological and Pharmaceutical Sciences.11 (02); 153-165.

Ajimera, R. (2024). What's the difference between fruits and vegetables? https://www.healthline.com /nutrition/ fruits-vs-vegetables#TOC_TI TLE_HDR_7 15/09/2024.

Alemu, T. K. (2024). Nutritional contributions of fruit and vegetable for human health: A review International Journal of Health Policy Planning. 3(1):1-9.

Camero C.M., Germanò M.P., Rapisarda A., D'Angelo V., Amira S., Benchikh F., Braca A., De Leo M (2018). Anti-angiogenic activity of iridoids from Galium tunetanum. Rev. Bras. de Farmacogn. 28:374–377. doi: 10.1016/j.bjp.2018.03.010.

Ceclu, L. & Oana-Viorela, N. (2020). Red beetroot: composition and health effects-a review. *Journal of Nutritional Medicine and Diet Care.* 6(1), 1-9

Chen, L., Zhu, Y., Hu, Z., Wu, S. & Jin, C. (2021). Antioxidant, antitumor, physical function,and chronic metabolomics activity. Food Science and Nutrition. 9(11): 6406–6420.

Dhingra, D., Michael, M., Raiput, H. & Patil, R. T. (2011). Dietary fibre in foods: a review. Journal of Food Science and Technology 49 (3): 255-266.

Feizy, J., Jahai, M., & Fasy (2020). Antioxidant activity and mineral content of watermelon peel. Journal of food and Bioprocess Engineering. 3(1): 35-40.

Feliciano R.P., Pritzel S., Heiss C. & Rodriguez-Mateos A.(2015). Flavonoid intake and cardiovascular disease risk. Curr. Opin. Food Sci. 2:92–99. doi: 10.1016/j.cofs.2015.02.006.

Fiveable (2024). Proximate analysis – Principles of food science. https://library.fiveable.me/key-terms/principles-food-science/proximate-analysis

Imran M., Ghorat F., Ul haq I., et al. Lycopene as a natural antioxidant used to prevent human health disorders. Antioxidants. 9 (8):706–727. doi: 10.3390/antiox9080706.

Infinita (2023). Laboratory food analysis: The nutritional value of foods.

Jeffery, E. (2005). Component interactions for efficacy of functional foods. Journal of Nutrition, 135, 1223–1225. 10.1093/jn/135.5.1223

Jennings, A. N. & Hallal, F. (2024). The top health benefits of watermelon. 15/09/2024.

Khan S., Khan T. & Shah A. J. (2018). Total phenolic and flavonoid contents and antihypertensive effect of the crude extract and fractions of Calamintha vulgaris. Phytomedicine. 47:174–183. doi: 10.1016/j.phymed.2018.04.046.

Manivannan, A. et al (2020). Versatile neutraceutical potentials of watermelon. A modest fruit loaded with pharmaceutically valuable phytochemicals. Molecules. 25(22): 5258.

Mazidi M., Katsiki N., Banach M. A (2019). Higher flavonoid intake is associated with less likelihood of nonalcoholic fatty liver disease: Results from a multiethnic study. J. Nutr. Biochem. 65 : 66 – 71 . doi: 10.1016/j.jnutbio.2018.10.001.

Medical New Today (2024). What is the difference between fruits and vegetables . https://www.medicalnewstoday.com/articles/fruits-vs-vegetables#affordable-options. Accessed 15/09/2024.

MedicalNewsToday (2025). How can antioxidant benefit our health? https://www.medicalnewstoday.com/articles/mushroom-coffee-benefits#summary

Meghwar, P., Saheed, S. M. G, Ullah, A., Nikolalakis, E., Panagopoulou, E., Tsoupras, Dimaoui, S. & Khaneghah, A. M. (2024). Nutritional benefits of bioactive compounds from watermelon: A comprehensive review. Food Bioscience. 61, 104609

Mirmiran, P., Houshialsadat, Z., Gaeini, Z. *et al.* (2020).Functional properties of beetroot (*Beta vulgaris*) in management of cardio-metabolic diseases. Nutr Metab. **17**, 3https://doi.org/10.1186/s12986-019-0421-0

Munteanu, I. G. & Apetrei C. (2021). Analytical methods Used in determining antioxidant activity: A review. I*nt. J. Mol. Sci. 22*(7), 3380; https://doi.org/10.3390/ijms22073380

Patel K., Kumar V., Rahman M., Verma A. & Patel D. K. (2018). New insights into the medicinal importance, physiological functions and bioanalytical aspects of an important bioactive compound of foods 'Hyperin': Health benefits of the past, the present, the future. Beni-Suef Univ. J. Basic Appl. Sci. 7:31–42. doi: 10.1016/j.bjbas.2017.05.009.

Rejali L., Ozumerzifon S., Nayeri H. & Asgary S. (2022). Risk reduction and prevention of cardiovascular diseases: biological mechanisms of lycopene. Bioactive Compounds in health and disease . 5(10):202–221. doi: 10.31989/bchd.v5i10.975.

Singh, B, & Hathan, B. S. (2014). Chemical composition, functional properties and processing of beetroot—a review. Int J Sci Eng Res. 5(1):679–684

Sirin, S., Dolanbay, S. N. & Aslim, B. (2023). Role of plant derived alkaloids as antioxidant agents for neurodegenerative diseases. Health Sciences Review. 6; 1-11.

Zeb A. (2020). Concept, mechanism, and applications of phenolic antioxidants in foods. Journal of Food Biochemistry. 44(9):e13394. doi: 10.1111/jfbc.13394.

Zhao L., Yuan X., Wang J., Feng Y., Ji F., Li Z., & Bian J.(2019). A review on flavones targeting serine/threonine protein kinases for potential anticancer drugs. Bioorganic Med.Chem. 27:677–685. doi: 10.1016/j.bmc.2019.01.027.

Numerical Assessment of a White Noise-Enhanced Advection-Diffusion Model Describing Water Pollution

Oluwatayo Michael Ogunmiloro[1], Kayode James Adebayo[1], Oluwagbenga Samuel Akinwumi[1]
[1]Department of Mathematics, Faculty of Science,
Ekiti State University, Ado - Ekiti, Nigeria.
corresponding author email: oluwatayo.ogunmiloro@eksu.edu.ng

Abstract.
This study concerns the dynamics of water pollution through a detailed model derivation using the advection-diffusion-reaction principle. The model is further expanded to include stochastic influences by integrating white noise. Utilizing a discretized Runge-Kutta fourth-order method (RK4) for the numerical solution, the effects of variable flow velocities, diffusion coefficients, and stochastic white noise on the dispersion of pollutants within aquatic environments were studied. The deterministic framework of the model depicts the pollutant dispersion phenomenon, while its stochastic extension introduces the element of environmental unpredictability characteristic of natural water systems. The comparative analysis between deterministic and stochastic scenarios reveals significant differences in pollutant dispersion patterns under diverse initial and boundary conditions. The findings show the essential role of incorporating stochasticity to more accurately reflect the erratic behavior of pollutants and the inherent unpredictability in the dispersion processes within natural water bodies.

Keywords: Stochastic, partial differential equation, discretized RK4

1. INTRODUCTION

Water pollution represents one of the mostpressingenvironmental challenges of the 21st century, affecting ecosystems, human health, and economic development across the globe, Goel (2006). The nature of water systems, coupled with anthropogenic activities, result in diverse pollution scenarios that necessitate sophisticated analytical approaches, (Yang *et al*., 2025). Mathematical modeling has emerged as a viable tool in understanding the dynamics of pollutant dispersion, providing tools to predict the behavior of pollutants under various conditions. Among these tools, the advection-diffusion-reaction models stand out for their ability to simulate the transport, spread, and transformation of pollutants within aquatic environments.

A range of studies has explored the mathematical modeling of water pollution. Teixeira & Auruch (2005) utilized the finite element method to stdy fluid-structure interaction while Krivykh (2016) focused on the practical implementation of modeling algorithms for groundwater pollution. Gray & Prider (1976) discussed the role of mathematical models in predicting pollution levels and proposed a specific numerical treatment for the generalized transport equation. Goodman (1966) developed a methodology for studying the interrelationships of water pollution control programs and constructed a mathematical model for a river stretch, which was programmed for electronic computers. Carstens & Amer (2019) demonstrated how pollutants move downstream, showing increasing pollution area but decreasing concentration, with spatial-temporal changes. Mazaheri *et al.* (2015) presented a simple mathematical model for river pollution point sources. Simeon & Koya (2015) developed a water pollution reaction-diffusion modeling system by showing a downstream movement of pollutants with reduced concentration, stagnation in certain regions, and harmful effects from chemical reaction products exceeding threshold values.

Moreover, some s tudies have investigated the use of discretized Runge-Kutta fourth-order methods for advection-reaction models. Calvo *et al*., (2001) and Kennedy & Carpenter (2003) developed linearly implicit Runge-Kutta methods for the numerical integration of the semi-discrete equations arising from spatial discretization, while Calvo (2001) showed that these methods were competitive with standard time integrators. Kennedy (2003) explored Adaptive Runge-Kutta (ARK) methods for convection-diffusion-reaction equations, presenting implicit-explicit RK methods that integrate stiff terms with an L-stable method and non-stiff terms with an explicit method. Chan *et al.*, (2014) introduced a novel approach to discretizing differential equations by applying it to the development of efficient numerical schemes for advection equations using two-derivative Runge-Kutta methods.

The application of advection-diffusion-reaction models in environmental sciences has a rich history, with deterministic approaches historically dominating the field. Early models focused on simulating the physical processes governing pollutant transport in water bodies, with works like Fischer *et al.*, (1979) laying the groundwork for understanding the mechanics of advection and diffusion. These models have been instrumental in designing pollution mitigation strategies and assessing environmental impacts. However, as noted by Jorgensen and Bendoricchio (2001), deterministic models, while useful, often simplify the

complex interplay of factors influencing ecological pollutant behavior, leading to a gap between predictions and real-world observations.

The recognition of this gap has spurred interest in stochastic modeling as a means to incorporate the uncertainty and variability characteristic of natural environments. Pioneering work by Neuman (2003) highlighted the potential of stochastic processes to enhance the realism of environmental models, acknowledging the limitations of deterministic approaches in capturing the spatial and temporal variability of natural systems. Subsequent studies have built on this foundation, exploring various aspects of stochastic modeling, from the incorporation of random noise to simulate turbulence Tartakovsky, (2007) to the development of hybrid models that combine deterministic and stochastic elements Yoon and Kang (2023).

In the specific context of water pollution, the work by Smith and Schwarz (2011) and the advancements by Tartakovsky (2013) stand out. They have explored the application of numerical methods, including the Runge-Kutta schemes, to solve increasingly complex stochastic differential equations that models pollution dynamics. These studies underline the importance of adopting a multifaceted modeling approach that acknowledges both the predictable patterns of pollutant dispersion and the unpredictable fluctuations resulting from environmental variability.

Understanding the transport and transformation of pollutants in water bodies is crucial for effective environmental management. Mathematical modeling, particularly advection-diffusion-reaction models, serves as a fundamental tool for simulating pollutant dynamics. This research builds upon these models by incorporating both deterministic and stochastic approaches to capture the complexity of real-world scenarios, aiming to improve predictions of pollutant dispersion and inform mitigation strategies. Previous studies cited have extensively employed advection-diffusion-reaction models to simulate pollutant behavior in aquatic environments. However, deterministic models often fall short in accounting for natural variability and uncertainties. Recent advancements have seen the integration of stochastic processes into these models, offering a more nuanced understanding of pollution dynamics. This study draws inspiration from works such as those by Tartakovsky (2013), who emphasize the role of stochastic modeling in environmental sciences, and Guo and Cheng (2019), who highlight the application of RK methods in solving complex PDEs in water pollution models.

In our methodology section, we explore the utilization of the discretized Runge-

Kutta 4th order method (RK4) for simulating water pollution dynamics through an advection-diffusion-reaction model. The ordinary RK4 method is widely recognized for its higher-order accuracy, making it adept at handling a broad range of differential equations with a notable degree of precision. This accuracy is particularly beneficial in environmental models where capturing subtle changes in pollution concentration over time and space is crucial. Moreover, RK4's stability, even for relatively larger time steps compared to lower-order methods, allows for efficient computation without sacrificing solution fidelity.

Despite these advantages, the RK4 method also presents challenges that necessitate careful consideration in its application. The method's requirement for multiple function evaluations per steptranslates to increased computational load which poses potential issues for extensive models or simulations extending over long durations. This aspect raises concerns regarding computational resources and efficiency, especially when dealing with large-scale environmental models. Additionally, RK4's fixed step size approach may not adequately adapt to the varying dynamics of a solution, potentially leading to inefficiencies or the need for manual adjustment to maintain an optimal balance between accuracy and computational demand. Moreover, while RK4 exhibits commendable performance in a wide array of scenarios, its application to stiff equations or highly nonlinear problems can be problematic. Stiff equations, characterized by rapidly changing solution components, may necessitate impractically small time steps for stability, rendering RK4 less effective or efficient compared to methods specifically designed for such cases, which led to our use of the discretized form.

Traditionally, these models have provided clear insights into the potential outcomes of pollution events under specific, predefined conditions. However, natural water bodies are subject to a myriad of unpredictable influences, from fluctuating water flows to sudden changes in pollutant sources, which deterministic models may not fully capture. Recognizing this gap, recent efforts in environmental modeling have turned towards stochastic methods, which introduce randomness into the equation, thereby mimicking the inherent variability of natural systems more closely. This study aims to bridge the deterministic and stochastic approaches, by providing a comprehensive analysis of water pollution dynamics that reveals both the predictable and unpredictable aspects of environmental systems. Building upon this rich body of literature, the present study aims to contribute to the ongoing dialogue on modeling water pollution dynamics. By comparing

deterministic and stochastic advection-diffusion-reaction models, this research seeks to illuminate the strengths and limitations of each approach, providing insights that could enhance future modeling efforts and inform more effective environmental management strategies. Through this comparative analysis, the study shows the necessity of embracing complexity and uncertainty in environmental modeling to better reflect the realities of natural water systems and improve the predictability of pollution outcomes.

2. METHODOLOGY

In order to formulate the model, the following assumptions were made.

- **Continuity and Differentiability:** Assumes pollutant concentration and parameters are continuous and differentiable, which may not hold in discrete environments.
- **Homogeneity of Stochastic Noise:** The white noise assumption suggests statistical homogeneity and independence, potentially oversimplifying environmental variability.
- **Spatial and Temporal Variability:** While accommodating variable flow and diffusion, accurately quantifying these parameters remains challenging.

Consider, C(x,t) as the concentration of a pollutant at position x and time t, u(x,t) as the variable flow velocity, and D(x,t) as the variable diffusion coefficient. The advection term, incorporating variable flow velocity, is given by

$$u(x,t) = \frac{\partial C}{\partial x}. \quad (1)$$

The diffusion term, incorporating a variable diffusion coefficient, is described as

$$\frac{\partial}{\partial x}(D(x,t) = \frac{\partial C}{\partial x}) \quad (2)$$

Assuming a constant reaction rate *k*, the reaction term is - *kC*, combining the advection, diffusion and reaction terms yields the following partial differential equation given by

$$\frac{\partial C}{\partial t} + u(x,t)\frac{\partial C}{\partial x} = \frac{\partial}{\partial x}\left(D(x,t)\frac{\partial C}{\partial x}\right) - kC. \quad \ldots\ldots\ldots\ldots(3)$$

To solve (3), we specify initial and boundary conditions. The initial distribution of pollutant concentration is given by:

$$C(x,0) = C_o(x) \quad (4)$$

We consider two types of boundary conditions. Dirichlet boundary condition specifies the concentration at the boundaries,

$$C(0,t) = f_o(t), C(L,t) = f_L(t) \quad (5)$$

where *L* is the length of the domain. The Neumann Boundary Condition Specifies the flux of the pollutant at the boundaries:

$$\frac{\partial C}{\partial x}|_{x=0} = g_o(t) \quad (6)$$

$$\frac{\partial C}{\partial x}|_{x=l} = g_l(t) \quad (7)$$

- **Advection Term**: $(u(x,t)\frac{\partial C}{\partial x})$ Represents the transport of pollutants by water flow, with velocity $u(x,t)$ capturing spatial and temporal variations. This term is crucial for modeling how pollutants are carried by moving water.

- **Diffusion Term**: $\frac{\partial}{\partial x}\left(D(x,t)\frac{\partial C}{\partial x}\right)$ Accounts for pollutant spreading due to concentration gradients, while the variable diffusion coefficient $D(x,t)$ reflects the impact of environmental factors like temperature and salinity on mixing processes.

- **Reaction Term**: $-kC$ Models chemical or biological reactions affecting pollutants, with k summarizing reaction kinetics. This term encompasses degradation, decay, or transformation processes.

- **Stochastic Noise Term**: $\eta\sigma(x,t)$ Introduces random fluctuations, capturing unpredictable environmental processes. The intensity σ scales the impact, while: $\eta(x,t)$ represents white noise with mean 0 and variance 1.

The introduction of stochastic noise into the advection-diffusion-reaction model provides a more realistic framework for modeling water pollution. This approach accounts for random fluctuations arising from various physical and environmental processes, such as turbulent flows, variable reaction rates, and environmental changes. Typically, these stochastic effects are represented by adding a noise term to the model, commonly modeled as Gaussian or white noise. The resulting model is a stochastic partial differential equation (SPDE). The modified equation that incorporates stochastic noise is expressed as:

$$\frac{\partial C}{\partial t} + u(x,t)\frac{\partial C}{\partial x} = \frac{\partial}{\partial x}\left(D(x,t)\frac{\partial C}{\partial x}\right) - kC\ \sigma\eta(x,t) \quad (8)$$

To clarify the application of the discretized Runge-Kutta 4th order (RK4) method to our advection-diffusion-reaction model, let's explicitly write out the expressions for k_1 to k_4 for a given grid point i at time step n. These expressions incorporate the spatial discretization for advection, diffusion, and reaction processes. Given the discretized form of our model equation at grid point i:

$$\frac{dC_i}{dt} = -u_i\frac{C_{i+1} - C_{i-1}}{2\Delta x} + D_i\frac{C_{i+1} - 2C_i + C_{i-1}}{\Delta x^2} - kC_i + \sigma\eta\frac{C_{i+1} - C_{i-1}}{2\Delta x} \quad (9)$$

Where Ci is the concentration at spatial point i, u_i is the flow velocity, Di is the diffusion coefficient, k is the reaction rate, Δx is the spatial step size, and the derivatives are approximated using central differences.

For each time step from t_n to t_{n+1}, we calculate:

k_1: The slope at the beginning of the time step, using the current state of the system.

$$k_1 = f(t_n, C_i^n) = -u_i\frac{C_{i+1}^n - C_{i-1}^n}{2\Delta x} + D_i\frac{C_{i+1}^n - 2C_i^n + C_{i-1}^n}{\Delta x^2} - kC_i^n + \sigma\eta\frac{C_{i+1} - C_{i-1}}{2\Delta x} \quad (10)$$

k_1: The slope at the midpoint of the time step, using the state estimated by k_1.

$$k_2 = f\left(t_n + \frac{\Delta t}{2}, C_i^n + \frac{\Delta t}{2}k_1\right) \quad (11)$$

k_3:Another slope at the midpoint, but using the state estimated by k_2.

$$k_3 = f\left(t_n + \frac{\Delta t}{2}, C_i^n + \frac{\Delta t}{2}k_2\right) \quad (12)$$

k_4: The slope at the end of the time step, using the state estimated by k_3.

$$k_4 = f(t_n + \Delta t, C_i^n + \Delta t k_3) \quad (13)$$

After calculating k_1, k_1, k_1 and k_4, the concentration at the next time step is updated using the weighted average of these slopes:

$$C_{i+1}^n = C_i^n + \frac{\Delta t}{6}(k_1 + 2k_2 + 2k_3 + k_4) \quad (14)$$

This process is repeated for each grid point *i* across the spatial domain and for each time step *n*, with appropriate handling of boundary conditions. The RK4 method's advantage lies in its higher-order accuracy, making it suitable for more complex or sensitive simulations where precision is critical. The algorithm implemented in python computational software is given below.

•Algorithm: Runge-Kutta 4th Order Method for Advection-Diffusion-Reaction Mode

- Define the spatial domain x in the interval [0, L] with N intervals. The spatial step size is given by $\Delta x = \frac{L}{N}$
- Define the time domain t in the interval [0, T] with a time step size Δt
- Initialize the concentration array C_i^o based on the initial condition C (x, 0).
- Define the flow velocity u (x, t), diffusion coefficient D (x, t), and reaction rate k

For each time step (from n = 0 to T $\Delta t - 1$, **do** /):

- **For each spatial point** (from i = 1 to N -1):.

1. Compute.$k_1 = f(t_n, C_i^n)$
2. Compute $k_2 = f\left(t_n + \frac{\Delta t}{2}, C_i^n + \frac{\Delta t}{2}k_1\right)$
3. Compute $k_3 = f\left(t_n + \frac{\Delta t}{2}, C_i^n + \frac{\Delta t}{2}k_2\right)$.
4. Compute $k_4 = f(t_n + \Delta t, C_i^n + \Delta t k_3)$
5. Update the concentration at the next time step:

$$C_{i+1}^n = C_i^n + \frac{\Delta t}{6}(k_1 + 2k_2 + 2k_3 + k_4)$$

6. **End for:**
7. Apply the boundary conditions to C_o^{n+1} and C_N^{n+1}
8. **End for:**

- **Return** the final concentration array C.

3. RESULTS

The numerical simulations of the model in (8) in view of (1) – (14) is performed using python computational software. The plots below show the evolution of the contaminant concentration profile in a scenario with spatially varying flow velocity. Each curve represents the concentration profile at different time points, illustrating how the pollutant dispersion is influenced by the changing velocity. As the flow velocity increases along the spatial domain, the advection term (transport of pollutants by the flow of water) becomes more pronounced,

especially in downstream regions. This leads to a faster movement of the concentration of pollution which enhances the spreading of the pollutant due to the combined effects of advection and diffusion. The increasing flow velocity effectively stretches the concentration profile along the flow direction, illustrating how spatial variations in flow velocity can significantly affect the transport and dispersion of pollutants in water bodies.

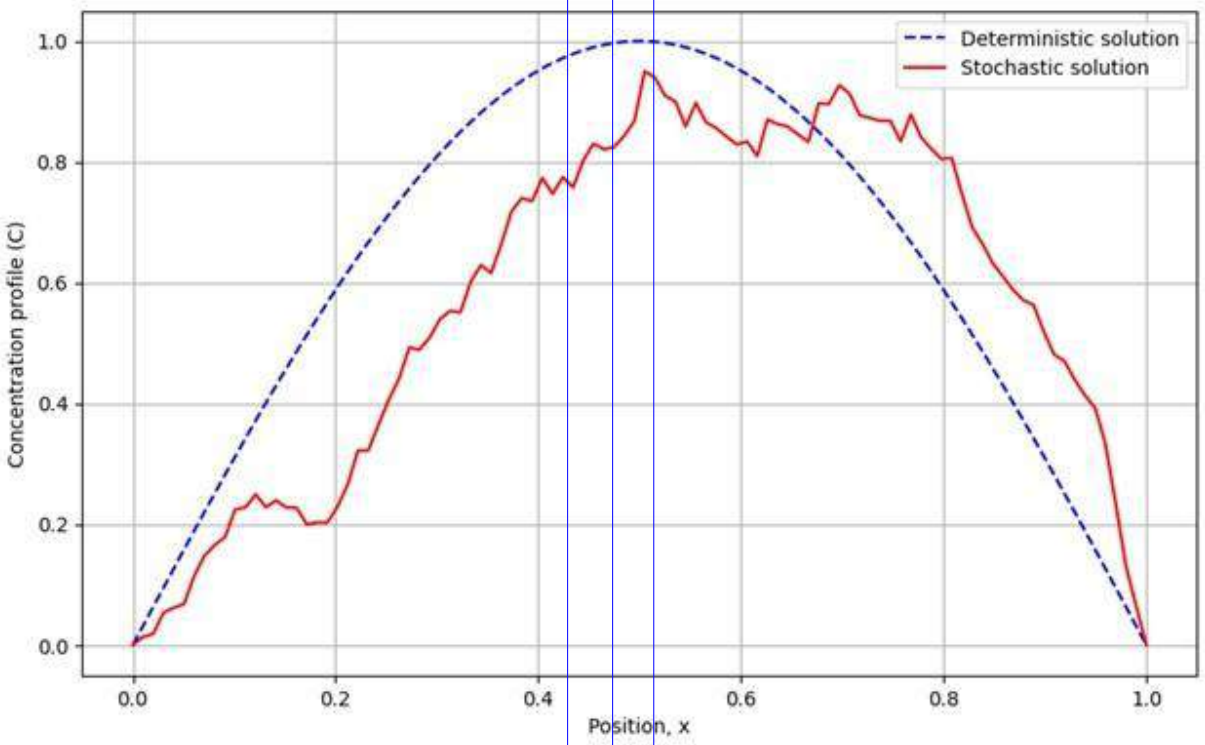

Figure 1: The Concentration profile under advection, diffusion, and reaction processes, with added noise to simulate environmental variability

Figure 1, describes evolution of the concentration profile under advection, diffusion, and reaction processes, with added white noise to simulate environmental variability. The results are visualized by plotting the initial and final concentration profiles, showing the impact of stochastic noise on the system's dynamics. The deterministic model uses the explicit scheme with no noise, while the stochastic model introduces Gaussian white noise to simulate random fluctuations.

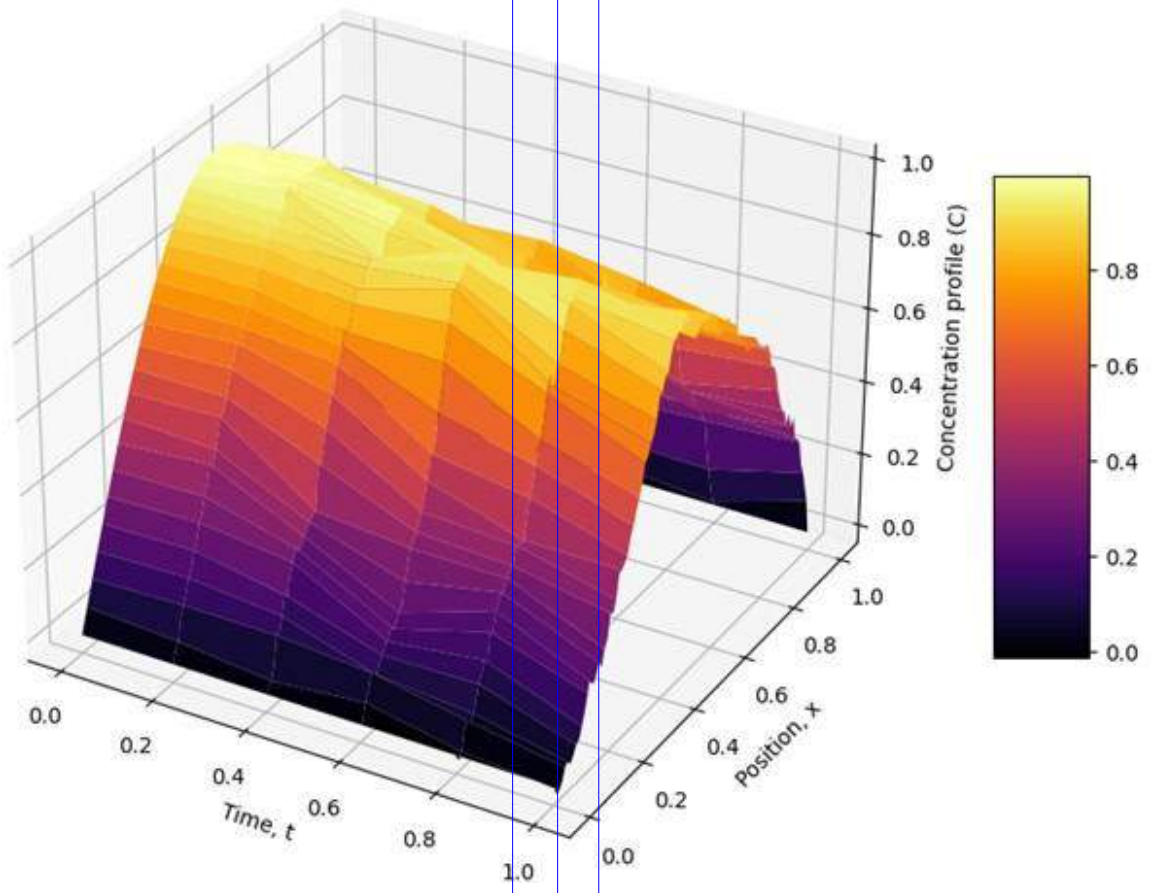

Figure 2: The 3D plot evolution of the concentration profile over time with stochastic noise.

Figure 2 shows the 3D plot that illustrates the evolution of the concentration profile over time, incorporating stochastic noise into the advection-diffusion-reaction model. The x-axis represents time, the y-axis represents the position along the domain, and the z-axis indicates the concentration of the pollutant. The plot shows how the concentration profile changes due to the combined effects of advection (movement), diffusion (spreading), reaction (decay), and the added complexity of stochastic fluctuations represented by noise. The colormap, ranging from cooler to warmer colors, signifies the varying concentration levels, with stochastic noise introducing noticeable fluctuations over time.

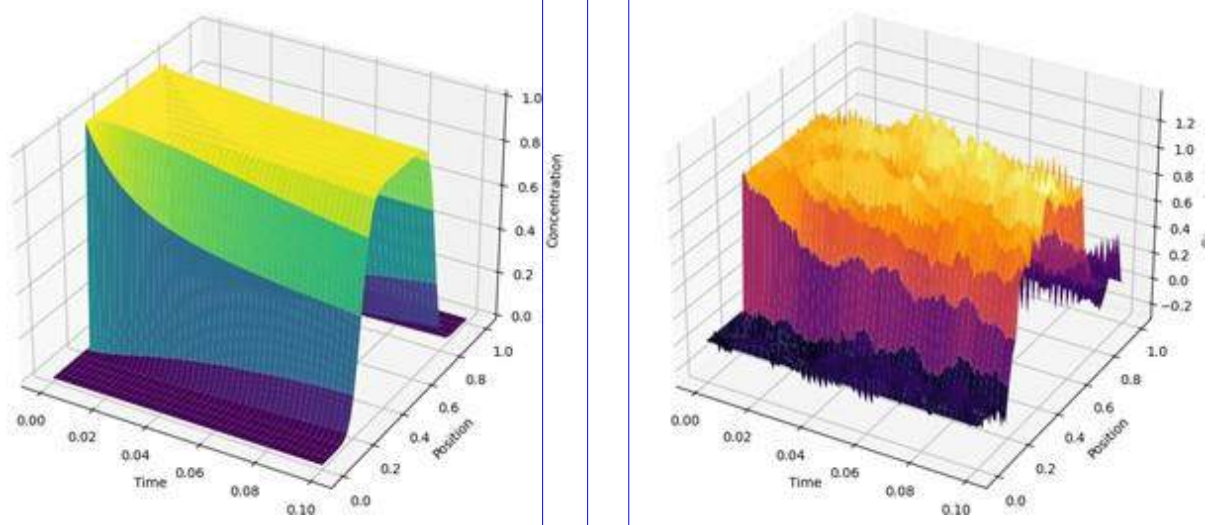

Figure 3: The 3D concentration profiles with two distinct initial values variations.

In Figure 3, the 3D visualizations illustrate the evolution of concentration profiles over time for two distinct initial values variations under the influence of stochastic noise.

Step Function Initial Condition (Left Plot): The concentration starts with a sudden change at the midpoint of the domain, simulating a pollutant release at one end. Over time, the stochastic noise along with advection, diffusion, and reaction processes cause the initially sharp boundary to disperse and become more erratic. This effect represents a sudden pollutant spill entering a water body.

Linear Gradient Initial Condition (Right Plot): The concentration gradually increases from one end of the domain to the other. As time progresses, the interplay of stochastic noise with the other processes lead to a smoothing and eventual homogenization of the gradient, albeit with noticeable fluctuations due to the stochastic component. This simulate a scenario where pollutant concentration gradually increases towards a source of pollution.

These visualizations show the significant impact of initial conditions on the dispersion and reaction dynamics in the presence of stochastic influences. The step function condition shows how a localized pollutant release disperses over time, while the linear gradient condition illustrates the evolution of a gradual pollutant concentration increase. In both cases, stochastic noise introduces variability that can represent natural fluctuations in environmental systems, emphasizing the importance of considering such effects in environmental modeling and risk assessment.

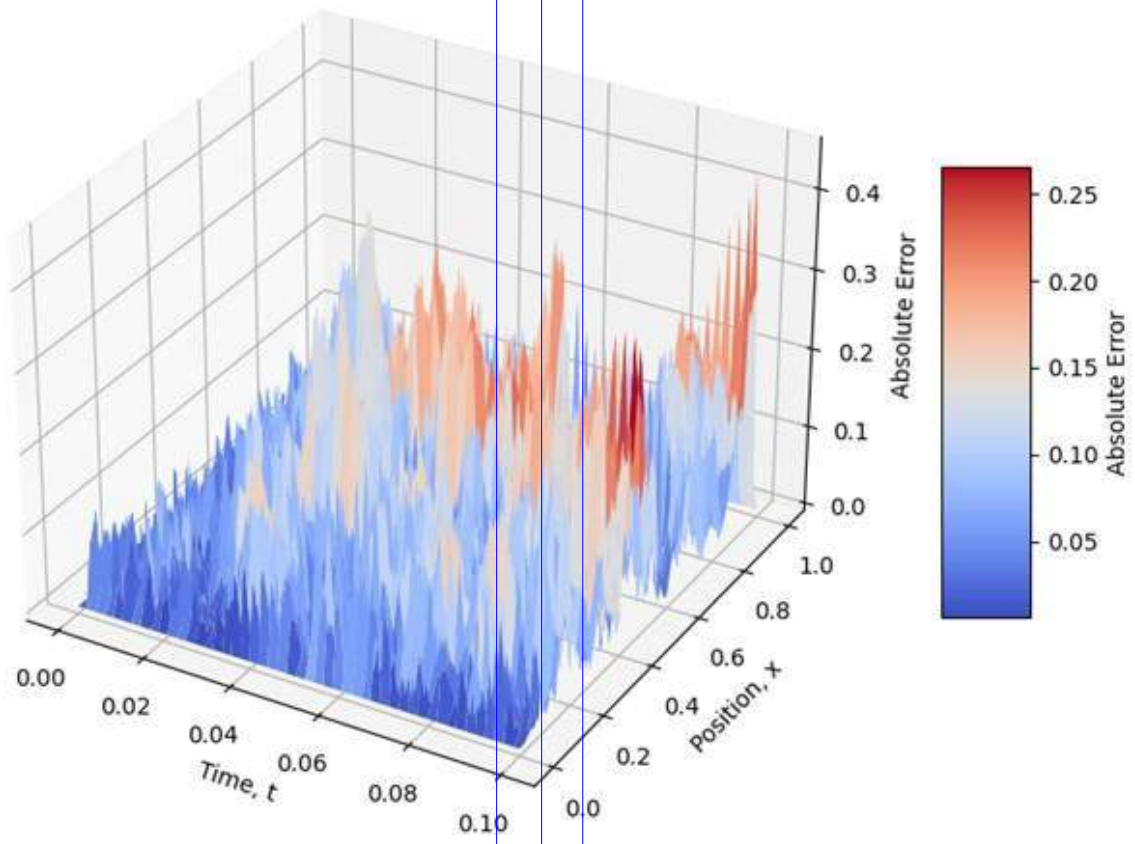

Figure 4: The absolute error profile between the deterministic and stochastic solution

Figure 4 shows the absolute error between the deterministic and stochastic curves. The introduction of stochastic noise leads to more erratic dispersion patterns, which revealed the unpredictability of pollutant behavior in natural systems. Specifically, scenarios with step function and linear gradient initial conditions exhibit pronounced differences when subject to stochastic influences, with the step function showing a more significant dispersion effect due to the initial concentration peak.**4.**

Conclusion

The formulation and comparative analysis of the deterministic and stochastic advection-diffusion-reaction model in this work showed the complexities involved in modeling water pollution dynamics. The deterministic part of the model gives more understanding into the baseline behavior of the pollutants, while the inclusion of stochastic term in the model showed the inherent variability of natural water systems, better than the deterministic part. This work contributes to the field of water pollution and conservation by demonstrating the impacts of different modeling approaches on the predicted dispersion of pollutants, which highlights the need for incorporating stochastic processes in environmental

modeling for more accurate and reliable predictions. Future work should focus on expanding the range of stochastic parameters and investigating their effects on pollution dynamics to further refine modeling practices.

References

Calvo, M. P., De Frutos, J., & Novo, J. (2001). Linearly implicit Runge–Kutta methods for advection–reaction–diffusion equations. *Applied Numerical Mathematics, 37*(4), 535–549.

Carstens, D., & Amer, R. (2019). Spatio-temporal analysis of urban changes and surface water quality. *Journal of Hydrology, 569*, 720–734.

Chan, R. P., Wang, S., & Tsai, A. Y. (2012, September). Two-derivative Runge-Kutta methods for differential equations. In *AIP Conference Proceedings* (Vol. 1479, No. 1, pp. 262–266). American Institute of Physics.

Fischer, H. B. (1979). *Mixing in inland and coastal waters*. Academic Press.

Goel, P. K. (2006). *Water pollution: Causes, effects and control*. New Age International.

Goodman, A. S., & Dobbins, W. E. (1966). Mathematical model for water pollution control studies. *Journal of the Sanitary Engineering Division, 92*(6), 1–20.

Gray, W. G., & Pinder, G. F. (1976). An analysis of the numerical solution of the transport equation. *Water Resources Research, 12*(3), 547–555.

Guo, G., & Cheng, G. (2019). Mathematical modelling and application for simulation of water pollution accidents. *Process Safety and Environmental Protection, 127*, 189–196.

Jørgensen, S. E., & Bendoricchio, G. (2001). *Fundamentals of ecological modelling*. Elsevier.

Kennedy, C. A., & Carpenter, M. H. (2003). Additive Runge–Kutta schemes for convection–diffusion–reaction equations. *Applied Numerical Mathematics, 44*(1–2), 139–181. https://doi.org/10.1016/S0168-9274(02)00185-5

Krivykh, I. V. (2016). Modeling groundwater pollution: Practical implementation of algorithms. *Environmental Modelling & Software, 82*, 123–135. https://doi.org/10.1016/j.envsoft.2016.03.009

Mazaheri, M., Samani, J. M. V., & Samani, H. M. V. (2015). Mathematical model for pollution source identification in rivers. *Environmental Forensics, 16*(4), 310–321.

Neuman, S. P. (2003). Maximum likelihood Bayesian averaging of

uncertain model predictions. *Stochastic Environmental Research and Risk Assessment, 17*(5), 291–305. https://doi.org/10.1007/s00477-003-0151-7

Simon, T., & Koya, P. R. (2015). Modeling and numerical simulation of river pollution usingdiffusion-reaction equation. *American Journal of Applied Mathematics, 3*(6), 335–340.

Tartakovsky, D. M. (2007). Probabilistic risk analysis in subsurface hydrology. *Geophysical Research Letters, 34*(5). https://doi.org/10.1029/2007GL029513

Tartakovsky, D. M. (2013). Assessment and management of risk in subsurface hydrology: A review and perspective. *Advances in Water Resources, 51*, 247–260.

Teixeira, P. D. F., & Awruch, A. M. (2005). Numerical simulation of fluid–structure interaction using the finite element method. *Computers & Fluids, 34*(2), 249–273.

Yang, W., Schmidt, C., Wu, S., Zhao, Z., Li, R., Wang, Z., & Zhang, J. (2025). Exacerbated anthropogenic water pollution under climate change and urbanization. *Water Research, 280*, 123449.

Yoon, S., & Kang, P. K. (2023). Mixing-induced bimolecular reactive transport in rough channel flows: Pore-scale simulation and stochastic upscaling. *Transport in Porous Media, 146*(1), 329–350.

MODELLING NIGERIA EXCHANGE RATE WITH OTHER CURRENCY USING AUTOREGRESSIVE MOVING AVERAGE (ARMA)

ILESANMI A.O[1]., OGUNBOYO O.F[2].,
ODUKOYA E.A[3] , ALADEJANA A.E[4].
[1,3,4]DEPARTMENT OF STATISTICS,
EKITI STATE UNIVERSITY, ADO-EKITI,
EKITI STATE, NIGERIA.

[2]EPIDEMIOLOGY AND BIOSTATISTICS DEPARTMENT,
UNIVERSITY OF MEDICAL SCIENCES ONDO,
ONDO STATE, NIGERIA

ABSTRACT
This research aimed at analyzing and forecasting the currency exchange rate between Naira and three other currencies (USD, Pounds and Deutsche) using Autoregressive Moving Average model (ARMA). The series were plotted on a graph to check the type of pattern that existed in the data and it was shown from the series plotted that Naira has been depreciating right from the year 1981 to 2023. Test for stationarity using Dickey Fuller (DF) was performed and the series for the three exchange rates were found to be non-stationary but were observed to be stationary after first order differencing. The results showed that, based on AIC, SIC, and HQC criteria, the ARMA (1,1) model performs better than the AR and MA models, making it the optimal choice for forecasting exchange rates from 2024 to 2030.

Key words and phrases: Time Series; Exchange Rate; Stationarity; Augmented Dickey-Fuller (ADF); Optimal Choice.

1. INTRODUCTION
The issues of exchange rate and the achievements of a realistic exchange rate for the naira have continued to generate a great challenge to macroeconomic policy formulators, owing to its unarguable significances in bringing about economic growth. This therefore explains in part why it is necessary for any growth conscious country to manage its foreign exchange.

Exchange rate is the rate at which a currencypurchases another (Jhingan, 2005). It is a reflection of the strength of a currency when measured against another country's currency. It is also regarded to as the value of one country's currency in relation to another currency (O'Sullivan et al, 2003). According to Oloyede (2002), it is the price of one currency in terms of another which is an

important decision-making variable in every nation, thus making it an important issue for any country desirous for economic growth as pointed out by Ahmed and Zarma (1997).

The prediction of the foreign exchange market performances becomes more difficult making domestic investors to face enormous risk. Iyeli *et al.*, (2011) explained how the government has tried maintaining a stable exchange rate but Naira depreciated throughout the 80's to date. It depreciated from N0.61 in 1981 to N2.02 in 1986 and further to N7.901 in 1990, all against the US Dollar. The policy of guided or managed deregulation pegged the naira at N21.886 against US Dollar in 1994. Further deregulation pushed it to N86.322 =$1.00 in 1999 Aliyu (2011). It depreciated further to N120.97 in 2002 and N135.5 in 2004. Thereafter, the exchange rate appreciated to N132.15 in 2005 and later N118.57 in 2008 towards the end of 2008. When the global financial crisis took its toll, the naira depreciated to N150.0124 at the end of 2009 Iyeli and Clement (2017). In 2010, the naira suffered some value loss and exchanged for N154.57 to the dollar according to CBN. The naira continued to lose value and recent news of exchange rate between naira and US Dollar showed an increase in rate which is N362.847 as at 29thSeptember, 2018 CBN(2018).This inconsistency in policies aggregate unstable nature of naira rate. Gbosi (2005).

As a matter of fact, the foreign exchange market is the most liquid financial market in the world. Traders include large banks, central banks, institutional investors, currency speculators, corporations, governments, retail investors and other f inancial institutions. The average daily turnover in the global foreign exchange and related markets is continuously growing. Foreign investors access the foreign banknotes which may be used to acquire foreign goods and settle overseas bills.

A lot of researchers discussed extensively about the effect of exchange rate volatility in relation to importation. Jonathan and Kenneth (2016) showed the link between exchange rate fluctuations and private domestic investment in Nigeria. The findings indicated that, the depreciation of the currency and interest rate does not stimulate private domestic investment activities in Nigeria. Ekanem (2002) explained that exchange rate can frustrate development efforts of import dependent economies to a large extent because critical development projects become more expensive. Mallic and Marques (2008) also asserted that changes in the exchange rate can lead to a rise in import prices and thus there is overall inflation. The response of local currency prices of imported products to changes in exchange rate may not be one-for-one, as it has been in the case of many advanced markets. Both the bilateral exchange rates and trading

partners are found to have significant imports Back and Koo (2009).

The goals of an exchange rate policy include determining an appropriate exchange rate and ensuring its stability. The stock exchange market has displayed a relatively high degree of volatility in response to the flexible in 1986. The depreciation of naira value in the Nigerian Stock Exchange (NSE) market relative to other currencies, US Dollar in particular is due to the excessive exposure of the stock market to external shocks, severe pressures on the external reserve and foreign exchange crisis CBN (2015). This is attributed to the sharp drop in foreign earning of Nigeria as a result of the persistent fall in crude oil's prices in the global market.

Chen et al. (2022) applied ARIMA to forecast the USD/EUR exchange rate using data from 2017 to 2021. The study compared ARIMA to other traditional models such as the random walk model, revealing that ARIMA outperformed the random walk approach, especially in volatile periods. The study employed a rolling forecast mechanism, which updated model parameters periodically, making it adaptable to real-time data shifts. ARIMA's strength lies in its capacity to model time series data with non-stationary behavior and patterns, which are typical of financial time series like exchange rates. Zhang and Li (2023) investigated the forecasting power of GARCH in predicting the volatility of the USD/GBP exchange rate. Their empirical study spanned from 2018 to 2022 and employed GARCH (1,1), a basic form of the model, to capture the conditional variance of exchange rate returns. The study found that GARCH models effectively forecast periods of high volatility, a crucial factor for foreign exchange traders. Moreover, their analysis suggested that incorporating GARCH models into traditional forecasting frameworks significantly improved predictive accuracy during market stress. A study by Gupta *et al*. (2021) used LSTM networks to predict the USD/CNY exchange rate from 2015 to 2020. The empirical results showed that LSTM outperformed traditional models like ARIMA and GARCH in forecasting accuracy, especially over longer time horizons. By leveraging deep learning techniques, the study was able to incorporate a broader range of features, such as macroeconomic indicators and market sentiment, into the model, l eading to better performance in highly dynamic markets. The study also demonstrated that LSTM's architecture helps mitigate the vanishing gradient problem, which is common in traditional RNNs when handling long sequences of time series data. In recent years, hybrid models combining traditional time series techniques with machine learning methods have been proposed to improve exchange rate forecasting accuracy. A notable study by Rahman and Ahmed (2022) combined ARIMA with a neural

network model (ARIMA-ANN) to forecast the EUR/USD exchange rate. The study used data from 2016 to 2021 and demonstrated that hybrid models outperform single-method models in both accuracy and stability. By first using ARIMA to capture linear trends and then applying a neural network to model non-linear patterns, the hybrid model provided a more robust framework for forecasting exchange rates. The empirical results showed that the ARIMA-ANN model reduced prediction errors compared to standalone ARIMA or ANN models, particularly during periods of market instability and high volatility. Park and Lee (2023) explored the use of hybrid models combining wavelet transform and machine learning techniques to enhance the accuracy of exchange rate forecasting. They applied this hybrid method to the USD/JPY exchange rate data from 2018 to 2022. By first decomposing the exchange rate time series into different frequency components using wavelet analysis, the study captured both high-frequency short-term fluctuations and low-frequency long-term trends. These components were then fed into a support vector machine (SVM) model for prediction. The empirical results showed that the hybrid wavelet-SVM model outperformed both standalone SVM and traditional time series models like ARIMA in terms of accuracy and stability, particularly during high-volatility periods. The s tudy highlighted that the wavelet transform's ability to isolate different time scales within the data significantly improved the model's performance by allowing it to focus on specific aspects of the exchange rate's behavior.

This paper therefore explores the relationship between naira and three other foreign currencies which are US Dollar (USD), British Pound (GBP) and Deutsche exchange rate and forecast the exchange rate using Autoregressive-Moving Average Model (ARMA). The best model was then used to forecast the exchange rate.

2.0 MATERIALS AND METHODS

The data used for this study is secondary data on Dollar- Naira, Pound-Naira and Deutsche-Naira exchange rate for a period of 42 years (1981- 2023) from the bulletin of Central Bank of Nigeria (CBN). The data are tested for stationarity and analyzed using Autoregressive-Moving Average Model (ARMA). The best model was used to forecast exchange rate between naira and the three currencies.

2.1 TIMESERIES MODELS SPECIFICATION

There are several models in time series analysis and they are as follows:

2.1. AUTOREGRESSIVE MODEL (AR)

An autoregressive model of order *p*, written as AR (p), can be given as:

$$X_t = \varnothing_1 X_{t-1} + \varnothing_2 X_{t-2} + \ldots + \varnothing_p X_{t-p} + \varepsilon_t \quad (1)$$

Where x_t is stationary series, $ø_1, ø_2 \ldots\ldots ø_p$, are the parameters of the AR ($ø \neq 0$). Where x_t is stationary series, $Ø_1, Ø_2 \ldots\ldots Ø_p$, are the parameters of the AR($ø_p \neq 0$). Unless otherwise stated, we assume that $Ɛ_t$ is a Gaussian white noise series with mean zero and variance σ_ε^2. The highest order p is referred to as the order of the model.

2.1.2 MOVING AVERAGE (MA) MODEL

As an alternative to the autoregressive representation in which the x_t on the left-hand side of the equation are assumed to be combined linearly, the moving average model of order q, abbreviated as MA (q), assumes the white noise($Ɛ_t$) on the right-hand side of the defining equation are combined linearly to form the observed data.

A series x_t is said to follow a moving average process of order q, or simply MA (q) process

$$X_t = \varepsilon_t + \theta_1 \varepsilon_{t-1} + \theta_2 \varepsilon_{t-2} + \ldots + \theta_q \varepsilon_{t-q} \quad (2)$$

Where$ø_1, ø_2 \ldots\ldots ø_q$, are the MA parameters. MA (q) models immediately define stationary, every MA process of finite order is stationary (Diebold et al., 2006). In order to preserve a unique representation, usually the requirement is imposed that all roots of (B) = $1+ø_1B+ø_2B_2+\ldots..+ ø_qB_q= 0$ are greater than one in absolute value. If all roots of $ø(B) = 0$ lie outside the unit circle, the MA process has an autoregressive representation of generally infinite order $\sum_{j=1}^{\infty} \phi_j \varepsilon_{t-j} = \varepsilon_t$ with $\sum_{j=1}^{\infty} |\phi_j| < \infty$.

MA process as with an infinite order autoregressive representation are said to be invertible.

2.1.3 ESTIMATION OF MOVING AVERAGE (MA) PARAMETERS

Consider MA(1) given below,

$$E(X_t) = E(\varepsilon_t) + E(\theta_1 \varepsilon_{t-1}) = 0$$

Then,

$$Var(X_t) = E(X_t - \mu)^2$$

$$Var(X_t) = E(\varepsilon_t^2 + 2\theta\varepsilon_{t-1}^2 + \theta^2\varepsilon_{t-1})^2$$

$$Var(X_t) = E(\varepsilon_t^2) + \theta^2 E(\varepsilon_{t-1}^2) - 2\theta E(\varepsilon_{t-1})$$

$$Var(X_t) = \sigma^2 + \theta^2\sigma^2 - 0$$

$$Var(X_t) = \sigma^2(1 + \theta^2) \quad (3)$$

The covariance is calculated as,

$$Cov(X_t X_{t-1}) = E((X_t - \mu)(X_{t-1} - \mu))$$

$$= E((\varepsilon_t - \theta\varepsilon_{t-1})(\varepsilon_{t-1} - \theta\varepsilon_{t-2}))$$

$$= E(\varepsilon_t\varepsilon_{t-1}) - \theta E(\varepsilon_t\varepsilon_{t-1}) - \theta E(\varepsilon_t^2) + \theta^2 E(\varepsilon_t\varepsilon_{t-1})$$

$$Cov(X_t X_{t-1}) = 0 - 0 - \theta\sigma^2 + 0$$

$$\gamma_1 = -\theta\sigma^2 \quad (4)$$

Therefore, lag 1 is given below,

$$\rho_1 = \frac{\gamma_1}{\gamma_0} = \frac{-\theta\sigma^2}{\sigma^2(1+\theta^2)} = \frac{-\theta}{1+\theta^2} \quad (5)$$

Also, consider MA(2) given below,

$$X_t = \varepsilon_t + \theta_1\varepsilon_{t-1} + \theta_2\varepsilon_{t-2}$$

$$E(X_t) = 0$$

$$\text{Then, } Var(X_{t-1}) = Var(\varepsilon_t) + \theta_1^2 Var(\varepsilon_{t-1}) + \theta_2^2 Var(\varepsilon_{t-1})$$

$$= E(\varepsilon_t^2) + \theta_1^2 E(\varepsilon_{t-1}^2) + \theta_2^2 E(\varepsilon_{t-1}^2)$$

$$= \sigma^2 + \theta_1^2\sigma^2 + \theta_2^2\sigma^2$$

$$\gamma_0 = \sigma^2(1 + \theta_1^2 + \theta_2^2) \quad (6)$$

$$Cov(X_t X_{t-1}) = Cov(\varepsilon_t - \theta_1\varepsilon_{t-1} - \theta_2\varepsilon_{t-2}, \varepsilon_{t-1} - \theta_1\varepsilon_{t-1} - \theta_2\varepsilon_{t-1})$$

$$= Cov(\varepsilon_t, -\theta\varepsilon_t) + Cov(\theta_1\varepsilon_{t-1}, \theta_2\varepsilon_{t-2})$$

$$= -\theta_1\sigma^2 + \theta_1\theta_2\sigma^2$$

$$= \theta_1\theta_2\sigma^2 - \theta_1\sigma^2 \quad (7)$$

$$\gamma_1 = \sigma^2(\theta_1\theta_2 - \theta_1)$$

Other lags are then estimated in this order.

2.1.4 AUTOREGRESSIVE-MOVING AVERAGE MODEL (ARMA)

Autoregressive (AR) models were first introduced by Yule in 1926. They were consequently supplemented by Slutsky

who in 1937 presented Moving Average (MA) schemes. It was Wold (1938), however, who combined both AR and MA schemes and showed that ARMA processes can be used to model all stationary time series as long as there is appropriate order of p, the number of AR terms and q the number of MA terms was appropriately specified. This means that any series X_t can be modelled as a combination of past X_t values and/or past ε_t (error terms) with parameters

$$X_t, X_{t-1}, X_{t-2}, \dots X_{t-p}$$

Autoregressive-moving average model is written as

$$X_t = \varnothing_1 X_{t-1} + \varnothing_2 X_{t-2} + \dots + \varnothing_p X_{t-p} + \varepsilon_t - \theta_1 \varepsilon_{t-1} - \theta_2 \varepsilon_{t-2} - \dots \theta_q \varepsilon_{t-q} \quad (8)$$

Equation (8) of the time series model will be simplified by a backward shift operator B to obtain:

$$\varnothing(B)^{X_t} = \theta(B)^{\varepsilon_t} \quad (9)$$

2.1.5 ESTIMATION OF ARMA PARAMETERS

As proposed by Box Jenkins (1976), the steps in estimating of Autoregressive-Moving Average model (ARMA) parameters are listed below: **identification** i.e. involves examining the given data to determine the values of p and q (the order of AR and MA) **parameter estimation:** There are three approaches to estimating ARMA parameters which are Two-stage regression estimation, Yule walker (Method of Moments) and Maximum Likelihood Method. In this study, we used Yule Walker equation for the estimation of ARMA parameters and **forecasting:** after the parameters have been estimated, the estimated parameters were used to forecast.

Using ARMA (1, 1) i.e. AR (1) in conjunction with MA (1), From equation 10, ARMA (1, 1) is defined as:

$$X_t = \varnothing_1 X_{t-1} + \varepsilon_t - \theta_1 \varepsilon_{t-1} \quad (10)$$

Multiply through by X_{t-p} and then take the expectation

$$X_t X_{t-p} = \varnothing_1 X_{t-1} X_{t-p} + \varepsilon_t X_{t-p} - \theta_1 \varepsilon_{t-1} X_{t-p}$$

$$E(X_t X_{t-p}) = \varnothing_1 E(X_{t-1} X_{t-p}) + E(\varepsilon_t X_{t-p}) - \theta_1 E(\varepsilon_{t-1} X_{t-p}) \quad (11)$$

When p = 0

$$\gamma_0 = \varnothing_1 \gamma_1 + E(X_t \varepsilon_t) - \theta_1 E(X_t \varepsilon_{t-1}) \quad \text{since } E(X_t \varepsilon_t) = \sigma_\varepsilon^2 \text{ and}$$

$$E(X_t \varepsilon_{t-1}) = \varnothing_1 E(X_{t-1} \varepsilon_{t-1}) + E(\varepsilon_t \varepsilon_{t-1}) - \theta_1 E(\varepsilon_{t-1}^2)$$

$$\gamma_{12}(-1) = \varnothing_1 \gamma_{12}(0) + 0 - \theta_1 \sigma_\varepsilon^2$$

$$\gamma_{12}(-1) = \varnothing_1 \sigma_\varepsilon^2 - \theta_1 \sigma_\varepsilon^2$$

$$\gamma_0 = \varnothing_1 \gamma_1 + \sigma_\varepsilon^2 - \theta_1 (\varnothing_1 \sigma_\varepsilon^2 - \theta_1 \sigma_\varepsilon^2)$$

$$\gamma_0 = \varnothing_1 \gamma_1 + \sigma_\varepsilon^2 - \theta_1 \varnothing_1 \sigma_\varepsilon^2 - \theta_1^2 \sigma_\varepsilon^2 \quad (12)$$

Also when p=1, From equation 12

$$\gamma_1 = \varnothing_1 \gamma_0 + 0 - \theta_1 \sigma_\varepsilon^2$$

$$\gamma_1 = \varnothing_1 \gamma_0 - \theta_1 \sigma_\varepsilon^2 \quad (13)$$

And then from equation 13

$$\gamma_0 = \varnothing_1 (\varnothing_1 \gamma_0 - \theta_1 \sigma_\varepsilon^2) + \sigma_\varepsilon^2 - \theta_1 \varnothing_1 \sigma_\varepsilon^2 - \varnothing_1^2 \sigma_\varepsilon^2$$

$$\gamma_0 (1 - \varnothing_1^2) = \sigma_\varepsilon^2 - 2(\theta_1 \varnothing_1 \sigma_\varepsilon^2) + \varnothing_1^2 \sigma_\varepsilon^2$$

$$\gamma_0 = \frac{\sigma_\varepsilon^2 - 2(\theta_1 \varnothing_1 \sigma_\varepsilon^2) + \varnothing_1^2 \sigma_\varepsilon^2}{1 - \varnothing_1^2}$$

$$\gamma_1 = \varnothing_1 \left(\frac{\sigma_\varepsilon^2 - 2(\theta_1 \varnothing_1 \sigma_\varepsilon^2) + \varnothing_1^2 \sigma_\varepsilon^2}{1 - \varnothing_1^2} \right) - \theta_1 \sigma_\varepsilon^2$$

$$\gamma_1 = \frac{(1 - \theta_1 \varnothing_1)(\varnothing_1 - \theta_1) \sigma_\varepsilon^2}{1 - \varnothing_1^2}$$

$$\rho_1 = \frac{\gamma_1}{\gamma_0} = \frac{\frac{(1 - \theta_1 \varnothing_1)(\varnothing_1 - \theta_1) \sigma_\varepsilon^2}{1 - \varnothing_1^2}}{\varnothing_1 (\varnothing_1 \gamma_0 - \theta_1 \sigma_\varepsilon^2) + \sigma_\varepsilon^2 - \theta_1 \varnothing_1 \sigma_\varepsilon^2 - \varnothing_1^2 \sigma_\varepsilon^2} \quad (14)$$

Equation (14) is known as the autocorrelation at lag 1

3.0 ANALYSIS

Considering the data plot of USD/ Naira, Pounds/ Naira and Deutsche/Naira below (Figure1), the movement of the data plot shows that an increasing trend pattern exists in the data. This is because of the movement of the values to relatively high values.

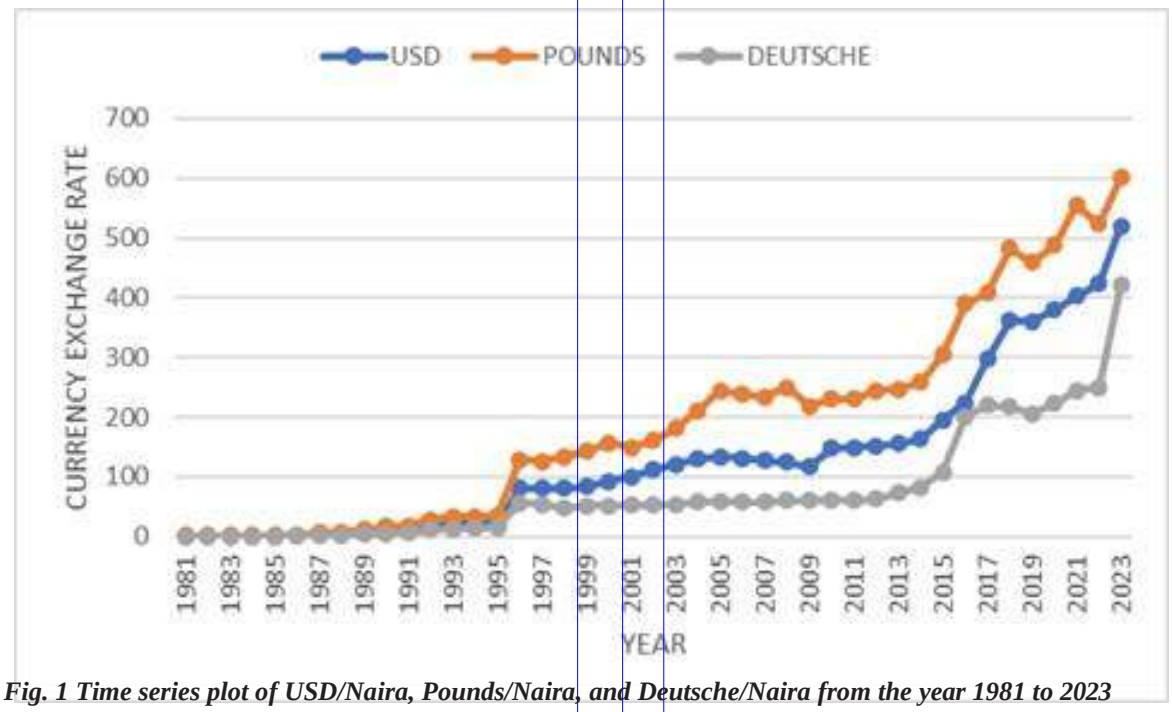

Fig. 1 Time series plot of USD/Naira, Pounds/Naira, and Deutsche/Naira from the year 1981 to 2023

3.1 Test for Stationarity

A time series x_t is said to be stationary if there is no trend and no seasonal variation and this assumes that the mean and the variance of the series are constant over time and that the co-variant structure of the series depends only upon the relative position in time of the two observations.

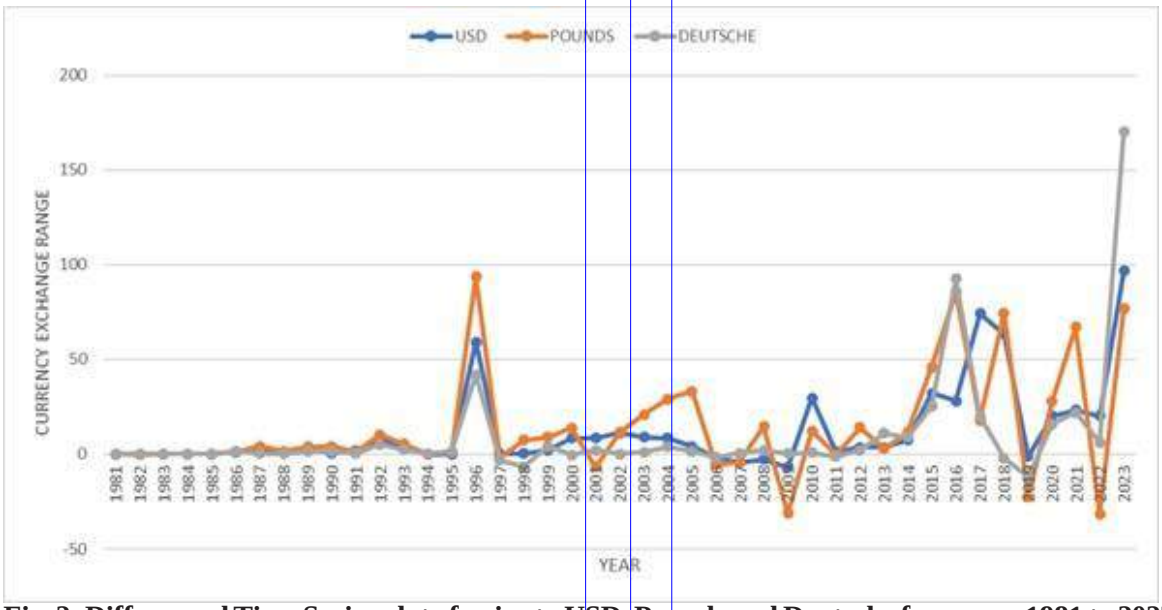

Fig. 2: Differenced Time Series plot of naira to USD, Pounds and Deutsche from year 1981 to 2023

The currency exchange rate were tested for stationarity firstly using the raw data (in levels) and then using differenced data as shown in figure 2. The resulted test statistic for the three currencies are greater than all the critical values which show that the raw data of the three currencies exchange rate is not

stationary. The resulted test statistic for the three currencies are lesser than all the critical values which show that the data is stationary after the first differencing.

3.2 VALIDATION OF THE MODELS

Once the time series data have been stationarized, the next step is to identify the order of the autoregressive and moving average terms. Akaike information criterion (AIC), Schwatz information criterion (SIC), and Hannan Quinn information criterion (HQC) will be used to choose the order. The order with the lowest value of criterion will be chosen.

TABLE 1: VALIDATION OF AR MODEL

MODEL	USD			POUNDS			DEUTSCHE		
	AIC	SIC	HQC	AIC	SIC	HQC	AIC	SIC	HQC
AR(1)*	**8.611**	**8.735**	**8.657**	**9.521**	**9.645**	**9.567**	**8.477**	**8.601**	**8.522**
AR(2)	8.655	8.821	8.716	9.553	9.718	9.644	8.499	8.665	8.560
AR(3)	8.691	8.898	8.767	9.568	9.774	9.643	8.547	8.754	8.623
AR(4)	8.739	8.987	8.830	9.604	9.892	9.695	8.585	8.833	8.676
AR(5)	8.780	9.069	8.886	9.651	9.941	9.757	8.632	8.921	8.738

From table 1, it was observed that the optimal model is AR (1) that is based on the selection criterion AIC, SIC, HQC. * is the best model for the three currencies (USD, Pounds and Deutsche)

TABLE 2: MA MODEL VALIDATION

MODEL	USD			POUNDS			DEUTSCHE		
	AIC	SIC	HQC	AIC	SIC	HQC	AIC	SIC	HQC
MA(1)*	**8.631**	**8.756**	**8.677**	**9.522**	**9.646**	**9.567**	**8.459**	**8.583**	**8.504**
MA(2)	8.670	8.835	8.730	9.542	9.707	9.603	8.506	8.672	8.567
MA(3)	8.697	8.904	8.773	9.567	9.774	9.643	8.546	8.752	8.621
MA(4)	8.743	8.992	8.834	9.614	9.862	9.705	8.593	8.841	8.684
MA(5)	8.785	9.074	8.891	9.657	9.947	9.763	8.630	8.920	8.737

From table 2, it was observed that the optimal model is MA (1) that is based on the selection criterion AIC, SIC, HQC. * is the best model for the three currencies (USD, Pounds and Deutsche).

TABLE 3: ARMA MODEL VALIDATION

MODEL	USD			POUNDS			DEUTSCHE		
	AIC	SIC	HQC	AIC	SIC	HQC	AIC	SIC	HQC
ARMA (1,1)*	**8.652**	**8.817**	**8.713**	**9.567**	**9.733**	**9.628**	**8.506**	**8.672**	**8.567**
ARMA(2,1)	8.695	8.901	8.770	9.589	9.796	9.665	8.547	8.754	8.623
ARMA(4,3)	8.825	9.197	8.961	9.714	10.09	9.850	8.671	9.044	8.808
ARMA(6,5)	8.966	9.503	9.163	9.832	10.37	10.03	8.837	9.375	9.034
ARMA(8,7)	9.125	9.828	9.382	9.989	10.69	10.25	8.971	9.674	9.223

From table 3, it was observed that the optimal model is ARMA (1,1) that is based on the selection criterion AIC, SIC, HQC. * Is the best model for the three currencies (USD, Pounds and Deutsche).

3.2.2 ARMA MODEL ESTIMATION

Autoregressive Moving- Average (ARMA) model of order 1 i.e. ARMA (1,1) is then estimated for each of the currencies exchange rate as shown below:

TABLE 4: ARMA MODEL ESTIMATION (USD)

Variable	Coefficient	Std. Error	t-Statistic	Prob.
C	27.94432	107.9807	0.258790	0.7975
AR(1)	0.943487	0.299094	3.154489	0.0035
MA(1)	-0.648614	0.332571	-1.950301	0.0599
R-squared	0.099250	Mean dependent var		8.485631
Adjusted R-squared	0.042953	S.D. dependent var		17.04077
S.E. of regression	16.67078	Akaike info criterion		8.547008
Sum squared resid	8893.272	Schwarz criterion		8.680323
Log likelihood	-146.5726	Hannan-Quinn criter.		8.593028
F-statistic	1.762968	Durbin-Watson stat		1.701459
Prob(F-statistic)	0.187790			
Inverted AR Roots	.94			
Inverted MA Roots	.65			

TABLE 5: ARMA MODEL ESTIMATION (POUNDS)

Variable	Coefficient	Std. Error	t-Statistic	Prob.
C	17.00541	5.152110	3.300669	0.0024
AR(1)	0.873274	0.139823	6.245588	0.0000
MA(1)	-0.999769	0.093960	-10.64040	0.0000

R-squared	0.127043	Mean dependent var	11.61533
Adjusted R-squared	0.072483	S.D. dependent var	23.38295
S.E. of regression	22.51957	Akaike info criterion	9.148463
Sum squared resid	16228.20	Schwarz criterion	9.281779
Log likelihood	-157.0981	Hannan-Quinn criter.	9.194484
F-statistic	2.328509	Durbin-Watson stat	1.773980
Prob(F-statistic)	0.113733		

Inverted AR Roots	.87
Inverted MA Roots	1.00

TABLE 6:ARMA MODEL ESTIMATION (DEUTSCHE)

Variable	Coefficient	Std. Error	t-Statistic	Prob.
C	13.27188	36.62194	0.362403	0.7194
AR(1)	0.880398	0.541432	1.626054	0.1137
MA(1)	-0.618387	0.591754	-1.045008	0.3038

R-squared	0.108426	Mean dependent var	6.284206
Adjusted R-squared	0.052703	S.D. dependent var	17.44849
S.E. of regression	16.98247	Akaike info criterion	8.584057
Sum squared resid	9228.942	Schwarz criterion	8.717373
Log likelihood	-147.2210	Hannan-Quinn criter.	8.630078
F-statistic	1.945790	Durbin-Watson stat	1.963495
Prob(F-statistic)	0.159411		

Inverted AR Roots	.88
Inverted MA Roots	.62

- For USD(Table 4): 0.6263 $Y_{t-1} + \varepsilon_t - 0.31206\varepsilon_{t-1}$
- For Pounds(Table 5): -0.3194 $Y_{t-1} + \varepsilon_t + 0.2541\varepsilon_{t-1}$
- For Deutsche(Table 6): -0.0121 $Y_{t-1} + \varepsilon_t + 0.34314\varepsilon_{t-1}$

From the list of equations listed above, the equation includes the percentage of past value resulting to the current value plus the percentage of past errors e.g. the current value of USD is the 94.35% of the past value plus the past error minus 64.86% of the immediate past error value of the past error in use to predict the current value.

TABLE 7: MEASURE OF THE FORECAST ACCURACY

CURRENCY	MODEL	ERROR		
		RMSE	MAE	MAPE
USD	AR	20.82	11.08	22.54
	MA	69.55	54.67	1578.85
	ARMA	**18.56**	**10.85**	**25.31**
POUNDS	AR	29.45	17.65	25.78
	MA	96.62	78.61	1442.31
	ARMA	**29.17**	**17.096**	**18.887**
DEUTSCHE	AR	17.55	7.36	53.34
	MA	44.05	31.996	2111.84
	ARMA	**16.20**	**7.03**	**52.80**

From table 7 above, the three models efficiency was measured and compared using RMSE (Root Mean Square Error),MAE (Mean Absolute Error) and MAPE (Mean Absolute Percentage Error). For each of the currency exchange rate, ARMA was found to be the best model to be used because it has the lowest RMSE, MAE and MAPE value for the three currencies exchange rate.

TABLE 8: FORECAST OF EXCHANGE RATE USING OPTIMAL ARMA MODEL (2024-2030)

YEAR	USD	POUNDS	DEUTSCHE
2024	436.41	553.62	269.66
2025	449.92	538.13	281.45
2026	467.95	545.70	287.48
2027	489.33	560.62	293.45
2028	512.80	577.90	299.41
2029	537.58	591.93	305.23
2030	563.19	608.92	311.05

4. DISCUSSION OF RESULT

In this work, the currency exchange rate between Naira and three other currencies (USD, Pounds and Deutsche) was analysed using ARMA. The series were plotted on a graph to check the type of pattern that existed in the data. From the series plotted, it shows that Naira has been depreciating right from year 1981 to 2023. The series of the three currencies were found to be in increasing trend pattern as shown in fig. 1. The currency exchange rate were tested for stationarity firstly using the raw data (in levels). Dickey Fuller (DF) Test was also performed using the series for the three exchange rates. The resulted test statistic for the three currencies are lesser than all the critical values which show that the data is stationary after the first differencing. Validation of the order of the autoregressive and moving average terms was done using Akaike information criterion (AIC), Schwatz information criterion (SIC) and Hannan Quinn information criterion (HQC) in order to choose the lowest value of criterion. From Table 1, it was observed that the optimal model is AR (1) that is based on the selection criterion AIC, SIC, HQC, is the best model for the three currencies (USD, Pounds and Deutsche) also the results from Table 2, revealed that the optimal model is MA (1) that is based on the selection criterion AIC, BIC, HQC is the best model for the three currencies (USD, Pounds and Deutsche) and the Table 3 as well revealed that the optimal model is ARMA (1, 1) that is based on the selection criterion AIC, SIC, HQC, is the best model for the three currencies (USD, Pounds and Deutsche). Autoregressive Moving- Average (ARMA) model of order 1 i.e. ARMA (1,1) is then estimated for each of the currencies exchange rate as shown in Table 4-6. The resulted equations for the three currencies include the percentage of past value resulting to the current value plus the percentage of past errors e.g. the current value of USD is the 94.35% of the past value plus the past error minus 64.86% of the immediate past error value of the past error in use to predict the current value. The three models efficiency was measured and compared in Table 7 using RMSE (Root Mean Square Error), MAE (Mean Absolute Error) and MAPE (Mean Absolute Percentage Error) and for each of the currency exchange rate, ARMA was found to be the best model used to forecast because it has the lowest RMSE, MAE and MAPE as shown in Table 8.

5.0 CONCLUSION

The exchange rates series between naira and three other currency were collected from central bank of Nigeria (CBN) are analyzed using AR, MA and ARMA models. This study reveals the fact that ARMA (1, 1) produces superior results than AR and MA models which was then used to forecast from 2024 to 2030. The finding also showed that the naira will continue to depreciate and suffer unstable exchange rate that will cause a

high degree of uncertainty in the Nigerian business environment if a surge in demand for the three currencies in the parallel market driven by banks.

REFERENCES

Ahmed, H. I., and Zarma, A., 1997. The impact of parallel market on the stability of exchange rate: Evidence from Nigeria. *NDIC Quarterly Publication*, 7(2), 42 – 61.

Aliyu, S. R. U. (2011) Impact of Oil Price Shock of Exchange Rate Volatility on Economic Growth in Nigeria: An Empirical Investigation, Research Journal of International Studies, Issue 11.

Benson, M and Victor, A.C (2012). Exchange Rate Fluctuation, Oil prices and Economic Performance:Empirical Evidencefrom Nigeria. *International Journal of Energy Economics and Policy*.

CBN (2015) Bulletin and Nigeria Economic Indicators. (http://www.economywatch.com/economic_statistics/country/Nigeria/year-2015)

CBN,(2018)FinancialStabilityReporthttps://www.cbn.gov.ng/out/2019/fprd/fsr%20december%202018%20(for%20publication).pdf

Chen, X., Zhou, Y., and Wang, H. (2022). Application of ARIMA in forecasting the USD/EUR exchange rate: A comparison with the random walk model. *Journal of Financial Analysis and Forecasting*, 15(3), 45-58.

Gbosi, A. N. (2005). Money, Monetary Policy and the Economy. Port Harcourt: Sodek.

Gupta, R., Singh, A., and Patel, K. (2021). Long Short-Term Memory (LSTM) networks for exchange rate forecasting: A deep learning approach using USD/CNY data. *Journal of Machine Learning in Finance*, 12(4), 150-168.

Iyeli, I. I., S. G. Nenbee and J. A. Opue (2011), Exchange Rate Volatility and its effects on Tradeable goods in Nigeria Annals of Humanities and Development Studies.Universal Academic Services, Beijing. China. Vol. 3.

Iyeli, I.I and Clement, U. (2017). Exchange rate volatility and economic growth in Nigeria, Journal of Economics, Commerce and Management, 5(7), 583-596

Jonathan O. E and Kenneth U (2016). The impact of exchange rate fluctuations on private domestic investment performance in Nigeria, Journal of Economics and Finance, 7(3), 07-15

Jhingan M. L. (2005). *International Economics*,5th Edition, Vrinda Publications (P) Limited Delhi.

Koo, R.C. (2009): Balance sheet recessions and 'the other half' of macroeconomics, in: European Journal of Economics and

Economic Policies: Intervention, 10(2), 136–157.

Mordi, M. C. (2006). Challenges of Exchange Rate Volatility in Economic Management of Nigeria, in the dynamic of exchange rate in Nigeria, CBN Bulletin Vol. 30(3).

Nkanta Frank Ekanem (2002), "Economic Instability: A case study of the effect of structural rigidity in the selected African Countries, Journal of African Development, Vol 5.

Oloyede, B. (2002). Principles of International Finance, Forthright Educational Publishers, Lagos.

O'Sullivan, A, and Steven, M. S. (2003). Economics: Principles in action. Upper Saddle River, New Jersey 07458: Pearson Prentice Hall.

Park, J., and Lee, D. (2023). Forecasting exchange rates using a hybrid wavelet and support vector machine model: The case of USD/JPY. *Journal of Computational Economics*, 35(5), 203-220.

Rahman, A., and Ahmed, S. (2022). Hybrid ARIMA-ANN models for EUR/USD exchange rate forecasting: An empirical study. *Advances in Neural Network Modeling*, 9(1), 89-104.

SushantaMallick and Helena Marques (2008) " Pass- through of Exchange Rate and Tariffs into import prices of India: Currency Depreciation versus Import Liberalization," Review of International Economics, Wiley Blackwell, Vol 16(4).

Zhang, L., and Li, M. (2023). Volatility forecasting of exchange rates using GARCH models: Evidence from USD/GBP. *International Review of Financial Studies*, 28(2),123-137.